A Methodological Assessment of Extreme Heat Mortality Modeling and Heat Vulnerability Mapping in Atlanta, Detroit, and Phoenix

A Dissertation
Presented to
The Academic Faculty

by

Evan Mallen

In Partial Fulfillment
of the Requirements for the Degree
Doctor of Philosophy in the
School of City & Regional Planning

Georgia Institute of Technology
December 2019

A Methodological Assessment of Extreme Heat Mortality Modeling and Heat Vulnerability Mapping in Atlanta, Detroit, and Phoenix

Approved by:

Dr. Brian Stone, Advisor
School of City & Regional Planning
Georgia Institute of Technology

Dr. Bill Drummond
School of City & Regional Planning
Georgia Institute of Technology

Dr. Ted Russell
School of Civil Engineering
Georgia Institute of Technology

Dr. Marie O'Neill
School of Public Health
University of Michigan

Dr. Andrew Grundstein
School of Geography
University of Georgia

Date Approved: October 30, 2019

To those who may benefit from this and future research

ACKNOWLEDGEMENTS

It will take many years of dedicated service to the community, the academy, my family, and my friends to repay their generous support during my time in graduate school. I am thankful to Dr. Brian Stone and the Urban Climate Lab for providing the training and experience necessary to succeed in my academic career, and to Drs. Larissa Larsen, Richard Rood, and Marie O'Neill for sparking my interest in this field and encouraging me to pursue this opportunity many years ago. I am grateful for my committee members, Drs. Bill Drummond, Armistead Russell, and Andrew Grundstein for their guidance and support throughout my time at Georgia Tech.

I thank my family for their lifelong encouragement to pursue my own goals, and my wife Anastasia for sacrificing so much that I may achieve them. I must also thank Milo, who has been with me through early mornings and long nights, providing companionship and an insistent reminder now and then, to take a walk.

TABLE OF CONTENTS

LIST OF TABLES

LIST OF FIGURES

LIST OF SYMBOLS AND ABBREVIATIONS

HVI	Heat Vulnerability Index
PCA	Principal Components Analysis
SAM	Statistical Attribution Model
WRF	Weather Research & Forecasting

SUMMARY

Extreme temperatures pose an increasingly high risk to human health and are projected to worsen in a warming climate with increased intensity, duration and frequency of heat waves, further amplified by the urban heat island, in the coming decades. To mitigate heat exposure and protect sensitive populations, urban planners are increasingly using decision support tools like heat vulnerability indices (HVIs) to identify high priority areas for intervention and investment. However, HVIs often capture only proxy heat exposure indicators at the land surface level, not air temperatures that humans experience, and are highly subjective in their construction methodology. This gap can be filled using regional climate models like the Weather Research & Forecasting (WRF) model to simulate air temperatures comprehensively over a city, coupled with a heat exposure-response function to objectively estimate mortality attributable to heat. But this method is often beyond the capabilities of local planning departments due to limitations in funding or technical expertise to run the model. Careful consideration of decision support tool selection will be an important factor in determining the future resilience of urban populations in a changing climate.

Through a comparative analysis, this study investigates the relationship and utility of HVIs and spatial statistical attribution models with a focus on 1) the extent to which HVI methods can replicate spatial prioritization from a WRF-driven mortality model; 2) the relative significance of place-based vulnerabilities used in the HVI; and 3) the potential to reliably replicate a WRF-driven mortality model using publicly available datasets. This information can help urban planners and public health officials improve their emergency

response plans and communication strategies for heat mitigation by specifically targeting short and long-term responses where there is greatest need. These techniques equip planners with a useful and accessible tool to protect vulnerable populations effectively and efficiently with minimal public funds and could advance the policies we use to adapt to a changing climate.

CHAPTER 1. INTRODUCTION

Extreme temperatures increasingly threaten vulnerable urban populations. Heat waves are responsible for more deaths annually than all other weather-related hazards combined, and are expected to increase in intensity, duration, and frequency in a warming climate (Habeeb et al., 2015; Luber & McGeehin, 2008). But the risks associated with heat exposure are not uniform across the urban landscape. The urban heat island (UHI) can further elevate air temperatures depending on the local microclimate, and spatially distributed heat-sensitive populations result in areas of high relative risk to heat exposure. Cities currently respond to extreme heat in the short-term through early warning systems and cooling centers. In the long term, research shows that UHI mitigation strategies can measurably reduce exposure (Stone et al., 2014). But locating areas of greatest heat risk and selecting appropriate mitigation strategies can present a major challenge.

Urban planners play a key role in enhancing local resilience to the effects of climate change. Planners have the unique ability to modify the structure and composition of the built environment in the long term and to assist in planning for short-term emergency heat response (APA, 2011). With limited resources, planners need a framework to prioritize heat management strategies to respond to localized heat vulnerability by locating areas of high priority for intervention and identifying which local strategies will be most effective to reduce heat vulnerability. A variety of decision support tools exist to guide these planning efforts with varying complexity. Researchers are increasingly using spatial heat mortality models driven by public health records to estimate and project heat-related mortality at high resolution within a city. However, these models use costly and

computationally intensive methods that are generally beyond the capability of the urban planning practitioner. A simpler tool is the heat vulnerability index (HVI), which aggregates indicators of vulnerability into a single score to highlight relative priority for intervention.

1.1 Heat Vulnerability Indices

Heat Vulnerability Indices (HVIs) are a type of Social Vulnerability Index (SOVI) specifically designed to help planning and public health practitioners understand spatial distribution of heat-related vulnerabilities to target areas for risk reduction via mapping (Gamble et al., 2018). HVIs overlay heat vulnerability indicators from the literature into a single score to convey relative vulnerability at the city, state, or even regional scale (Morabito et al. (2015); Buscail et al., (2012); Tomlinson et al., (2011).

HVIs are generally accessible to the planning practitioner, often using familiar datasets and analysis techniques. Much of the data used in HVIs are publicly available, such as through the National Land Cover Database or in the US Census (Bao et al., 2015; Wolf et al., 2015). Analysis and mapping techniques can often be run in a geographic information system. As such, HVIs are relatively straightforward to construct and are therefore accessible to the urban planning community. Several state and local public health practitioners use vulnerability mapping to identify populations most vulnerable to climate change (Manangan et al., 2014; Marinucci et al., 2014). Public health departments are likewise using HVI methods from the literature in places like Michigan (Seroka et al., 2011), Minnesota (Minnesota Climate and Health Program, 2012), New York State (Nayak et al., 2017), San Francisco (SFDPH, 2013), and Chicago (Wilson et al., 2017).

A population's vulnerability to environmental hazards can be characterized as a function of their exposure, sensitivity, and adaptive capacity (Figure 1). In the case of heat-related deaths, exposure refers to the intensity and spatial distribution of elevated temperatures. Extreme heat exposure can vary temporally through a warming climate, as temperatures steadily rise over time, or spatially through the urban heat island effect, through which some zones of a city may be much warmer than others. Sensitivity refers to how well a population can cope with increased exposure, or the extent to which increased exposure will affect them physically. For example, those with heat-sensitive pre-existing conditions like diabetes will have greater sensitivity to heat than those without an underlying health condition (Reid et al., 2009). A city's climate also influences local sensitivity due to acclimatization. For example, the population of a southern city will be less sensitive to heat than a northern city, as these locations closer to the equator are more regularly exposed to higher temperatures (Curriero et al., 2002). Lastly, adaptive capacity is the ability of a population to actively mitigate or cope with increased personal exposure (Cutter et al., 2008; USGCRP, 2016). Individuals with access to air conditioning, for example, exhibit a greater adaptive capacity than those without air conditioning, independent of their sensitivity to heat. These three components of vulnerability have been shown to influence heat-related morbidity and mortality and can be useful predictors of heat risk.

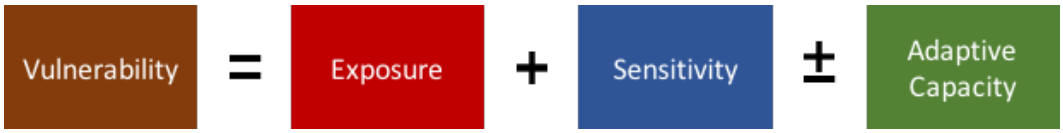

Figure 1 - Components of heat vulnerability.

Heat Vulnerability Indices (HVIs) are one method used to determine heat vulnerability, focusing on these three components of risk. HVIs can provide a more in-depth analysis of specific risk factors associated with heat, allowing urban planners to identify areas of higher relative heat vulnerability. While HVIs incorporate indicators of heat exposure, sensitivity, and adaptive capacity, they typically do not incorporate estimates of actual health outcomes, such as historical heat-related mortality counts by zone. So, while HVIs do help visualize relative risk of heat-related mortality, they are fundamentally reflective of proxy measures of vulnerabilities rather than a direct measure of heat illness, and do not quantify heat-related mortality. As such, the utility of HVI scores to guide heat management and intervention strategies is largely undetermined.

1.2 Statistical Attribution Models

Researchers are increasingly using statistical attribution models to estimate the health impacts of environmental exposures that are difficult to directly measure. For example, the number of deaths resulting from a heat wave is hard to determine directly, as the cause of death recorded on death certificates may be attributed to an underlying health condition exacerbated by extreme heat, such as a cardiovascular or respiratory illness. As an alternative to such direct attribution approaches to quantifying heat-related mortality, health researchers are increasingly developing statistical attribution models based on the established association between observed temperature and all-cause mortality over time (Bobb et al., 2014; Kalkstein et al., 2011). As illustrated in Figure 1, all-cause mortality is often found to increase sharply during heat wave events, such as in Paris during the summer of 2003. Exposure-response functions for heat mortality are statistically derived from the

association between temperature and total mortality over a fixed period of time and support the estimation of heat mortality in response to historical or projected heat exposures.

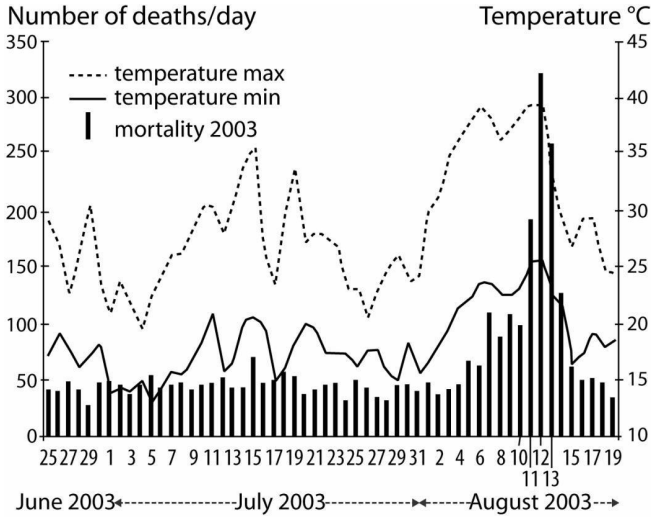

Figure 2 - Number of deaths at varying temperatures during Paris heat wave (Dousset et al., 2010).

Figure 3 summarizes how a change in mortality for a population can be predicted based on a change in heat exposure, the historical rate of all-cause mortality for a location, and an established health-response function for heat, represented as the additional mortality expected per unit change in temperature.

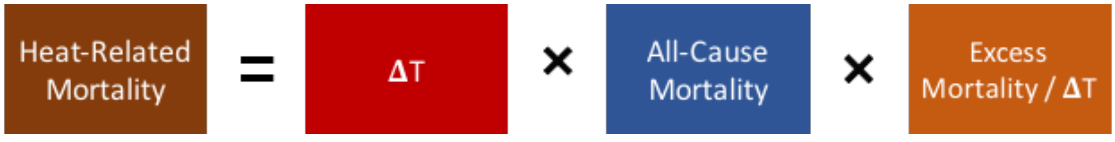

Figure 3 - Exposure-response function applied to heat-related mortality.

Such functions can also be applied within cities to pinpoint areas that may be at risk of higher heat-related mortality, such as those with a greater urban heat island intensity or dense population centers. A major impediment to developing such intra-urban scale

estimates of heat mortality is an insufficient number of weather stations across cities to measure how heat exposure varies over space. While satellites provide accurate measurements of land surface temperatures, these surface temperatures have not been found to correlate highly with the near-surface air temperatures employed in heat exposure-response functions (Ho et al., 2016; Weng, 2011).

To address this limitation, it is often necessary to comprehensively model air temperatures using regional climate models like the Weather Research & Forecasting Model (WRF). This type of model can generate high resolution and spatially comprehensive air temperature datasets using complex weather simulations over a specific region. Such simulations can even model land cover scenarios to test various impacts of development or climate adaptations. Models like WRF allow for statistical attribution models to take on a spatial orientation, modeling variation in heat-related mortality over space due to the urban heat island rather than simply over time. In this document, I refer to such an orientation as a spatial statistical attribution model, or spatial SAM.

While HVIs can provide a low-cost approach to mapping heat vulnerability, they may not well represent actual heat risk. As a result, researchers are increasingly seeking to evaluate HVI methods using heat-related morbidity and mortality observations. spatial SAMs can provide high-resolution mortality estimates based on local observations to fill this model evaluation gap. However, these functions are generally less accessible to the planning practitioner because of technical demands and processing costs. Alternatively, HVI construction is much less technically demanding and can provide useful insights into which areas have higher relative risk.

1.3 Study Purpose

The principal objective of this study is to analyze the relationship between HVIs and spatial SAMs, and to explore alternatives to the WRF-derived temperature inputs with the aim of enhancing accessibility of these methods as decision support tools. In a warming climate, it is increasingly important for cities to adopt strategic plans to protect our most vulnerable populations from heat-related morbidity and mortality. Planning and Public Health practitioners can improve both short and long-term response strategies with guidance from decision support tools like HVIs or spatial SAMs. With guidance from these tools, planners are able to develop effective and efficient response strategies targeted to particular neighborhoods and populations. While there are many studies using HVI methods, no study has yet compared HVI outcomes to more complex statistically attributed heat mortality models.

The findings from this study are intended to influence policy and planning decisions in several ways. First, understanding the relationship between these vulnerability mapping methods can improve the accessibility of these models to be run in-house within planning or public health departments, without the need to rely on outside consultation. This can reduce costs of major plan development and allow for greater coordination between multiple levels of planning efforts in the city government and community. Second, a better understanding of the model inputs, construction methods, and output utility can help planners design more effective strategies that directly address specific vulnerabilities. Such targeted strategies can help planners design better short- and long-term strategies and direct capital investments where they will be most beneficial. Third, the development of a more

accessible spatial SAM can eliminate the need for WRF-driven temperature inputs, thereby reducing the time and cost of the spatial SAM procedure.

CHAPTER 2. LITERATURE REVIEW AND GAPS

2.1 Introduction

This section summarizes the current knowledge and gaps in which to situate this research. Here I discuss the physiological impacts of heat, the need for decision support tools, and measuring heat-related health impacts, to establish a theoretical grounding and motivation for this work. Next, I review the literature on statistical attribution model construction, HVI construction methodology, and the utility of each. Finally, I highlight gaps in the literature that inform my central research questions, described in greater detail in Chapter 3.

2.2 Physiological Impacts of Heat

Extreme temperatures already pose a major risk to human health (Koppe et al., 2004; Kovats & Hajat, 2008; Stone et al., 2014) and are projected worsen in a warming climate with increased intensity, duration and frequency of heat waves in the coming decades (Battisi & Naylor, 2009; Diffenbaugh & Scherer, 2011; Habeeb et al., 2015; Knowlton et al., 2007). Exposure to high temperatures can result in clinical syndromes of heat stroke, heat exhaustion, heat syncope, heat cramps, or even death (Bouchama & Knochel, 2002; Kovats & Hajat, 2008; Luber & McGeehin, 2008). In the United States, extreme heat events, or heat waves, are responsible for more deaths annually than any other weather-related hazard combined (Habeeb et al., 2015; Luber & McGeehin, 2008). Studies estimate between 670 and 1,300 deaths are related to heat in the US every year (Berko et al., 2014; Bobb et al., 2014). Heat-related mortality could increase by as much as 95% by

2050 without proper risk mitigation steps (Knowlton et al., 2007). For the country as a whole, annual heat-related deaths may increase by 28,000-34,000 additional deaths by mid-century (Voorhees et al., 2011).

Heat exposure is further exacerbated by elevated temperatures in urban areas, a phenomenon known as the urban heat island effect. Dark-colored building materials absorb and store heat energy from the sun, releasing it over time as sensible heat in the urban environment. Lack of vegetation can also lead to higher temperatures through a reduction in shading as well as reduced evapotranspiration. The urban canyon can further trap heat as it radiates back and forth between tall buildings in the urban core (Oke, 1987; Stone, 2012). Together, these drivers can create small islands of elevated temperature that are not limited to dense urban centers but can occur anywhere these conditions are prevalent. Kenward et al. (2014) found the 60 largest cities in the United States to have maximum single-day air temperature differences of 17.5°F on average, as compared to proximate rural areas. This difference was found in extreme cases to be as high as 27°F at night, and that cities averaged at least 8 more days over 90°F each summer than proximate rural areas. The UHI leads to higher heat stress in urban areas in both intensity and duration of heat exposure, an effect expected to amplify even further in climate change projections (Fischer & Lawrence, 2012).

2.3 Decision Support Tools

Urban planners are in a unique position to address climate adaptation at the municipal level, applying global and regional trends to local context (APA, 2011). However, planners often do not have the technical expertise or resources to obtain

downscaled climate data or local impacts of climate change and may not have perfect information on impacts and response strategies. Lack of awareness and communication about climate impacts at the local scale is a key barrier to local climate adaptation planning, including heat mitigation (Baker, 2012; Biesbroek, 2013; Measham et al., 2011). Furthermore, there is a communications gap between planners and scientists that can hinder the flow of information from science to policy (Moser, 2014; Winkler, 2011). Despite this barrier, the American Planning Association suggests that planners should strive to recognize and effectively communicate the risks of heat at the local level (APA, 2011). To use public resources effectively and efficiently, planners need to be able to identify areas of high risk and understand what interventions are appropriate to enhance local resilience to heat.

Planners can use decision support tools such as heat vulnerability mapping to better understand spatial differences in heat-related vulnerabilities to tailor interventions to specific vulnerabilities (Gamble et al., 2018). Some cities like Chicago have developed publicly accessible heat vulnerability tools that show relative heat vulnerabilities within the city based on local exposures and population sensitivities to heat (Wilson et al., 2017). Other public health departments are also beginning to adopt similar tools to guide heat mitigation and response policy (Minnesota Climate and Health Program, 2012; Nayak et al., 2017; SFDPH, 2013; Seroka et al., 2011; Wilson et al., 2017).

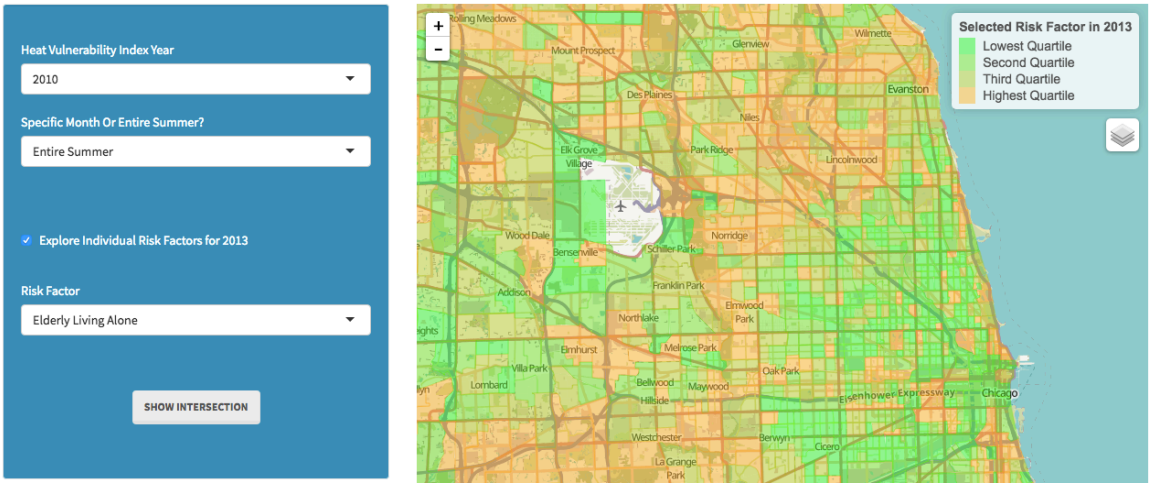

Figure 4 - Chicago Heat Vulnerability Tool (Wilson et al., 2017).

While these tools do not contain all possible indicators of heat vulnerability, planners can work within a bounded rationality framework to guide policy toward enhanced heat resilience and protect vulnerable populations. Planning incrementally based on the best knowledge available can help us adapt to a changing climate and the risks of extreme heat exposure we face today based on what we already know regardless of future warming scenarios (Quay, 2010).

2.4 Measuring Heat-Related Health Impacts

There are two main methods of quantifying the relationship between heat exposure and health impacts identified in the literature: direct attribution and statistical attribution (USGCRP, 2016). Direct attribution relies on observed health outcomes directly linked to observed temperatures. Health outcomes include medical records such as hospital admissions or death certificates. Unfortunately, death certificates very rarely record heat exposure as a cause of death (Harlan et al., 2013), even though codes do specifically exist in the International Classification of Diseases (WHO, 2004). Furthermore, even if death

certificates list heat, they generally do not list weather conditions at or preceding the time of death (USGCRP, 2016). Most death certificates will not list heat as a cause of death because heat exacerbates pre-existing conditions that are then listed as the cause of death (Anderson et al., 2011; Berko et al., 2014). As a result of these practices, the direct attribution method often underestimates total heat-related mortality.

On the other hand, the statistical attribution method compares observed mortality to observed temperature and other socio-demographic factors relative to long-term averages (USGCRP, 2016) to determine the relationship between the two. These studies often compare total cases of illness or death during a short-term period of extreme heat to baseline rates during a control period without extreme heat to determine excess illness or death that can be attributed to heat (Bustinza et al., 2010; Knowlton et al., 2009; Ye et al., 2012).

Some studies will include all deaths in a long-term study period, while others will focus only on days above a certain temperature threshold (Mills et al., 2015). The period and threshold often take the form of a designated heat wave. Robinson (2001) generally defines a heat wave as "an extended period of unusually high atmosphere-related heat stress, which causes temporary modifications in lifestyle and which may have adverse health consequences for the affected population." An increasingly common approach to defining heat waves is to use temperature thresholds relative to the normal temperature in a particular location at a particular time (Hawkins et al., 2015; Robinson, 2001) or to use a percentile approach in which temperatures in a particular location are compared to the historical record at that location, at that time of year (Habeeb et al., 2014; Maier et al., 2014). A heat wave is triggered not at an absolute temperature, but at a temperature that is

sufficiently different from the "norm" to overwhelm the body's capacity to cope with the heat, given an individual's level of acclimatization at that time, in that place (Robinson, 2001). Some studies will incorporate other weather variables in addition to temperature, such as wind, air pressure, cloud cover, or humidity (Kalkstein et al., 2011).

The statistical attribution method is not inherently subject to restrictions on the cause of death, as with the direct attribution method. As a result, heat mortality estimates tend to be higher using this method compared to the direct attribution method and may be at risk of over-estimating heat mortality (Bobb et al., 2014; Kalkstein et al., 2014). However, this method can be useful to track changes in mortality over time, either historically or through projections using climate change and land cover scenarios. I discuss the construction and utility of this method further in the following section.

2.5 Statistical Attribution Model Construction and Utility

The statistical attribution model is driven by the principle that the future rate of change in a health impact is influenced by the existing health status of the population, the change in exposure, and the interaction effect of the exposure on that population's health status (USGCRP, 2016). Applied specifically to heat, this method models heat-related mortality as a function of all-cause mortality (observed mortality within a specific area), times the change in exposure to heat (either over time due to a warming climate or over space due to the UHI effect), times the excess mortality observed per degree change in temperature, also known as the exposure-response function.

Figure 5 - General formula for statistical attribution model (top) and adapted for heat (bottom).

A particular strength of the statistical attribution model is that it is inherently linked to a locality's unique relationship with heat, also known as acclimatization. Acclimatization has major implications for heat-health research as a key aspect of heat sensitivity (Boeckmann et al., 2014; Davis et al., 2003; Hondula et al., 2014; Kalkstein et al., 1989; Knowlton et al., 2007; Robinson, 2001; Toloo et al., 2013). Sensitivity is greatly dependent on individual and regional acclimatization, or the human body's ability to protect itself from heat stress through mechanisms such as cardiovascular performance, salt conservation by sweat glands and kidneys, and increase in the capacity to secrete sweat (Bouchama & Knochel, 2002). Populations can also behaviorally acclimatize through personal decisions like clothing choice or regional development decisions (Curriero et al., 2002). On a large-scale, this could mean development of green space for neighborhood cooling or promoting street trees along major pedestrian corridors. On a smaller scale, it could mean installing air conditioning in new housing. This personal and regional acclimatization gives each city a unique relationship with heat, which is reflected in different sensitivities in the exposure-response function for a given city.

This is illustrated in Figure 6 below, from a study comparing temperature-related mortality in Northern and Southern cities in the U.S. (Curriero et al., 2002). People who regularly live in hot environments are generally less sensitive to heat because they are regionally acclimatized to the hotter weather. Note that Southern cities appear to have a higher relative risk of mortality to cooler weather, while Northern cities have a higher relative risk of mortality in hot weather, with a sharp upward trend at high temperatures. This is because the residents of these cities are acclimatized to particular temperature ranges and become stressed in unusually high or low weather conditions. Several studies have also identified this U-shaped relationship between temperature and mortality, with greater relative risk at high and low temperatures (Basu et al., 2008; Braga et al., 2002; Breitner et al., 2014; Curriero et al., 2002; Patz et al., 2010; Zeng et al., 2016). The human body also experiences strong intra-seasonal acclimatization as the body slowly adapts to changing seasonal weather. This means that a heat event occurring earlier in the season can be far more dangerous than one occurring later in the season after the population has had time to physiologically and behaviorally adjust to the warmer weather (Kalkstein & Davis, 1989).

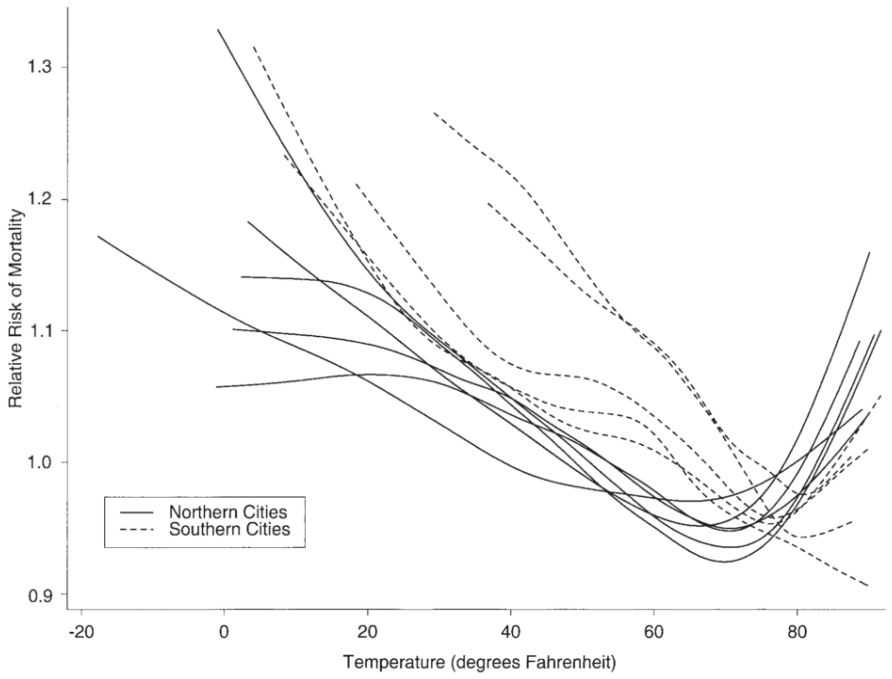

Figure 6 - Temperature-mortality response for northern and southern cities (Curriero et al., 2002).

The recent development of global datasets on the association between temperature and mortality enables both historical and projected heat mortality to be estimated for many large cities around the world. For example, Gasparrini et al. (2015) analyzed daily death counts and temperatures from 384 locations over several years to determine the relationship between mortality and temperature. From these observations, the authors determined the excess mortality per degree temperature change, the third component in Figure 5 - General formula for statistical attribution model (top) and adapted for heat (bottom).

. By determining a unique exposure-response function for each location and using it to modify observed local all-cause mortality rates, this procedure already takes into account any behavioral and physiological acclimatization to heat and cold in the local population. Using location-specific mortality rates and response functions provides a more complete

picture of a population's sensitivity to extreme temperatures and their adaptive capacity to cope with them.

While these models have traditionally been used to analyze changes over time, such as through historical temperature records or climate projections, very little research has applied this model over space to model heterogeneities derived from the urban heat island effect (Vescovi et al., 2005; Lindley et al., 2007). Very few cities have weather stations or air temperature sensor networks dense enough to provide a spatially comprehensive air temperature dataset necessary for this method (Wolf et al., 2013). As microclimates can have a major impact on air temperature, having only few stations represent air temperature across a city or region is not enough to comprehensively model exposure (Arnfield, 2003). Many studies instead use land surface temperature (LST) as a proxy for near-surface air temperature (Jenerette et al., 2007; Liu et al., 2011; Yuan et al., 2007). Studies have not found a strong correlation between surface and air temperature, with R-square values less than 0.5 (Ho et al., 2016; Kloog et al., 2012). However, it is common practice in the literature to characterize an entire city by a single station, often the airport (Habeeb et al., 2014; Kuras et al., 2012; Mallick et al., 2012; Mohsin et al., 2012; Oke, 1982; Stone, 2007). But this method clearly does not account for the UHI effect, as it considers the entire city as one homogeneous thermal body. The airport is also rarely near the city center and does not accurately reflect land cover that is commonly found within the city.

To address this data limitation, regional scale climate models have been used to construct a gridded surface of air temperature estimates across large urbanized regions (Stone et al., 2014). Most commonly, the Weather Research & Forecasting (WRF) model, the model often employed to develop local weather forecasts in the United States, can

reliably estimate a wide range of meteorological variables including temperature, humidity, and wind speed, at a high spatial and temporal resolution (e.g., hourly estimates for every ½ kilometer grid cell). WRF is also often used to model landcover scenarios and their impacts on the urban heat island (Boumans et al., 2014; Chen et al., 2014; Stone et al., 2014; Zhou et al., 2010)

In combination with regional climate model output on heat exposure, a statistical attribution model can be used to estimate annual or event-specific heat-related mortality across a city. Stone et al. (2014) used this method to analyze heat-related mortality under various heat mitigation scenarios such as increased vegetation or albedo across three metropolitan regions, finding heat-related mortality to decrease by 50 to 99% in response to specific heat mitigation strategies. Similarly, the Louisville and Dallas Urban Heat Management Studies produced by Georgia Tech's Urban Climate Lab both use a WRF-driven spatial SAM to estimate the impacts of land cover change scenarios on heat-related mortality.

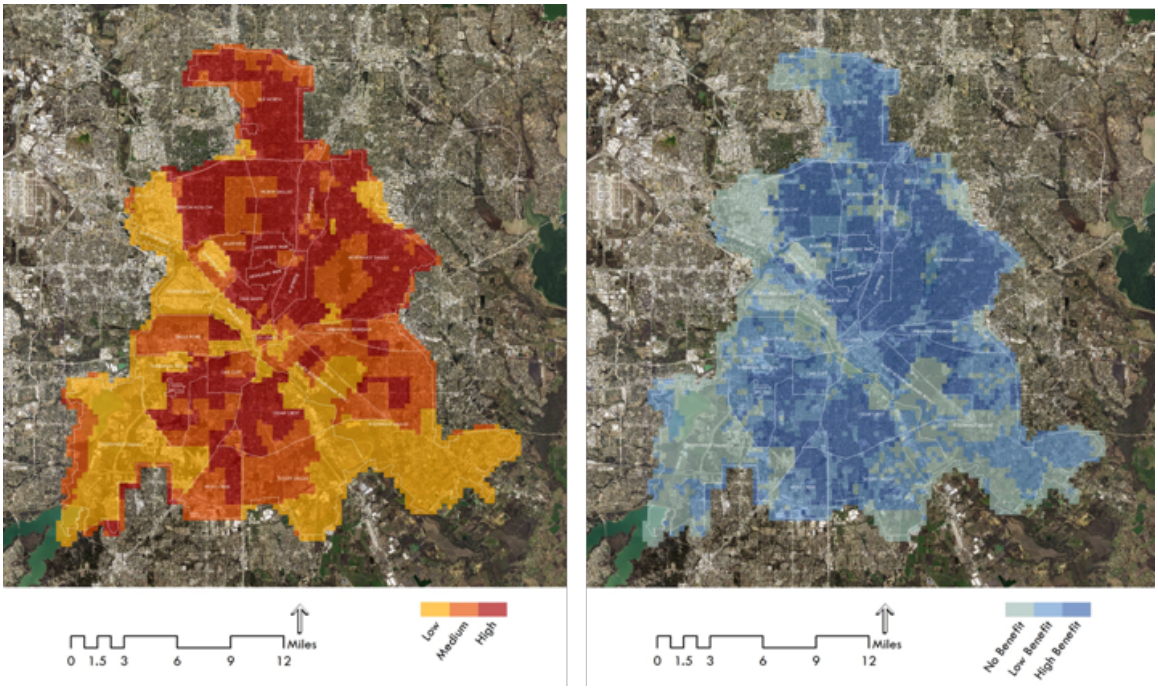

Figure 7 - Urban heat island attributable heat mortality in Dallas, TX (left) compared to neighborhood-specific offset mortality with cooling strategies (right) (Urban Climate Lab).

Such mortality modeling provides a decision support tool to help planning and public health practitioners design targeted interventions to reduce heat exposure and mortality in vulnerable neighborhoods. But these models often require more advanced tools, such as numeric climate models like WRF, than local planners have the capacity to employ without external technical support. Instead, many local planners have turned to Heat Vulnerability Indices to guide heat mitigation and response planning, which I describe further in the following section.

2.6 Heat Vulnerability Index Construction and Utility

HVIs are designed to help planners understand the spatial distribution of heat-related vulnerabilities for heat risk assessment and reduction (Gamble et al., 2018; Hess et

al., 2012). They are often created by combining indicators of hazard exposure and population vulnerabilities as a spatial overlay and mapping to quickly identify areas of highest priority for intervention (Buscail et al. 2012; Morabito et al., 2015; Tomlinson et al., 2011). HVI data often consists of publicly available and easily accessible datasets such as the Census or American Community Survey, CDC public datasets, or remote sensing data like Landsat (Bao et al., 2015). Conceptually, heat vulnerability is often characterized as a function of sensitivity, exposure, and adaptive capacity (Wolf et al., 2015).

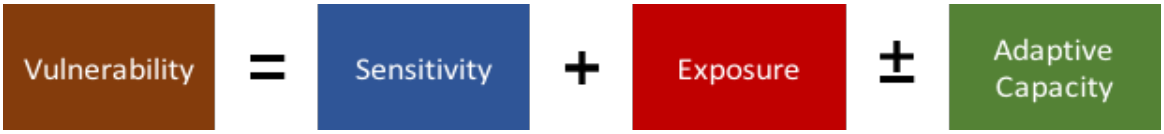

Figure 8 - Components of heat vulnerability.

2.6.1 Sensitivity

Sensitivity involves the level to which an individual may be impacted by the heat given pre-existing physiological conditions that may help or hinder these impacts. Examples of this are the very young or the very old, who may have more trouble regulating their body temperature (Bouchama & Knochel, 2002). Additionally, those with chronic mental disorders, cardiopulmonary, respiratory, or renal diseases, diabetics, or those taking medications that interfere with salt and water balance such as diuretics are at higher risk of being negatively impacted by high temperatures (Bouchama & Knochel, 2002; Harlan & Ruddell, 2011; Nitschke et al., 2013; Reid et al., 2009; Rocklov et al., 2014; Sun et al., 2014). Those who are living alone (often also elderly) are also at higher risk with fewer people to check on them in the case of an emergency and are more likely to ignore heat risk and lack support to cope with the heat (Reid et al., 2009; Semenza et al., 1999).

Elderly populations are widely considered to be at greater risk because they usually have chronic illnesses and higher probability of social isolation (Dolney et al., 2006); Ebi et al., 2004; Robinson, 2001; Schwartz, 2005). Similarly, children are often considered more vulnerable for higher susceptibility to heat (Bunyavanich et al., 2003; Xu et al., 2014).

2.6.2 Exposure

Exposure to high temperatures does not impact everyone equally, as each person has different capabilities to cope with the heat. This includes not only regional and seasonal acclimatization effects as described in Section 2.4, but also populations that are more sensitive to heat stress. It is well documented in the literature that particular populations can be more vulnerable than others to elevated temperatures due to a variety of stressors. Overall risk can be considered a function of environmental exposure, sensitivity, and adaptive capacity (KC et al., 2015).

Environmental exposure includes environmental factors that can exacerbate the overall exposure to heat. A common cause of elevated exposure is the urban heat island effect, characterized by elevated temperatures in urban areas due to low levels of vegetation in the urban environment and subsequent reductions in evapotranspiration, built surface materials efficient at absorbing and storing thermal energy, high density urban morphology that traps outgoing radiation, and the emission of waste heat from buildings and vehicles (Oke, 1987; Stone, 2012).

This exposure is often measured as a proxy, represented by indicators such as total impervious surface cover or lack of vegetative cover (Bao et al., 2015; Reid et al., 2009). Additionally, exposure may be exacerbated by factors like residential building type, with

tall buildings collecting greater heat in the higher floors as heat rises, or by roofing material with dark, absorptive materials storing more thermal energy than reflective ones (Stone, 2012). As a more direct proxy for heat exposure, HVIs commonly use satellite-derived land surface temperature (LST) to characterize heat exposure, as they are spatially comprehensive across the study region (Johnson et al., 2009; Johnson et al., 2012; Rinner et al., 2014; Tomlinson et al., 2011).

2.6.3 Adaptive Capacity

Adaptive (or absorptive) capacity refers to the abilities or resources available to an individual or group to help them cope with the exposure to high temperatures (Cutter et al., 2008; KC et al., 2015). This largely includes socioeconomic factors, such as the ability to afford to own and operate air conditioning to reduce personal exposure to heat, which has been shown to be a useful indicator of heat risk (Curriero et al., 2002; Davis et al., 2003; Kuras et al., 2015; Naughton et al., 2002; Sheridan, 2007). Therefore, indicators relating to lower socioeconomic status, such as those living under the poverty line, those with low education, and racial minorities are common indicators in vulnerability literature (O'Neill et al., 2003; Reid et al., 2009; Schwartz, 2005). Poverty status is also a common vulnerability indicator, as those who do not have access to or cannot afford to use cooling devices like air conditioning lack this control measure over their personal heat exposure (Curriero et al., 2002; Reid et al., 2009).

Research has indicated that low socioeconomic status can also increase environmental exposure. Harlan et al. (2006) and Jenerette et al. (2007) found that there is a "luxury effect" on the environment, in which wealthy residents have a greater ability to

plant and maintain vegetation on their properties, thereby increasing resilience to heat exposure in the process. Similarly, renters are more vulnerable than homeowners, as they tend to have less control over their building envelope, instead relying on a landlord to implement features such as strong weatherization, reflective building materials, local vegetation, or even operable windows (Reid et al., 2009) As a result, those with lower financial capabilities tend to live in more exposed neighborhoods, so it is those who are most sensitive to heat that are also the most exposed to it.

2.6.4 HVI Study Design

There is no standardized common set of indicators to include in HVI studies. In a review of HVI studies by Bao et al. (2015), the authors identified studies ranging in total indicators as low as 5 and as high as 25 to include in their HVI. The number of indicators across each study are summarized in Figure 5 below. Appendix 1 shows the wide range of indicators used in the Bao et al. (2015) sample of HVI studies, organized by exposure, sensitivity, and adaptive capacity categories. Displayed this way, some patterns emerge. All of the studies agreed that elderly population is an important factor to include as an indicator of heat sensitivity. Living alone, ethnicity, and poverty were also commonly selected as adaptive capacity indicators. As for exposure, LST was most often selected to represent exposure to high temperatures. See Appendix 3 for a table of HVI indicators used in sample HVI studies.

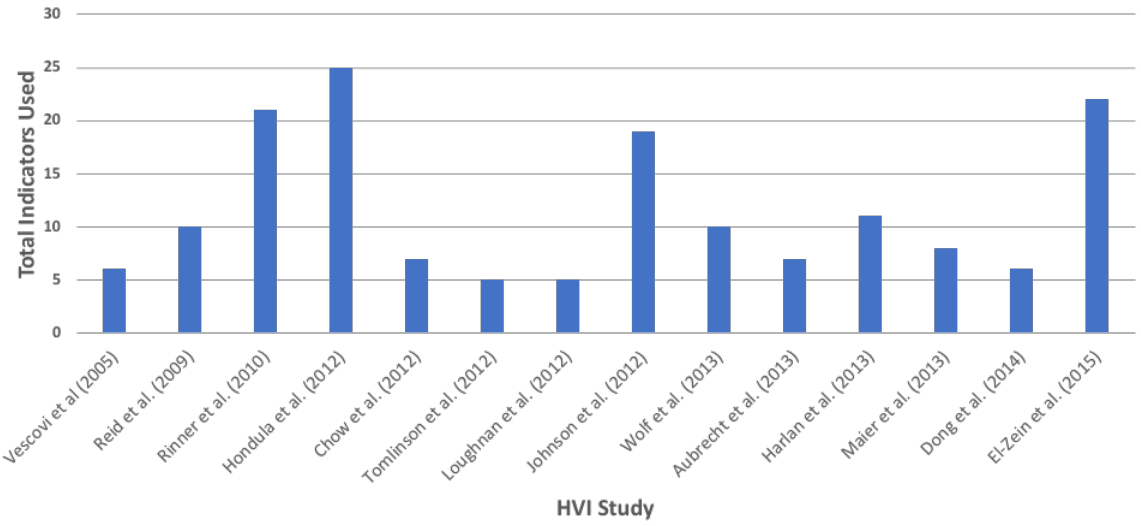

Figure 9 - Total number of indicators used in select sample of HVI studies (adapted from Bao et al., 2015).

In a review of 37 HVI studies, Wolf et al. (2015) characterized three types of HVI study design. The first type was characterized as an a-priori or inductive index without testing empirical health data. This is a "top-down" approach using census data as indicators, often combined using methods of dimensionality reduction such as Principal Components Analysis (PCA). This type is referred to as "inductive" because it uses indicators that either directly or indirectly represent heat risk factors to generate the HVI without direct measures of heat morbidity or mortality (Tate, 2012). The second type is an a-priori or inductive index that does include heath data testing, also known as HVI evaluation or validation. This type utilizes the same "top-down" approach as the first type, but with spatial health data used to validate the HVI results. This spatial health data is often a form of direct attribution such as hospital admissions or in some cases, death certificates. The third type is a bottom-up approach that begins with health outcomes and subsequently explores vulnerability factors. This type often uses health outcome data to weight the components in the HVI or correlate HVI indicators with the outcomes to highlight relative

significance and eliminate indicators with low significance in an effort to create a more succinct HVI (Conlon et al., n.d.).

2.6.5 HVI Scoring Methods

With so many potential indicators, HVIs usually combine these indicators using various statistical methods into a single "score" that indicates relative risk within the study area (Bao et al., 2015; Reid et al., 2009). As with the general HVI study design, there are a wide variety of aggregation methods to derive the HVI score. Most researchers normalize the individual indicators between 0 and 1 to standardize them before aggregating into a composite HVI score (Bao et al., 2015). Each indicator is designed to increase with vulnerability, where 1 is highly vulnerable and 0 is low vulnerability. But from that point, the methods may differ. Detailed below are some of the commonly used aggregation methods.

2.6.5.1 Equal Weight

Some HVI scores are left unweighted and assumed to have equal contributions to vulnerability (Aubrecht et al., 2013; Tapsell et al., 2002; Turvey, 2007; Vescovi et al., 2005; Wolf et al., 2014). Such HVIs may simply standardize each indicator, for example by z-score, then sum the z-scores to create an overlay of vulnerability. This final sum is determined to be the HVI score. This method is also known as an "unweighted additive overlay" (Manangan et al., 2015).

2.6.5.2 Weighted

Other researchers choose to use weighting schemes to reflect relative significance of the various indicators. Often this is derived from "expert judgment" such as a panel of experts to place weighting on the indicators to differentiate those with higher influence on vulnerability from those with low influence (Brooks et al., 2005; Ozceylan et al., 2012). Rinner et al. (2010) uses ordered weighted averaging (OWA), or a family of multi-criteria operators allowing the decision-maker to place their own weights of importance to specify attitude towards decision risk from risk-averse ("pessimistic") to risk-taking ("optimistic") (Ahn et al., 2012; Rinner et al., 2010). Rinner et al. (2010) uses OWA, or a family of multi-criteria operators allowing the decision-maker to place their own weights of importance to specify attitude towards decision risk from risk-averse ("pessimistic") to risk-taking ("optimistic") (Ahn et al., 2012; Rinner et al., 2010). Loughnan et al. (2012) and Zhu et al. (2014) used 9 experts from public health, meteorology, social sciences to determine heat-related indicators to assist in the construction of their HVI. This was a subjective hierarchy process of ranked indicators, which were then placed into a PCA, described further below.

2.6.5.3 Principal Components Analysis (PCA)

One common method of aggregation is to use PCA for dimension reduction and to reduce potential for autocorrelation between related variables (Ried et al., 2009; Zhu et al., 2014). PCA is a variable-reduction technique that can take many potentially collinear indicators and reduce them to mutually independent factors. Each factor may be characterized depending on the indicators with which they are most strongly associated.

For example, one factor may be associated with impervious surfaces associated with a greater urban heat island intensity, thereby characterizing the factor as "exposure." Each geographic unit of analysis, such as a census tract, is assigned a score for each factor, often based on its z-score, and each factor score is combined to create the composite HVI score. This score is then mapped, displaying relative vulnerability across a defined geographic domain.

Table 1 - HVI scores assigned to each factor in the PCA using the Reid et al. (2009) methodology.

Range of Z-Score	Assigned HVI Component Score
-2 or lower	1
-2 to -1	2
-1 to 0	3
0 to 1	4
1 to 2	5
2 or higher	6

The PCA method, and in particular the Reid et al. (2009) methodology, have been commonly reproduced and adapted in the literature. Reid et al. (2009) analyzed the relative vulnerability of major metropolitan areas in the United States at the census tract level using commonly accessible census data for demographic and socioeconomic indicators, and remote sensing imagery of land cover data to estimate environmental exposure indicators. KC et al. (2015) used a modified form of the Reid et al. (2009) model to map overall climate vulnerability for the entire state of Georgia by county. See figure 6 below for examples of

such HVI maps. Wilson et al. (2017) also used a modified Reid et al. (2009) index to create the Chicago Heat Vulnerability Tool.

(a) 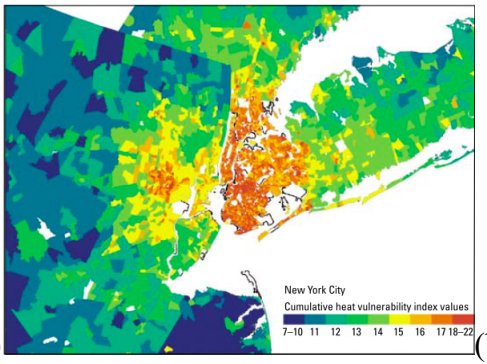

(b) 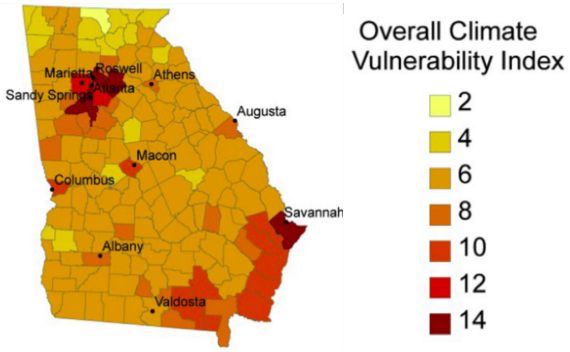

Figure 10 - Examples of HVI maps for (a) New York City by census tract (Reid et al., 2009) and (b) Georgia by county (KC et al., 2015).

2.6.6 Evaluation

While HVIs can provide relative priority for intervention, they may not represent actual vulnerability in the real world. As a result, researchers are increasingly seeking to evaluate their HVIs using observed heat-related morbidity and mortality observations, similar to the Wolf et al. (2015) "bottom-up" typology. Several studies have found positive correlation between HVI score and excess mortality obtained via the direct attribution method (Bao et al., 2015; Maier et al., 2014; Wolf et al., 2015). Maier et al. (2014) validated the use of HVI mapping techniques by correlating HVI score with direct attribution heat-related mortality data. They found a 13.4% increase in mortality for every increase of 1 HVI score on "oppressive" days with extreme heat (defined by the 95th percentile maximum Apparent Temperature), and a 12.4% increase in mortality for each unit increase in HVI score even on non-oppressive days. Furthermore, the authors found no statistically significant relationship between HVI score and mortality on oppressive days

for counties with low HVI scores, but the relationship became significant at higher HVI values. This finding lends support to the utility of HVI mapping techniques in identifying areas with greater vulnerability. Strategies like this may be a useful for issuing heat warnings to the most vulnerable populations to ensure they take proper measures to reduce their exposure. However, evaluation studies such as these are often at a coarse scale, such as the county or MSA level, and thus do not reflect the intra-urban scale disparities in exposure due to the urban heat island. While many HVI studies focused on the census tract or block group scale, it is difficult to validate them on such a fine scale without spatially comprehensive heat mortality data.

2.7 Knowledge Gaps in the Literature

Four primary gaps emerge as a result of this literature search. These gaps regard sensitivity analysis, evaluation methodology, HVI utility, and statistical attribution model accessibility. These categories are described below:

2.7.1 Methodological Sensitivity Analysis

Studies on HVIs use a variety of construction methods in the literature, and the vast majority of studies use only one method from the literature or design their own, and present those findings (Bao et al., 2015). As a result, there is no single agreed upon method for HVI construction, and the choices for HVI design can be highly subjective. Furthermore, emerging research has shown that HVI outcomes can be heavily dependent on the indicators selected. Conlon et al. (n.d.) studied sensitivity to indicator inputs in Detroit using a common set of socioeconomic and demographic indicators but varying the heat exposure indicator. Each HVI used the same construction method based on the PCA-

derived Reid et al. (2009) index. This constituted a set of theoretically acceptable HVI results, yet this one change alone resulted in high variation in the HVI score outcome. Figure 11 below shows the frequency of each census tract in Detroit to be in the top quartile of heat vulnerability as determined by the HVI score across the four HVIs constructed for the study. The results show that agreement in relative vulnerability across all four HVIs is rare, and that some tracts display high vulnerability in only one or two HVIs.

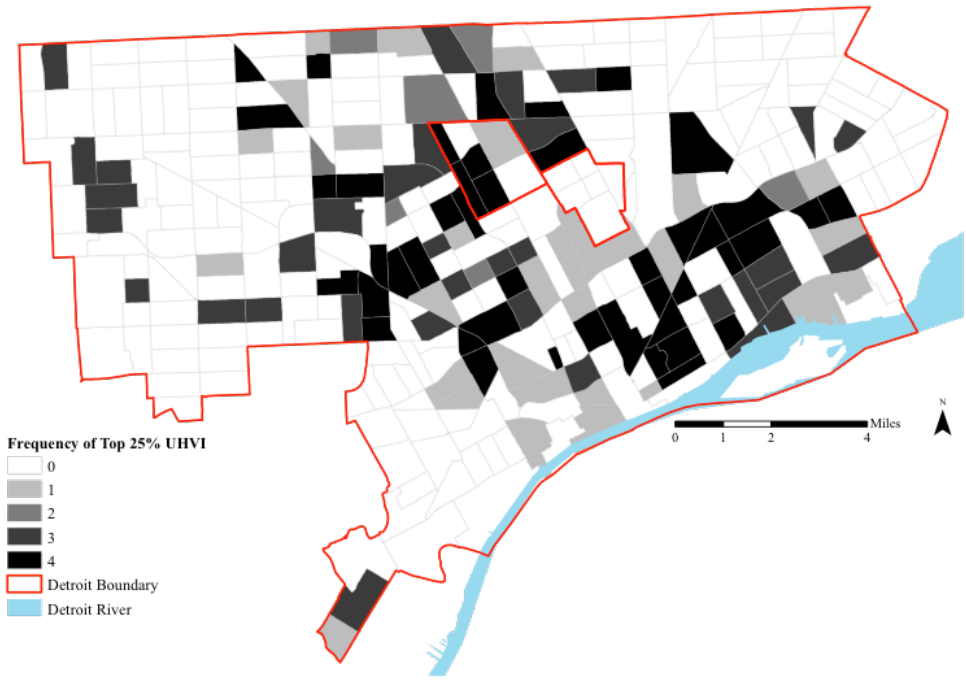

Figure 11 - Map of number of times each census tract fell into the top quartile of an HVI calculation using 5 different sets of input variables (Conlon et al. (in review, Environmental Health Perspectives)).

To date, very little research compares indicator sensitivity to HVI outcome and even less explores methodological sensitivity despite calls for such research (Bao et al., 2015). While some sensitivity analysis research has been conducted on social vulnerability indices (Tate, 2012; Tate, 2013), no similar HVI research has been conducted

and validated using a common heat mortality dataset. This presents a major gap in HVI research, as Conlon et al. (n.d.) has demonstrated that small changes in HVI construction can lead to measurable differences in the results. If planners are to use HVIs to guide policy, it is important to understand the impacts of these HVI design decisions. Therefore, methodological sensitivity analysis would help address this major gap in the literature.

2.7.2 Evaluation Research

Direct attribution and evaluation studies are difficult to conduct in heat mortality research, as it is difficult to attribute deaths directly to heat. Extreme heat exposure exacerbates pre-existing conditions that in turn are listed as the cause of death (Davis et al., 2003; Kovats et al., 2008; Stone, 2012). In fact, only the Maricopa County Department of Public Health has a surveillance system specifically designed to identify deaths related to or caused by heat and weather (Harlan et al., 2013). This type of surveillance is very uncommon in practice.

Due to these difficulties, HVI evaluation studies use a wide variety of techniques to specifically attribute heat to excess mortality. These deaths are also based on assumptions such as observing deaths during a heat wave compared to usual death rates for the same time of year, using 911 calls during a heat event, or analyzing only deaths due to certain causes like cardiovascular or renal failure (Bao et al., 2015; USGCRP, 2016). They are themselves estimates of deaths that may be attributable to heat, rather than confirmed heat-related deaths. Maier et al. (2014) compared HVI score to this type of direct attribution data across the state of Georgia, but not at the intra-urban scale. However, a spatially comprehensive mortality estimate could be derived from the spatial SAM used in studies

like Stone et al. (2014) or the heat management plans from Louisville and Dallas. **To date, no HVI study has compared an HVI score to an intra-urban spatially comprehensive statistical attribution method.**

2.7.3 HVI Utility

Despite the large body of HVI literature over the past decade, HVIs have not been shown to greatly impact policy (Bao et al., 2015; Wolf et al., 2015). To quote Wolf et al. (2015): "Heat vulnerability mapping has been used in an attempt to communicate policy recommendations, raise awareness and induce institutional networking and learning, but has not yet had a substantive influence on policymaking or preventive action." One possible reason could be that the statistical methods employed to create the aggregate HVI score, such as PCA, may be obscuring the precise reasons why one neighborhood is considered more vulnerable than others. For an effective and efficient intervention, it is useful for the planner to understand both where and why a particular neighborhood is vulnerable. With some HVIs using up to 25 individual indicators of heat vulnerability, it can be easy to lose the message as to exactly which vulnerabilities to address with the limited funds available. Furthermore, Bao et al. (2015) recommends that future HVI research attempt to simplify their models through specific indicator selection for easier interpretation and more targeted responses. **To date, little HVI evaluation research has analyzed the significance of individual indicators against observed heat-related mortality.** A deeper analysis of the relative significance of these indicators could help planners construct HVIs with higher reliability and can help them design more efficient response strategies targeting specific vulnerabilities.

2.7.4 Statistical Attribution Model Accessibility

One major strength of HVI studies is that they focus primarily on publicly accessible data sources, such as the US census or remotely sensed datasets. For this reason, HVIs can be generally considered accessible tools to the average urban planner or public health practitioner. **However, no similar attempt has been made to develop a spatial SAM using publicly accessible datasets.** Instead, this method has relied on complex and technically demanding models like WRF to generate a spatially comprehensive air temperature dataset to drive the heat mortality model. If the WRF component could be replaced with publicly accessible air temperature datasets, then the spatial statistical attribution method would become much more readily available to planners and public health practitioners.

2.8 Statement of Proposition to be Tested

The primary intent of this research is to address the knowledge gaps detailed in the section above by understanding the spatial relationship between heat vulnerability as determined by HVI scoring methods and heat mortality as derived from a spatial statistical attribution model through mapping. I address the methodological sensitivity gap directly by varying the complexity of HVI construction methodology to examine the influence on score outcomes. Using the spatial statistical attribution model as spatially comprehensive mortality estimates will address the evaluation gap detailed above. Using the mortality estimates to examine individual indicator significance may help address the HVI utility gap by identifying which specific vulnerabilities to target via intervention. Finally, I address the statistical attribution model accessibility gap by exploring the impacts of

replacing WRF-derived air temperatures with publicly available datasets. The conceptual framework in Figure 12 below summarizes the relationships to be tested and where each research question is situated in the framework. This framework is discussed in greater detail in Chapter 3.

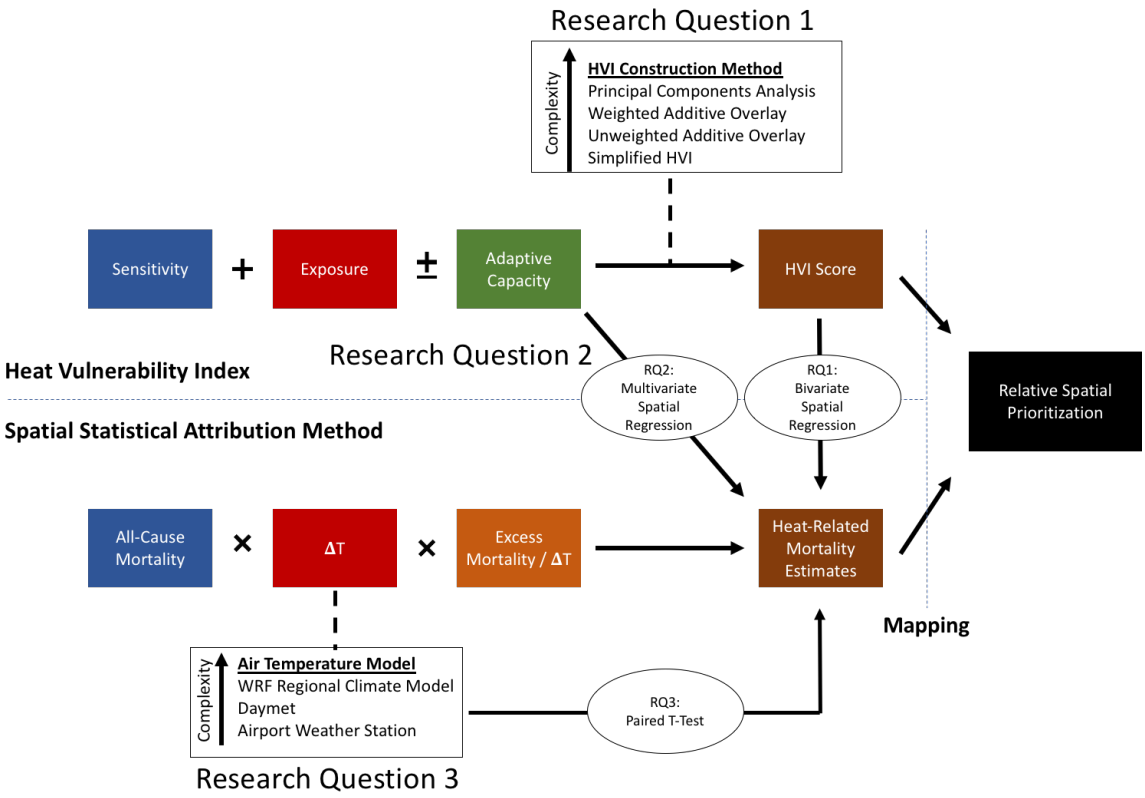

Figure 12 - Conceptual framework for this study design.

CHAPTER 3. DESCRIPTION OF THE STUDY

3.1 Introduction

With the primary gaps in the literature identified, this chapter details how this study addresses these gaps, and provides the structure for the following chapters. This section provides an overview of the selected HVI indicators and construction methods and Spatial SAM procedures, including the data acquisition and processing protocols. This section also contains an introduction to the study sample and statistical methods employed.

At the end of this chapter, I introduce my central research questions and hypotheses, and briefly summarize the methods used to answer them. Each research question directly addresses one or more gaps in the literature, with the aim of improving model accessibility for planning and public health practitioners.

3.2 Selected HVI Indicators and Methods

In this study, I compare four established a-priori heat vulnerability methods of varying complexity to heat-related mortality estimates derived from statistical attribution models. The primary research design varies HVI construction methods to analyze sensitivity to construction method, rather than variable input sensitivity already analyzed by Conlon et al. (*n.d.*). Each HVI contains the same set of indicators across each method, and across each study city. Given the popularity of the Reid et al. (2009) index in the literature and the findings of indicator significance from Bao et al. (2015), I used a slightly modified version of the indicator set used in Reid et al. (2009), replacing Impervious

Surface with LST due to its frequency of use in HVI studies. Table 2 below summarizes these indicators.

Table 2 - Indicators of heat vulnerability selected for this study.

Sensitivity	Exposure	Adaptive Capacity
Diabetes Prevalence	Land Surface Temperature	Living Below Poverty Line
Living Alone		Less than High School Education
Over Age 65		No AC Access
Over Age 65 and Living Alone		No Full AC Access
NonWhite		

The HVI aggregation methods to be compared are as follows:

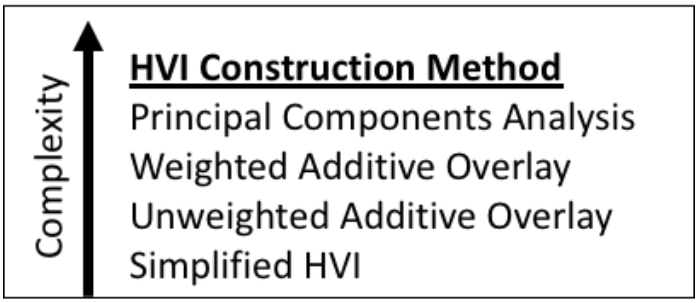

Figure 13 - HVI construction methods ordered by complexity.

3.2.1 Simplified HVI

In this construction method, I created an unweighted additive overlay out of only two indicators: over age 65 to represent sensitivity, and Land Surface Temperature (LST) to represent exposure. This simplified model is similar to one recommended by the Centers

for Disease Control and Prevention (Manangan et al., 2015) and a recommendation from Bao et al. (2015) to strive for simpler HVI methods. This model differs from the CDC model in that it includes only indicators that are a subset of the larger Reid et al. (2009) HVI indicator set. If this HVI is shown to correlate strongly with the spatial statistical attribution method, then more complex HVI methods may not be necessary for relative spatial prioritization.

3.2.2 Unweighted Additive Overlay

This method uses all of the indicators from the Reid et al. (2009) index, but without PCA as the aggregation method. Each indicator is converted to a z-score, scored using the Reid et al. (2009) scheme shown in Table 1, then summed to create the aggregate HVI score for each study city.

3.2.3 Weighted Additive Overlay

This method is a variation on the above additive overlay, but with weights assigned to each indicator in accordance with recommendations from the Centers for Disease Control and Prevention (Manangan et al., 2015) before being summed to a composite HVI score. The Manangan et al. (2015) study recommended a domain weighting approach in which the factors representing each of the three vulnerability components (sensitivity, exposure, and adaptive capacity) were weighted equally. In this study design, that means each of the indicators would be weighted by 1/n, where n is the number of indicators within each component.

3.2.4 Principal Components Analysis

This is the most common, yet most complex, method for HVI construction, with which the Reid et al. (2009) study was originally conducted. This procedure combines the set of indicators first using Principal Components Analysis (PCA) to create statistically independent components, then each component is scored using the scoring scheme detailed in Reid et al. (2009) and summed to create the final PCA HVI score.

3.3 Study Sample

This study primarily relies on data from an NSF funded project entitled "Hazards SEES: Enhancing Emergency Preparedness for Critical Infrastructure Failure During Extreme Heat Events" (NSF award number: 1520803), referred to as 3HEAT in this study. Principal investigators Brian Stone, Matei Georgescu, and Marie O'Neill head 3Heat with each leading research teams at Georgia Institute of Technology, Arizona State University, and University of Michigan, respectively. This study compares the above HVI methods in each of the three 3HEAT study cities: Atlanta, GA, Detroit, MI, and Phoenix, AZ.

Table 3 - Climate and population comparison between the three study cities.

	Atlanta, GA	**Detroit, MI**	**Phoenix, AZ**
Climate Region	Southeast	Upper Midwest	Southwest
Climate Type	Humid Subtropical	Humid Continental	Subtropical Desert
Mean Summer High Temperature (°F)	87.9	81.4	104.8
Population (2010)	420,003	713,777	1,445,632

These cities represent three very different climate regions as defined by NOAA (Karl et al., 1984). Detroit lies in the Upper Midwest near the border of the Ohio Valley climate region, while Atlanta and Phoenix are in the Southeast and Southwest, respectively.

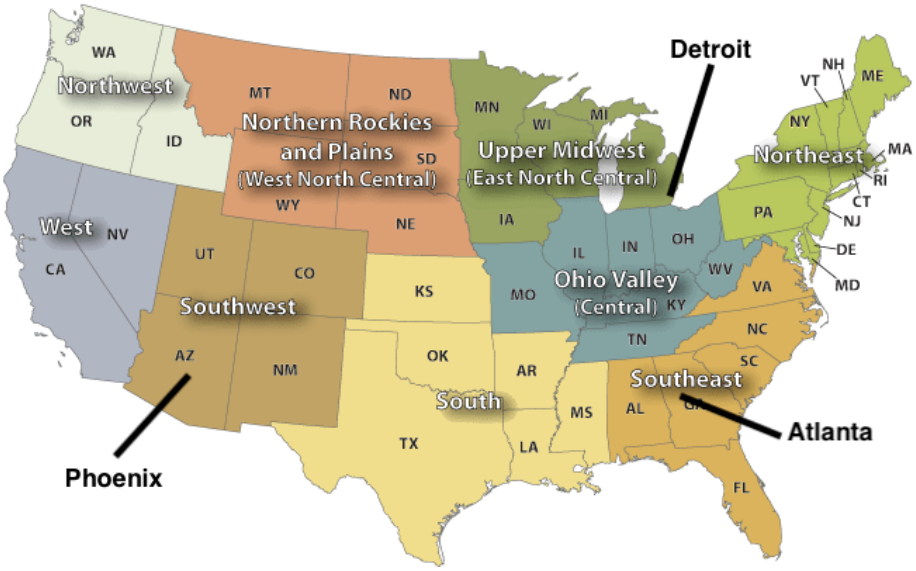

Figure 14 - Regional distribution of study cities.

Each city's population also has a unique relationship with heat, as the residents develop personal and physiological acclimatization to their local climate. Figure 15 below shows the exposure-response curves for heat mortality for the three study cities from Gasparrini et al. (2015). Exploring the relationships between HVI models and spatial statistical attribution models in each city enhances the external validity of the findings, as some relationships may hold in one type of city, but not in another.

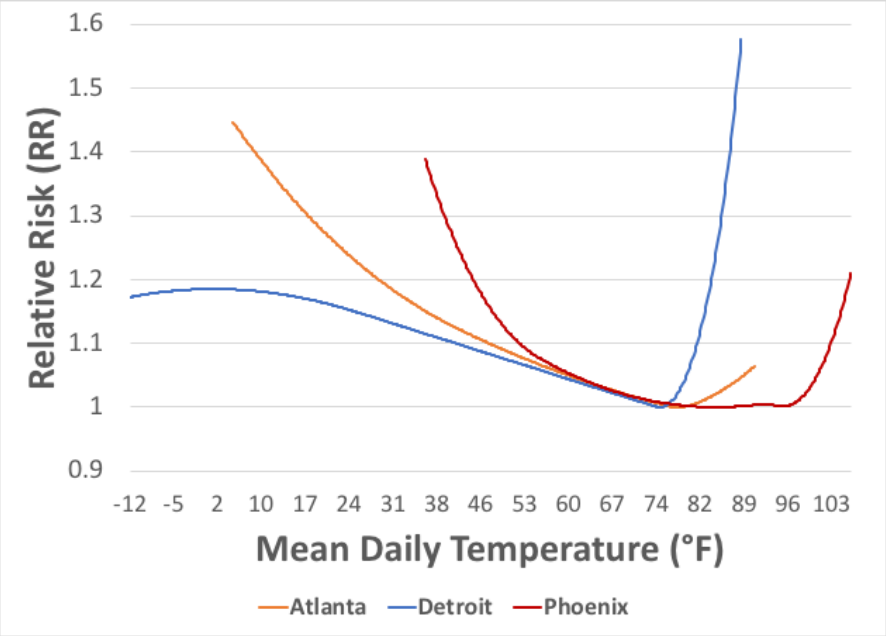

Figure 15 - Heat mortality relative risk curves for Atlanta, Detroit, and Phoenix (Gasparrini, 2015).

3.4 Data

3.4.1 HVI Construction

All HVI data comes from publicly available data sources. Social vulnerability indicator data was collected from the American Community Survey 5-year estimates at the tract level from the Social Explorer website. Each variable is normalized by tract population to be used as a proportion of the tract population ranging from 0 to 1, with larger numbers implying higher vulnerability. All tracts with zero population are removed from the analysis.

The primary pre-existing health variable, an indicator of population sensitivity, is diabetes prevalence. This data was obtained from the CDC Chronic Disease and Health Promotion Open Data portal. This data is available at the census tract scale through the

CDC 500 Cities Project. The primary exposure variable is Land Surface Temperature (LST), obtained using remotely sensed imagery from NASA's MODIS satellites. This dataset provides 8-day average LST datasets that are clear of all obstructions such as clouds. Average LST is determined for each tract in ArcGIS using zonal statistics and converted to a z-score to illustrate relative heat exposure rather than absolute surface temperature.

Additionally, lack of access to air conditioning (AC) is an important adaptive capacity factor in this analysis. AC data is not available at the census tract level, but it can be modeled using MSA-level data from the American Housing Survey. By applying the AC prevalence by housing type at the MSA level to each matching housing type quantified in the American Community Survey at the census tract level, I estimate the AC prevalence at the census tract level for use in this HVI analysis.

3.4.2 Statistically Attributed Mortality Estimates

The most important and defining factor of the spatial SAM is the high-resolution temperature datasets required to run the analysis. In this study, I use three WRF-derived air temperature datasets representing historic heat waves for each study city. The dates of each heat wave are summarized in Table 4 below. In this study, we define heat waves as periods where the 97.5th percentile daily average temperature is exceeded on five or more consecutive days. The period with the highest mean temperature was selected for WRF modeling in this study.

Table 4 - WRF-modeled historic heatwaves for Phoenix, Atlanta, and Detroit.

Atlanta	Detroit	Phoenix
1995-08-05	1994-06-08	2006-07-11
1995-08-06	1994-06-09	2006-07-12
1995-08-07	1994-06-10	2006-07-13
1995-08-08	1994-06-11	2006-07-14
1995-08-09	1994-06-12	2006-07-15
1995-08-10	1994-06-13	2006-07-16
1995-08-11	1994-06-14	2006-07-17
1995-08-12	1994-06-15	2006-07-18
1995-08-13	1994-06-16	2006-07-19
1995-08-14	1994-06-17	2006-07-20
1995-08-15	1994-06-18	2006-07-21
1995-08-16	1994-06-19	2006-07-22
1995-08-17	1994-06-20	2006-07-23
1995-08-18	1994-06-21	2006-07-24
1995-08-19	1994-06-22	2006-07-25
1995-08-20	1994-06-23	2006-07-26
1995-08-21	1994-06-24	2006-07-27
1995-08-22	1994-06-25	2006-07-28
1995-08-23	1994-06-26	2006-07-29
1995-08-24		2006-07-30
1995-08-25		2006-07-31
		2006-08-01
Pre-Heatwave	**Heatwave**	**Post-Heatwave**

The WRF models were run using nested domains at 16-km, 4-km, and 1-km resolution for each study city. Figure 16 below shows the 1-km WRF grid overlaid with each study city. The WRF simulations generate surface and air temperature, humidity, wind speed and direction, solar and terrestrial longwave radiation, cloud cover, precipitation, and air pressure, though this analysis uses only surface-level air temperature for the purposes of this research. The 1-km WRF grid domain far exceeds the city limits, but this analysis utilizes only the grid cells within a 2-km proximity to each city's political boundaries.

The WRF model results were evaluated using proximate airport weather station data during each city's target period, including sites near the urban core and the urban fringe. In Phoenix, the root mean square error (RMSE) for the urban and fringe sites were 4.7°F and 4.9°F respectively, with greater amplitude in the model than observed (warmer days and cooler nights). Detroit model evaluation used four weather stations, with RMSE ranging between 4.1°F and 4.7°F, and Atlanta used two stations with RMSE of 4.0°F at both sites. This evaluation shows that while WRF is a state of the art climate model, it is still a model with error. Despite this error, WRF is representative of the best spatially comprehensive air temperature datasets available for the urban environment.

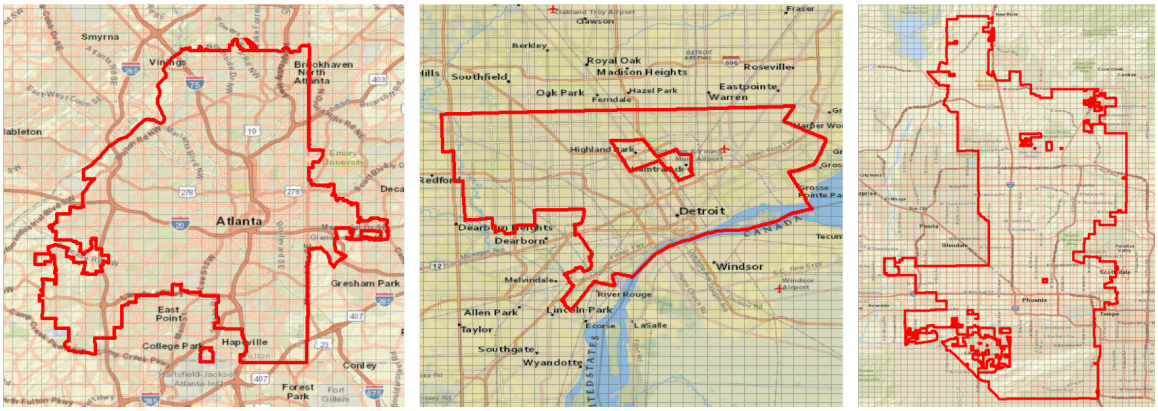

Figure 16 - WRF grids relative to city limits for Atlanta (left), Detroit (center), and Phoenix (right).

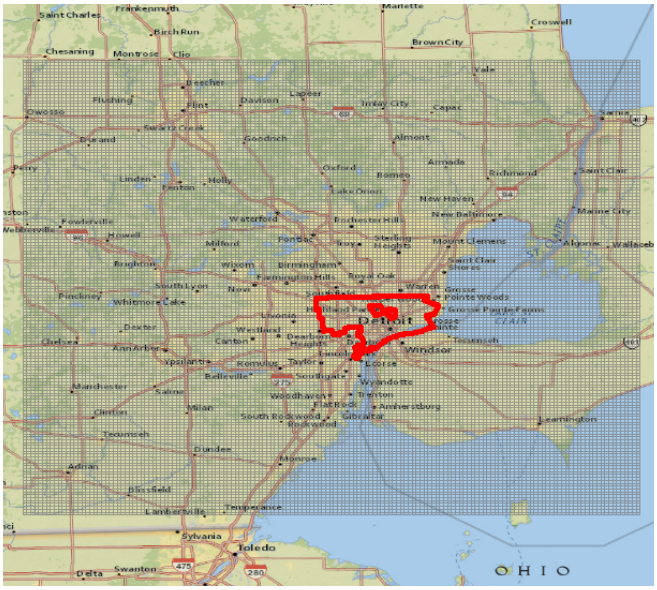

Figure 17 - Full extent of Detroit WRF grid relative to city limit.

Additional data to calculate the statistically attributed heat mortality estimates were collected from two primary sources. The baseline mortality component was downloaded from CDC WONDER, and consists of average daily all-cause mortality for 5 years centered on the year 2010. These baseline mortality rates were binned by age (every 10 years after age 5) and sex to account for different sensitivities among different cohorts. The unique exposure-response functions for each city are from the Gasparrini et al. (2015) study, a published distributed lag non-linear model relating observed temperature and mortality rates from all causes over time.

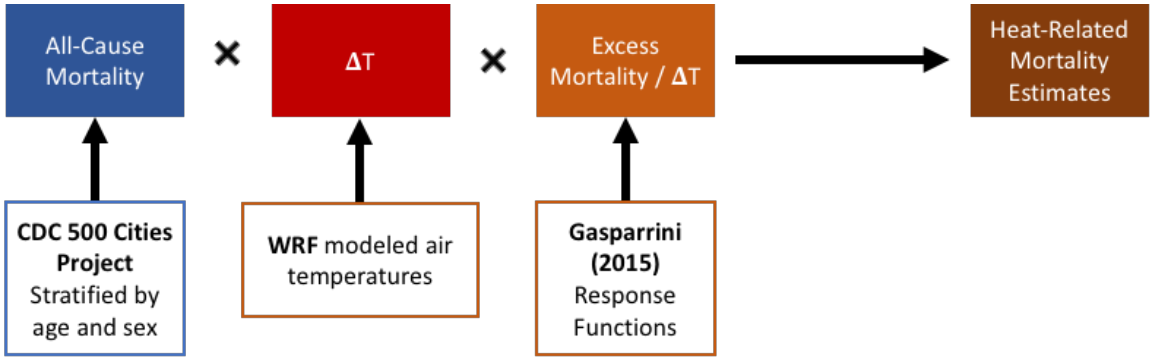

Figure 18 - Summary of spatial SAM procedure.

The mortality estimates were calculated via an R script, which first adjusts the baseline mortality by multiplying the baseline daily mortality rate for each age and sex cohort by a population relative risk ratio at each mean daily temperature per WRF grid cell, provided by Gasparrini et al. (2015). Then this modified daily mortality rate is multiplied by the count of people in each cohort per grid cell, to estimate total deaths during the heat wave period. Only deaths that occur at warm temperatures are counted as deaths attributable to heat (see Figure 20). This threshold is determined to be the inflection point between increased relative risk ratios due to colder temperatures and increased relative risk ratios due to warm temperatures. See Table 22 for the inflection points in each city. All WRF grid-level mortality estimates were re-aggregated to census tract totals for comparison with the tract-level HVI scores. In order to avoid confounding results due to inflated infant mortality, all populations below the age of 5 have been set to zero for this analysis.

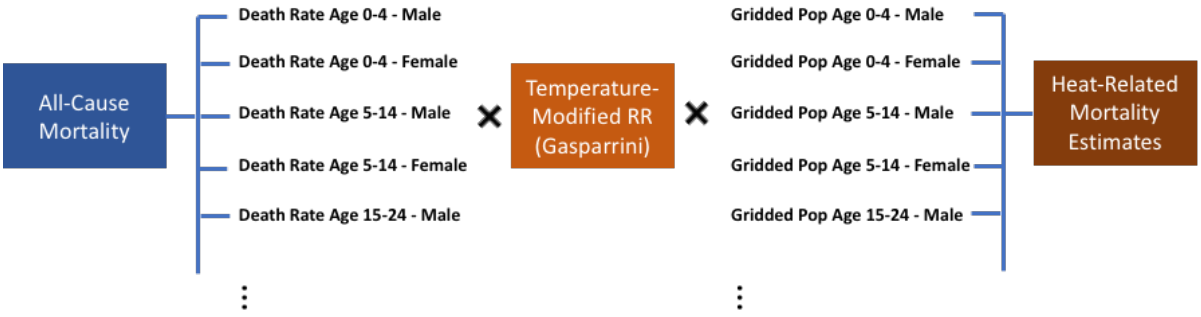

Figure 19 - Summary of response function applied to age and sex cohorts.

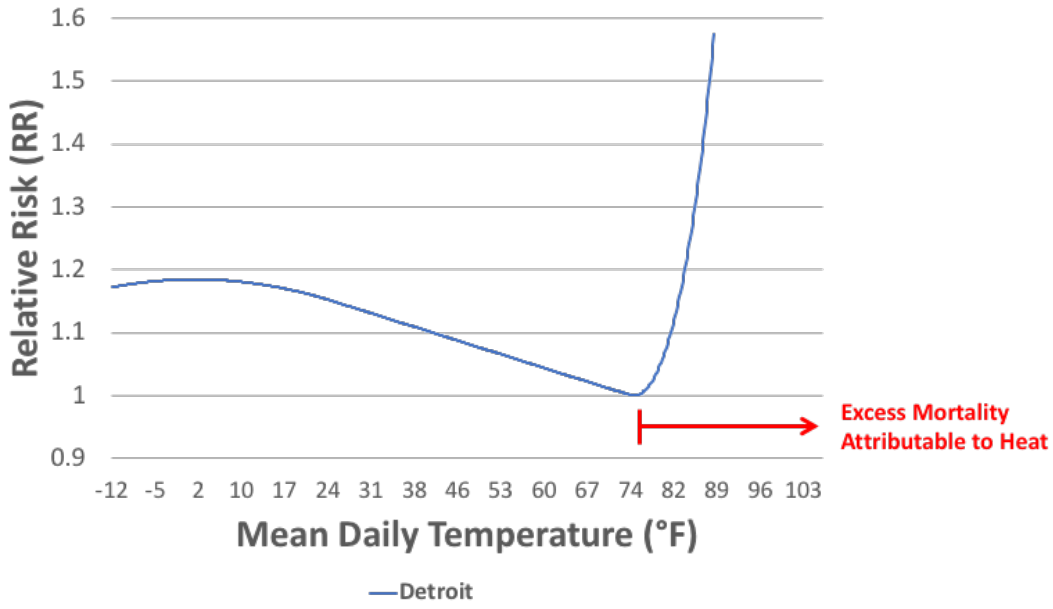

Figure 20 - Only warm-temperature modeled mortality are considered deaths attributable to heat.

The Gasparrini et al. (2015) study monitored deaths in 384 locations across the world between 1985 and 2012 and concurrent daily average temperature. A standard time-series Poisson model was fit for each city between temperature and mortality, controlling for trends and day of the week. The temperature-mortality associations unique to each city were estimated using a distributed lag non-linear model with a 21-day lag, then pooled the data in a multivariate metaregression including country indicators, temperature average,

and temperature range. The result used in this study is a set of city-specific tables of relative risk (RR) by temperature (T) for Atlanta, Detroit, and Phoenix.

While the Gasparrini et al. (2015) is a valuable resource for the spatial SAM analysis, it does have limitations. While the study uses daily average temperature, previous research has found a stronger association between minimum temperature and mortality (Robinson, 2001). Future research should explore creating additional exposure-response functions using minimum temperature. Additionally, the Gasparrini et al. (2015) response functions have a wide range of uncertainty at higher temperatures for each city. In following with the procedure of previous studies (Stone et al., 2019; Urban Climate Lab, 2017), this research uses the mean RR value at each temperature T. Furthermore, the focus of this study is on the relative spatial prioritization of heat-related mortality and heat vulnerability, rather than the uncertainty of the spatial SAM procedure itself. Future research should include this range of uncertainty for a complete picture of the spatial SAM outcomes.

The spatial SAM procedure can be mathematically represented at the grid cell level using Equation 1 below. For each grid cell, the total mortality estimate (ME) is the sum across all age and sex cohorts (i) for all cohorts (c) of the product of each cohort's baseline daily average mortality (m_i), the grid cell temperature-modified relative risk (RR_{Tj}) on day j, and the grid cell's population for cohort i, summed over each day of the modeled period (j) up to the total modeled days (d). RR_T is determined by looking up the corresponding mean RR value at temperature T for day j in a table from Gasparrini et al. (2015). Across all temperature datasets, there was no grid cell with a daily average

temperature that exceeded the bounds of the Gasparrini et al. (2015) dataset, so all temperatures and associated RR were properly accounted for in this procedure.

$$ME = \sum_{j=1}^{d} \sum_{i=1}^{c} (m_i \times RR_{Tj} \times P_i) \quad \text{(Equation 1)}$$

3.5 Model comparison

Mortality estimates and HVI results are compared using two methods. Bivariate spatial regression between mortality estimates and composite HVI scores are used to analyze the correlation between the two models across the tracts. Through a second approach, multiple spatial regression between mortality estimates as the dependent variable and each HVI indicator prior to the PCA analysis is used to show which indicators are statistically significant predictors of heat-related mortality as derived by the exposure-response function. In the multivariate regression, the indicator "over age 65 and living alone" was removed for potential threats of multicollinearity with "over age 65" and "living alone." Similarly, "no AC" was removed to reduce threats of multicollinearity with "no full AC." Spatial regressions were run in the free software package GeoDa with a first-order queen contiguity spatial lag model.

3.6 Central Research Questions

Research Question 1: *To what extent can established HVI methods predict total heat-related mortality estimates as derived by the statistical attribution method?*

This analysis was conducted using a bivariate spatial regression between HVI scores and total mortality estimates at the census tract level for each study city. To address methodological sensitivity, I used a set of HVI construction methods of varying HVI complexity detailed above. The HVI score for each method is the independent variable, while the WRF-derived total mortality estimates serves as the dependent variable and remains constant across each regression. The extent of predictive power is captured in the R-Square for each regression.

Hypothesis 1: Varying HVI method will influence predictive power, and more complex HVI methods will reduce predictive power by including irrelevant information.

Research Question 1a: *Do different HVI construction methods within the same city produce statistically independent HVI scores?*

To further analyze the impacts of methodological sensitivity in HVI construction, I directly compare each HVI method to the rest in the set using a paired t-test on each score per census tract. This analysis does not utilize the heat mortality estimates. A statistically significant t-score determines statistical independence between the HVI models within each study city.

Hypothesis 1a: Varying HVI construction method will result in significantly different HVI score distributions within each city.

Research Question 1b: *To what extent can HVI scores predict the top quartile of vulnerability as determined by the statistical attribution method?*

From a planning standpoint, the quantification of heat related deaths and HVI score may be less important than the relative spatial prioritization alone. Similar to the Conlon et al. (n.d.) study in Detroit, I examine the spatial distribution of heat-related mortality as a binary top quartile designation, rather than as a discrete count of deaths. This top quartile highlights areas for intervention without quantifying the exact count and gives planners an idea of where to target heat mitigation efforts.

This research question is analyzed using bivariate logistic regression between the HVI score as the independent variable, and a binary variable of "highly vulnerable" areas, with 1 indicating the top quartile total estimated heat mortality, and 0 indicating all else. The results of this regression captures the likelihood of a given census tract being designated "highly vulnerable" based on the HVI score as a predictor variable. A measure of Tjur's R-Square (Tjur, 2009) measures the strength of the correlation for each model.

Hypothesis 1b: The top quartile method will produce a better fit than a spatial regression using total mortality counts.

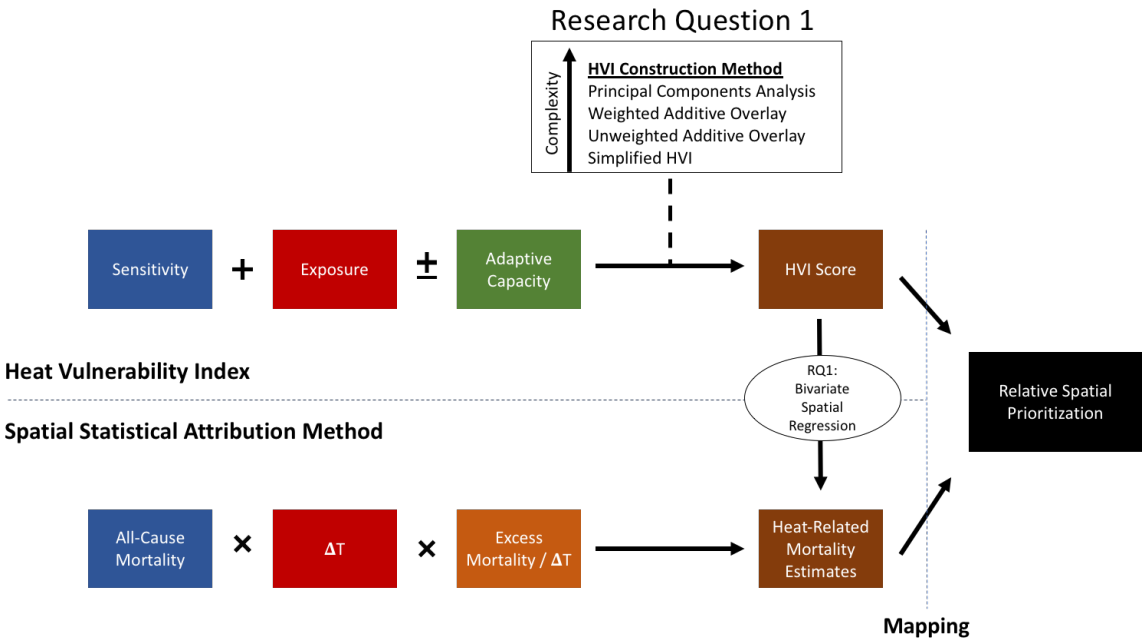

Figure 21 - Conceptual framework for research question 1.

Research Question 2: *Which heat vulnerability indicators are significant predictors of heat-related mortality as derived by the statistical attribution method?*

In determining heat vulnerability, it may be that not all indicators are significant predictors of heat-related mortality. In this analysis, I use the individual indicators as independent variables in a spatial regression rather than combine them into a single HVI score. The total mortality estimates are used as a dependent variable, as with research question 1. Any indicators that are significant at the $\alpha = 0.1$ level in the regression is considered significant predictors of heat-related mortality. Indicators at risk of multicollinearity have been removed from the regression.

Hypothesis 2: Very few vulnerability indicators will significantly predict heat-related mortality, and the results will differ between cities due to their unique sensitivity to heat.

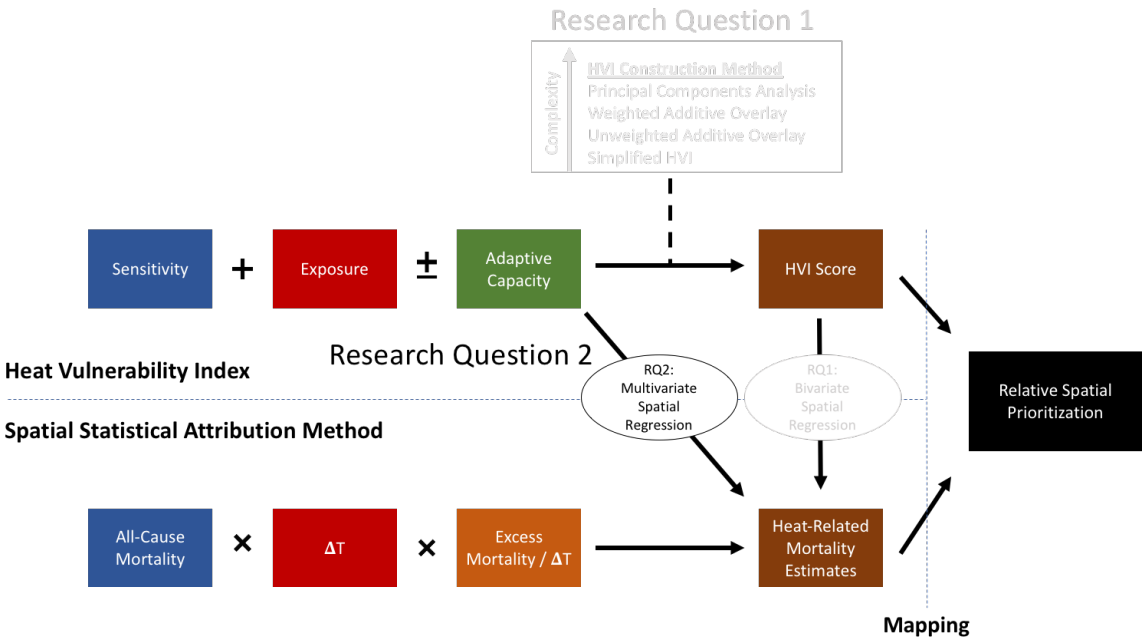

Figure 22 - Conceptual framework for research question 2.

Research Question 3: *To what extent can the WRF-driven statistical attribution method be replicated using publicly available data sources?*

As stated in the knowledge gaps section, studies using the spatial statistical attribution method have relied on technically and computationally demanding models like WRF. This research question seeks to examine the impacts of replacing the WRF-derived air temperature component with publicly available datasets. Similar to Research Question 1, the complexity of these datasets is also varied.

At the simplest level, I replace WRF-derived air temperatures with a single weather station located at the airport. Airport weather station data is often the most long-term, reliable, and complete temperature dataset available, and is therefore commonly used to represent an entire city (Habeeb et al., 2014; Huang et al., 2011; Kuras et al., 2012; Mallick et al., 2012; Mohsin et al., 2012; Oke, 1982; Stone, 2007). This data was collected for the

same heat wave period as WRF but is applied evenly to each WRF grid cell for the mortality calculations. Slightly more complex, I also use the Daymet modeled air temperature dataset from Oak Ridge National Laboratory. This dataset represents modeled air temperatures comprehensively across the country at a 1-km resolution, similar to the WRF model resolution for this study. This is a much simpler air temperature model, so it is less likely to capture the type of urban heat island dynamics as WRF but may be a more accessible substitute if it can produce similar results in the spatial statistical attribution process.

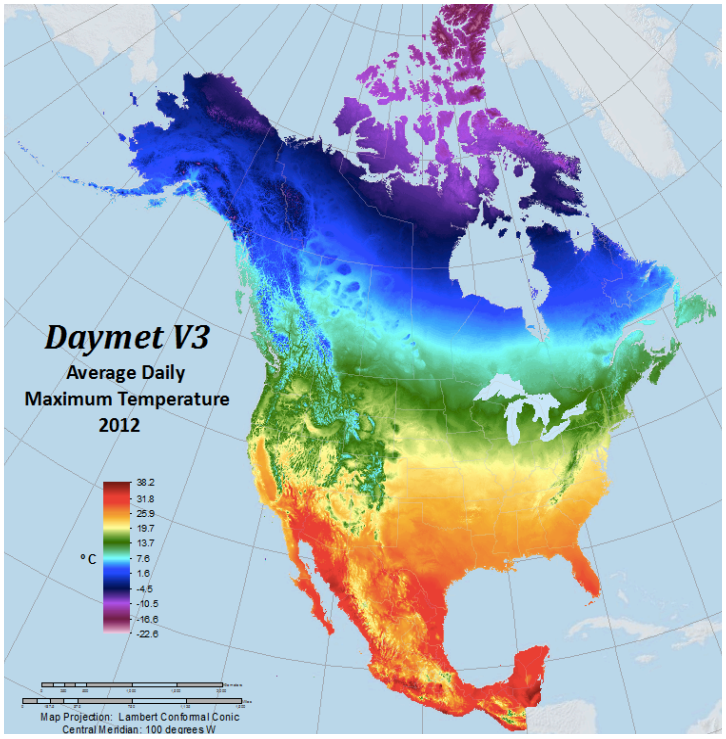

Figure 23 - Daymet modeled air temperatures for North America (daac.ornl.gov).

Similar to research question 1a, I use a paired t-test to test for statistical independence between the WRF-derived mortality estimates and the public temperature model mortality estimates at the tract level. Statistically significant t-scores indicate

statistical independence between the model results, while a non-significant result suggests that the public model provides an adequate substitute to the WRF model.

Hypothesis 3: Publicly accessible temperature datasets will produce similar mortality estimates, depending on the spatial resolution of the dataset.

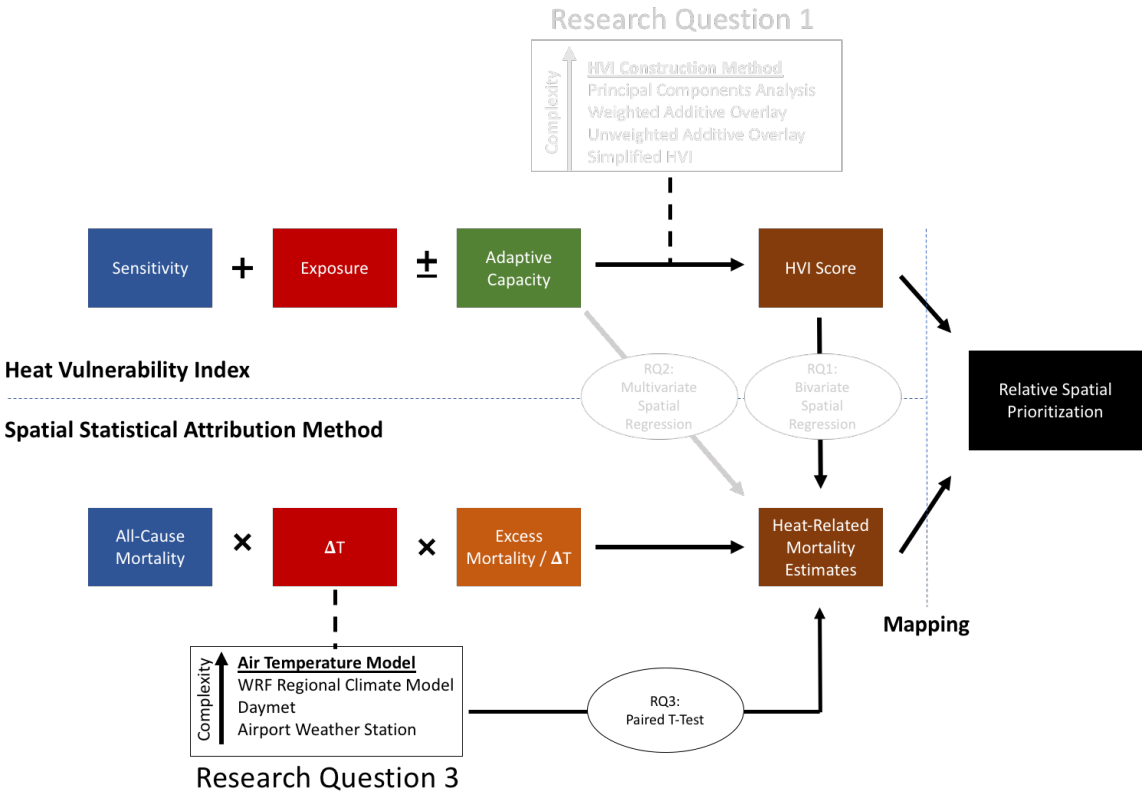

Figure 24 - Conceptual framework for research question 3.

3.7 Method of Analysis

3.7.1 HVI Construction

HVI construction was conducted via scripting in the statistics package SPSS. Scripting ensures that all processes are conducted quickly and consistently across all three cities and can be reproduced with minimal human error. For the PCA HVI construction method, PCA was employed to reduce the total number of variables to four statistically independent factors. The PCA uses varimax rotation to ensure orthogonality between the factors. This transformation ensures that the factors are statistically independent of one another and maximizes the variance of the factor loadings on each variable. This process makes it easier to identify each variable with a single factor, thereby enhancing the ability to classify each factor as a component of vulnerability (i.e. sensitivity, exposure, or adaptive capacity) using its associated variables. All PCA processing was conducted using IBM SPSS 24. Factor scores were created for each tract and converted to z-scores to indicate vulnerability relative to other tracts. Each tract is assigned an HVI score based on the z-score for each factor according to the Reid et al. (2009) scheme in Table 1. Since an increase in each variable implies an increase in vulnerability, higher factor scores also imply higher vulnerability. Therefore, a higher z-score means greater relative vulnerability relative to the study city average. The composite HVI score is then defined as the sum of the HVI scores for each factor.

3.7.2 Mapping Analysis

All mapping calculations, such as conversion between census tract populations and WRF grid cell-level populations was completed in ArcGIS. However, the bivariate and

multiple spatial regressions are conducted using the spatial statistics software GeoDa. HVI scores, vulnerability indicators, and mortality estimates are joined in ArcGIS to census tract shapefiles, then compared using a first-order queen contiguity spatial lag model in GeoDa.

3.8 Conclusion

This chapter provides an overview of the research design and methods for this study. In the following chapters, I provide more in-depth details for each method. Chapter 4 covers the methods, results, and discussion on Research Questions 1, 1a, 1b, and 2, as these are primarily on the same topic of comparing HVI outcomes to WRF-driven spatial SAM outcomes. Chapter 5 primarily covers Research Question 3, exploring the influence of temperature model inputs on spatial SAM outcomes.

CHAPTER 4. HVI AND SPATIAL SAM ANALYSIS

4.1 Introduction

This chapter explains the method details and results of Research Questions 1, 1a, 1b, and 2. RQ1 analyzes the extent to which HVI outcomes can predict WRF-derived spatial SAM outcomes. The results of this question address a gap in the literature pertaining to very little research exploring HVI sensitivity to construction method, and that no HVI study has compared HVI scores to an intra-urban spatially comprehensive statistical attribution model like the spatial SAM. RQ1a further analyzes the statistical independence between each HVI construction method, and RQ1b analyzes the extent to which each HVI construction method can predict the top quartile spatial SAM. RQ2 explores the significance of individual indicators in predicting spatial SAM outcomes. This study is the first of its kind to study this question, and further addresses the issue that HVI methods may make obfuscate clear responses strategies by including confounding or misleading indicators in the analysis.

A deeper understanding of these relationships can help planning and public health practitioners select appropriate HVI construction methods and better translate the outcomes into more effective response strategies. A clearer sense of relative spatial priority can help direct capital investments and community initiatives in both short- and long-term heat planning.

4.2 Method Details

4.2.1 Data Availability

It is important to note that to complete this study, it was necessary to use contemporary data sources that did not provide data perfectly matching each WRF-modeled historic heat wave detailed in Table 4. While it was possible to match much of the data to the 2006 heat wave in Phoenix, Atlanta's 1995 heat wave and Detroit's 1994 heat wave were too early for many of the datasets used in this analysis. More specifically, MODIS LST is limited to the year 2000 and beyond, CDC WONDER is available after 1999, American Housing Survey data used in AC assignment is limited to 2015, and CDC 500 Cities Project data is limited to 2016 for diabetes data. As a result of this data mismatch, all American Community Survey data and CDC WONDER baseline mortality are centered on the year 2010 using 5-year estimates (2008-2012). All census tracts similarly 2010 geographies, which are valid for all of 2010-2019. In effect, this study assumes that a modern heat wave follows similar heat patterns to the historic heat wave modeled in WRF.

4.2.2 HVI Data Processing

In this section, I detail the acquisition and processing of all HVI indicators used in this study. The HVI indicators are listed in Table 5 below.

Table 5 - Indicators of heat vulnerability selected for this study.

Sensitivity	Exposure	Adaptive Capacity
Diabetes Prevalence	Land Surface Temperature	Living Below Poverty Line
Living Alone		Less than High School Education
Over Age 65		No AC Access
Over Age 65 and Living Alone		No Full AC Access
NonWhite		

4.2.2.1 Diabetes Prevalence

Diabetes data was acquired from the CDC 500 Cities Project, which provides diabetes prevalence at the 2010 census tract level for Atlanta, Detroit, and Phoenix for the year 2016. The data used in this study is the crude prevalence, converted to population proportions for each census tract. The full 500 cities dataset was downloaded and then reduced to only the three target cities through joins in ArcGIS.

4.2.2.2 American Community Survey

Several of the sensitivity and adaptive capacity indicators were obtained from the American Community Survey, including living alone, over age 65, over age 65 and living alone, race other than white, living below poverty line, and less than high school education. To center on the year 2010, I used the ACS 2008-2012 5-year estimates for all downloaded variables. All data was downloaded at the 2010 census tract level for each county. Wayne County, MI completely contains Detroit, and Maricopa County completely contains

Phoenix, but Atlanta requires data from both Fulton and Dekalb Counties. All data was obtained using Georgia Tech Library access to Social Explorer. To calculate all necessary indicators, I downloaded the following tables from Social Explorer:

Table 6 - Social Explorer tables used in this analysis.

Social Explorer Table	Description
A00001	Total population
A02002	Sex by Age
C01001	Age (detailed version)
A03001	Race
A10008	Households by household type
A12001	Educational Attainment for population 25 years or older
A10001	Housing Units
A13004	Ratio of Income in 2012 to Poverty Level
B11001	Household Type (including living alone)
B25011	Tenure by Household type (including living alone) and age of householder
A10032	Housing Units in Structure
A10053	Occupied Housing Units by Units in Structure

All tracts with zero population were first removed from this analysis. Over 65 was defined as the sum of all age groups 65 and above, then divided by the total tract population. NonWhite is defined as the reciprocal of the white population proportion, or [1 – (White population / Total population)]. Less than high school education is defined as the proportion of population above age 25 who do not have a high school diploma. Living alone is defined as the number of households with a single occupant, which means each household represents one person, divided by the total tract population to derive tract population proportion living alone. Over age 65 and living alone is the sum of all households with a single occupant over the age of 65 divided by the total tract population. Finally, living below the poverty line is defined as the sum of the population below 1.0 times the poverty line, divided by the population for whom poverty status is determined.

Additionally, the Sex by Age table was downloaded to obtain population cohorts stratified by age and sex for the spatial SAM analysis. This analysis was introduced in section 3.4.2 and explained further in section 4.2.4 below.

4.2.2.3 Air Conditioning Prevalence

Air conditioning prevalence is not available at the census tract level. Instead, the data was downloaded from the 2015 American Housing Survey metropolitan datasets for each city. This dataset breaks down AC prevalence by housing type. Since the number of housing units by housing type is also available through the American Community Survey, I can apply the MSA-level AC prevalence individually to each housing type within each census tract to calculate an overall AC prevalence estimate for the census tract.

Two separate levels of AC are considered in this analysis for use in the HIV: No AC, and No Full AC. No AC is defined in the American Housing Survey sample data as a designation of "unit does not have air conditioning" divided by the total number of units within each housing structure type. No Full AC classification includes all units that have some form of air conditioning, but not central air conditioning. This class is defined as: [Total units – units with central air conditioning] / [Total units] within each housing structure type. The structure types included in this analysis are single family attached, single family detached, multi-family (any building with 2 or more units), and mobile homes. The prevalence of air conditioning for each housing type are shown in the tables below, represented as proportions of the total units per housing type.

Table 7 – Lack of AC access by housing type, Atlanta.

	Single Family Detached	Single Family Attached	Multi-Family	Mobile
No AC	0.0088	0.0071	0.0045	0.0434
No Full AC	0.0520	0.0437	0.0321	0.2653

Table 8 – Lack of AC access by housing type, Detroit.

	Single Family Detached	Single Family Attached	Multi-Family	Mobile
No AC	0.1050	0.0631	0.1069	0.0665
No Full AC	0.2564	0.1434	0.3266	0.2898

Table 9 – Lack of AC access by housing type, Phoenix.

	Single Family Detached	Single Family Attached	Multi-Family	Mobile
No AC	0.0142	0.0000	0.0047	0.0188
No Full AC	0.0252	0.0194	0.0180	0.1754

Overall census tract AC prevalence was calculated using the sum of the count of each housing structure type multiplied by the AC prevalence of that type, all divided by the total count of housing units of all types. As an illustrative example, in Phoenix, No AC prevalence would be calculated as follows:

No AC = ([# Single family detached units] * 0.0142 + [# Single family attached units] * 0.0000 + ([# Multi-family units] * 0.0047 + ([# mobile home units] * 0.0188) / [Total housing units]

4.2.2.4 Land Surface Temperature

Land Surface Temperature (LST) represents the primary exposure indicator in the HVI. In this analysis, I use MODIS 8-day average LST to better represent average LST over a heat wave period, rather than a single snapshot LST derived in each flyover of the satellite. The average LST was chosen over the snapshot to avoid issues with cloud cover obscuring the satellite image. As each modeled heat wave period is roughly one week in length, the 8-day average is a good indicator of LST over each modeled period. All MODIS data was downloaded from the USGS Earth Explorer tool. MODIS data is in Kelvin with a scale factor of 0.02, so the data was converted to degrees Fahrenheit using Equation 2 below:

$$F = ([\text{MODIS data}] * 0.02 - 273.15) * 9/5 + 32 \qquad \text{(Equation 2)}$$

MODIS data begins in the year 2000, so only Phoenix can match the MODIS data with the WRF model of 2006. For Phoenix, I simply matched the MODIS 8-day average as closely as possible to the WRF-modeled period, spanning July 11, 2006 to July 25, 2006. The closest MODIS dataset for this period has an acquisition date of July 20 to July 27, 2006.

The MODIS dataset for Phoenix is shown in the figures below. Figure 25 shows the entire city in the environmental context, mostly arid landscape. However, there is a lake in the north of the city, with much lower surface temperatures. Phoenix also displays a unique LST dynamic in that the sparsely populated desert landscape can display higher temperatures more than some urban areas, which is the opposite effect from an expected

urban heat island dynamic. This is because it is only in the urban areas where residents are able to establish and maintain vegetation through irrigation. In the surrounding desert landscape, it is less likely for vegetation to survive and provide cooling. This dynamic is highlighted below in Figure 26. LST in Phoenix ranged from 87.9 °F to 137.9 °F.

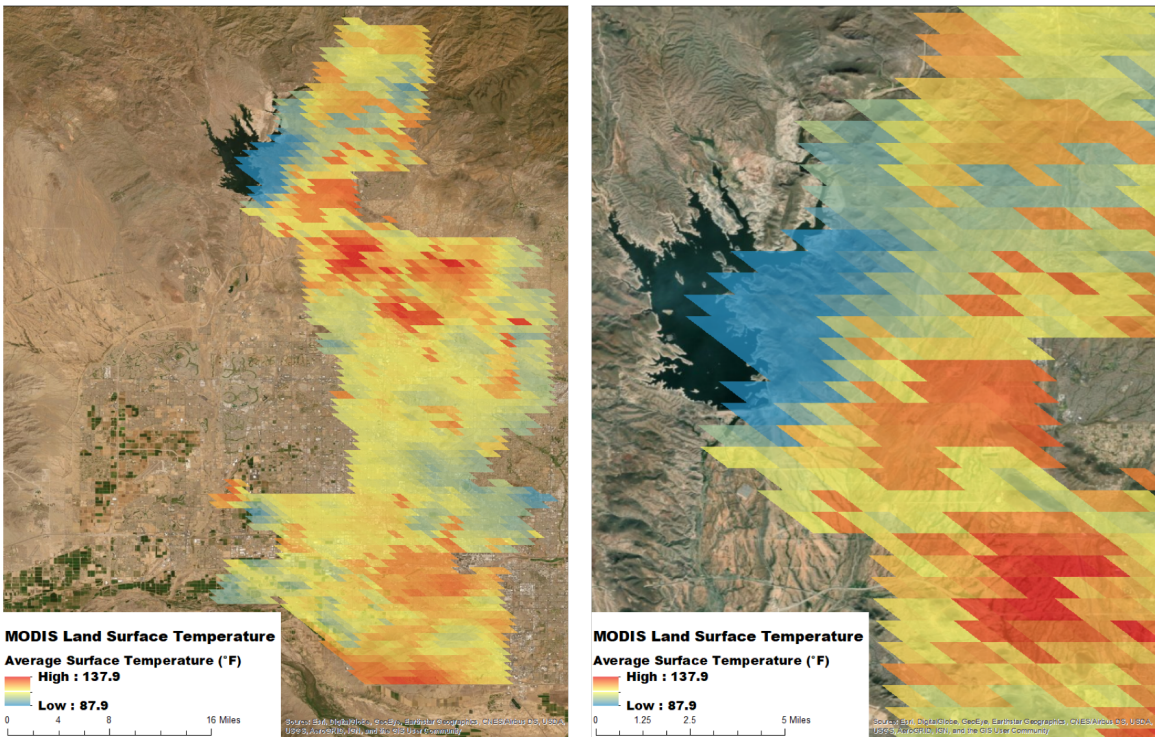

Figure 25 - Phoenix MODIS LST, full-city (left) and zoomed for detail (right)

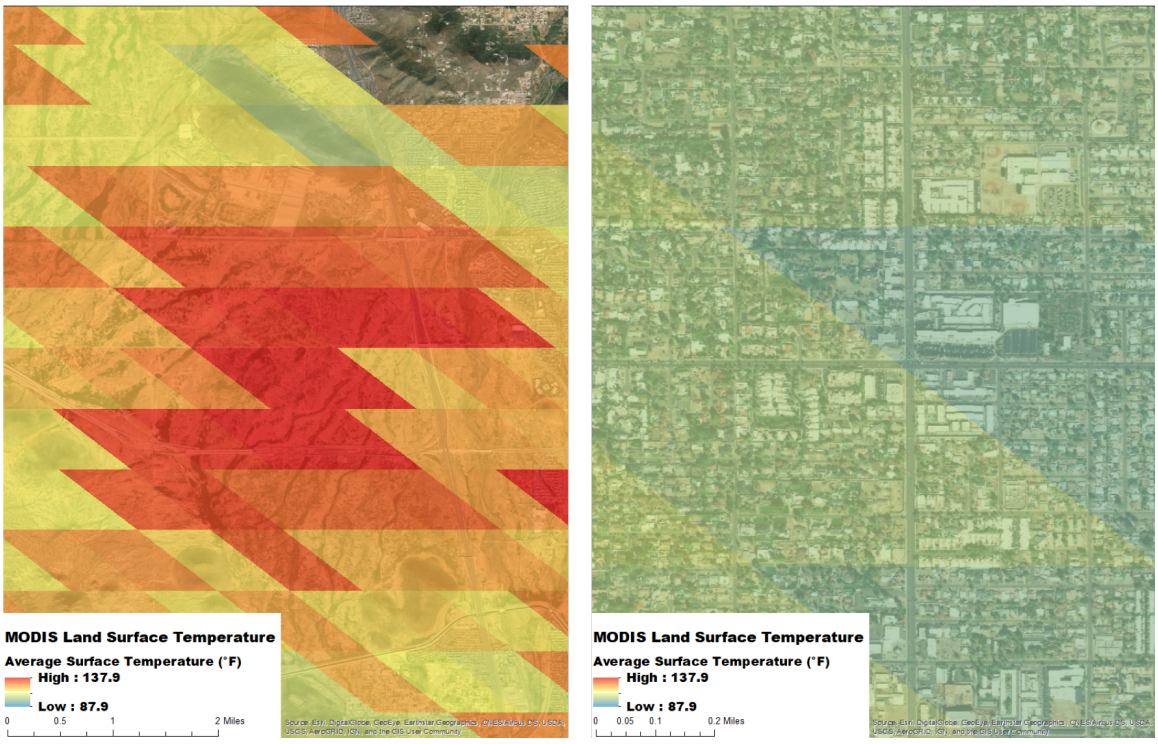

Figure 26 - Phoenix MODIS LST with rural hot spot (left) and urban cool spot (right)

Since the Detroit WRF model uses 1994 temperatures, and Atlanta uses 1995 temperatures, it was necessary to first identify a similar heat wave for each city from the year 2000 or later. To do this, I downloaded daily weather data from the National Climatic Data Center's Global Historical Climatology Network Daily (GHCND) dataset (NOAA) for each city spanning the modeled heat wave period up to July 2019. Weather variables included minimum temperature, average temperature, maximum temperature, and wind speed. I then created an 8-day running average across the he entire dataset for each city to compare to the average temperature of the modeled heat wave period to find a similar heat wave for the MODIS data, described below.

Table 10 - GHCND weather stations for each city.

Station	Atlanta Hartsfield International Airport	Detroit Metro Airport	Phoenix Airport
GHCND ID	USW00013874	USW00094847	USW00023183
Latitude	33.6301	42.2313	33.4277
Longitude	-84.4418	-83.3308	-112.0038
Elevation	307.8m	192.3m	337.4m

For Atlanta, the heat wave period spans August 12, 1995 to August 18, 1995. This heat wave is summarized below, represented as mean daily average values:

Table 11 - Atlanta heat wave period characteristics.

Wind Speed (m/s)	Tavg (°F)	Tmax (°F)	Tmin (°F)
5.5285	87	99	75

Using the 8-day running averages in the GHCND dataset, I identified August of 2007 as a similar heat wave period to the one from 1995, as shown in the table below in descending order of average temperature.

Table 12 - 8-day running averages for Atlanta weather record.

Start Date	Wind Speed (m/s)	Tavg (°F)	Tmax (°F)	Tmin (°F)
8/8/07	5.99	88.81	99.63	78.00
8/9/07	6.24	88.69	99.75	77.63
8/7/07	6.32	88.63	99.13	78.13
8/4/07	6.04	88.56	99.38	77.75
8/6/07	6.46	88.44	99.00	77.88
8/10/07	6.40	88.25	99.50	77.00
8/5/07	6.40	88.13	98.50	77.75
8/3/07	5.73	87.75	98.63	76.88
8/15/07	6.35	87.75	99.38	76.13

With this information, I downloaded a MODIS 8-day LST dataset spanning August 5 to August 12, 2007. This data is shown below in Figure 27. As highlighted in the image on the right, Atlanta displays much more conventional urban heat island dynamics as compared to Phoenix, with warmer urban areas and cooler vegetated neighborhoods outside the urban core. The LST in Atlanta ranged between 91.3 °F and 106.7 °F.

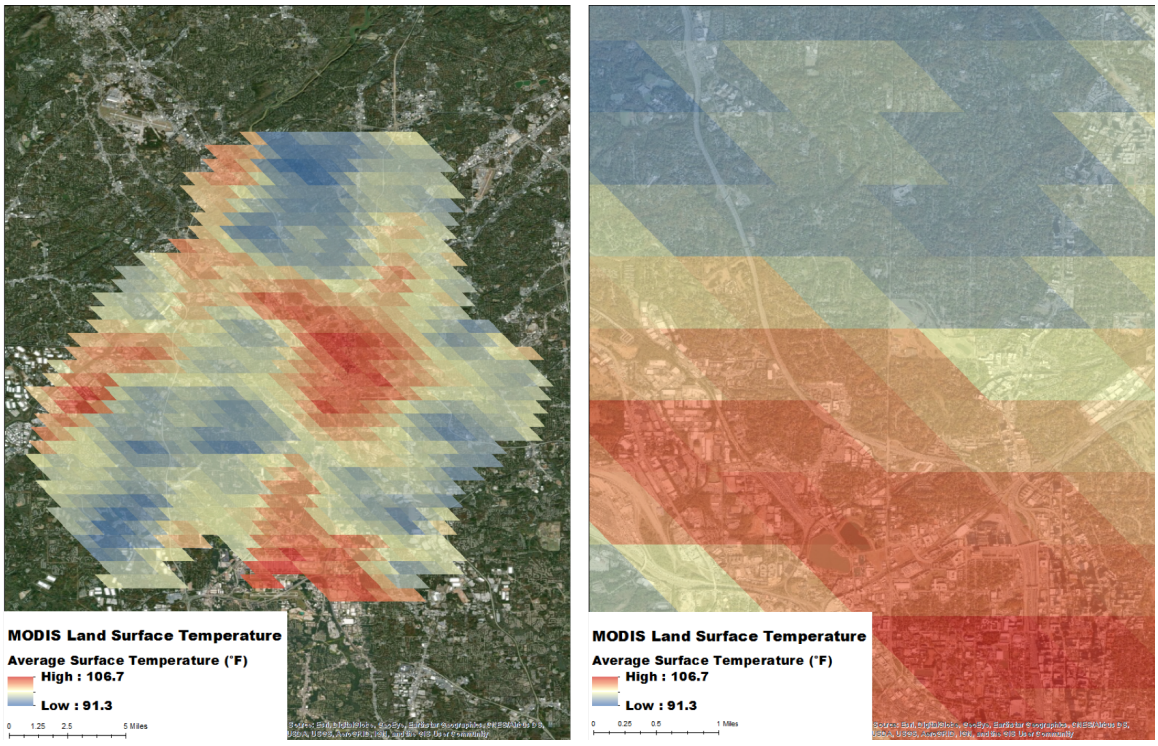

Figure 27 - Atlanta MODIS LST, full-city (left) and zoomed for detail (right)

For Detroit, the WRF-modeled heat wave period was from July 15 to July 19, 1994. The heat wave period characteristics are summarized in Table 13 below as mean daily averages. Table 16 shows the 8-day running averages for the closest heat wave period in July of 2011.

Table 13 - Detroit heat wave period characteristics.

Wind Speed (m/s)	Tavg (°F)	Tmax (°F)	Tmin (°F)
6.6200	84.9	96	73.8

Table 14 - 8-day running averages for Detroit weather record.

Start Date	Wind Speed (m/s)	Tavg (°F)	Tmax (°F)	Tmin (°F)
7/17/11	5.98	84.00	94.00	74.00
7/18/11	6.18	83.94	93.63	74.25
7/16/11	6.18	83.63	93.88	73.38
7/15/11	6.15	82.94	93.25	72.63
7/19/11	6.23	82.88	92.50	73.25

Using this information, I identified a MODIS 8-day average LST period of July 12 to July 19, 2011. This data is displayed below in Figure 28. Like Atlanta, Detroit displays urban heat island patterns with a warmer urban core as compared to a more heavily vegetated western periphery. The Detroit River to the southeast greatly reduces the LST in that area of the city. Across the city, Detroit LST ranges from 74.8 °F to 101.4 °F.

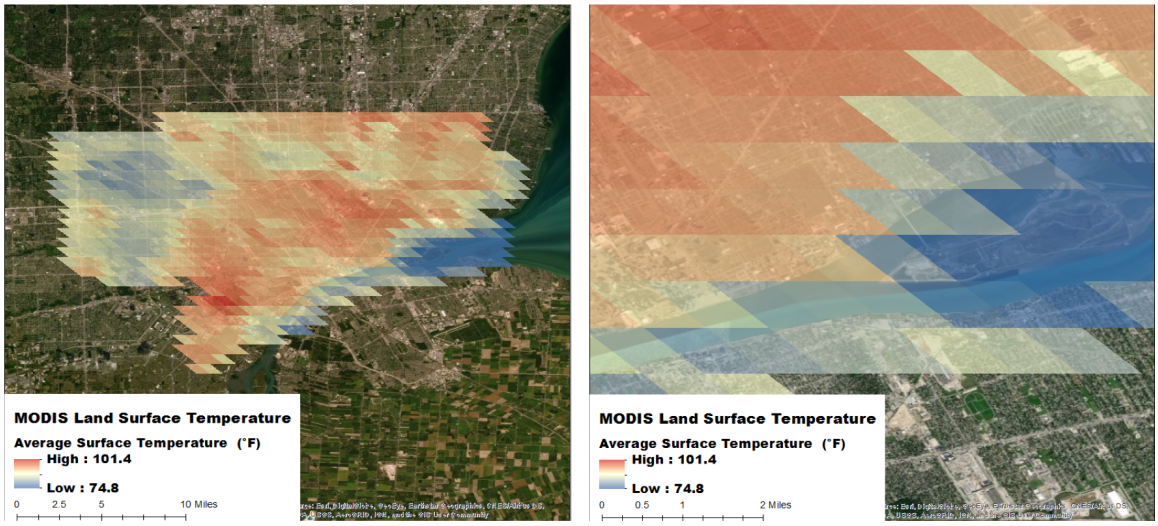

Figure 28 - Detroit MODIS LST, full-city (left) and zoomed for detail (right)

For use in the HVI, all MODIS data were resampled from 1km resolution to 250m resolution, then averaged to 2010 census tract geographies using the Zonal Statistics as Table tool. This results in a measure of average LST for each census tract to be used with the other tract-level HVI indicators discussed above.

4.2.3 HVI Construction

Once all of the HVI indicators were processed at the census tract level, the full table was exported to Excel to construct the simplified HVI, unweighted overlay HVI, and weighted overlay HVI. For these three HVI methods, I converted all indicators to z-scores and assigned indicator HVI scores according to the Reid (2009) methodology in Table 15 below. This method converts z-score to an HVI component score to ensure that all indicators contribute positively, and that no indicators reduce the overall HVI score.

Table 15 - HVI score assignment procedure.

Range of Z-Score	Assigned HVI Component Score
-2 or lower	1
-2 to -1	2
-1 to 0	3
0 to 1	4
1 to 2	5
2 or higher	6

4.2.3.1 Simplified HVI

The simplified HVI is defined as consisting of only two indicators: over age 65 representing heat sensitivity, and LST representing heat exposure. In this HVI, I simply added the HVI indicator score for over age 65 and LST to calculate the final simplified HVI score.

4.2.3.2 Unweighted Overlay HVI

In the unweighted overlay HVI, all HVI indicator scores are added across all ten indicators. All indicators are equally weighted.

4.2.3.3 Weighted Overlay HVI

In the weighted overlay HVI, each HVI category is weighted equally between sensitivity, exposure, and adaptive capacity. As shown in Table 5 above, there are five

indicators in the sensitivity category (over 65, living alone, over 65 and living alone, diabetes, and nonwhite), one indicator in the exposure category (LST), and four indicators in the adaptive capacity category (poverty, less than high school education, no AC, and no Full AC). The weighted overlay is defined as the sum of all indicator HVI scores, divided by the number of indicators in each respective category.

4.2.3.4 Principal Components Analysis HVI

As the most complex HVI method, the PCA HVI required several more processing steps. The Principal Components Analysis procedure was conducted in SPSS 24. Before selecting the number of components to use in the analysis, it was important to first examine the scree plot and total variance explained by varying the number of components. In general, it is common to limit the number of components where the added benefit begins to show diminishing returns for total variance explained. Visually, this is where the scree plot begins to level out.

Figure 29 shows the scree plot for Atlanta, and Table 16 shows the total variance explained. Both show that 4 components is adequate for this analysis, as the added benefit of each new component begins to sharply diminish. For Atlanta, 4 components cumulatively explain just over 84% of the variance in the dataset.

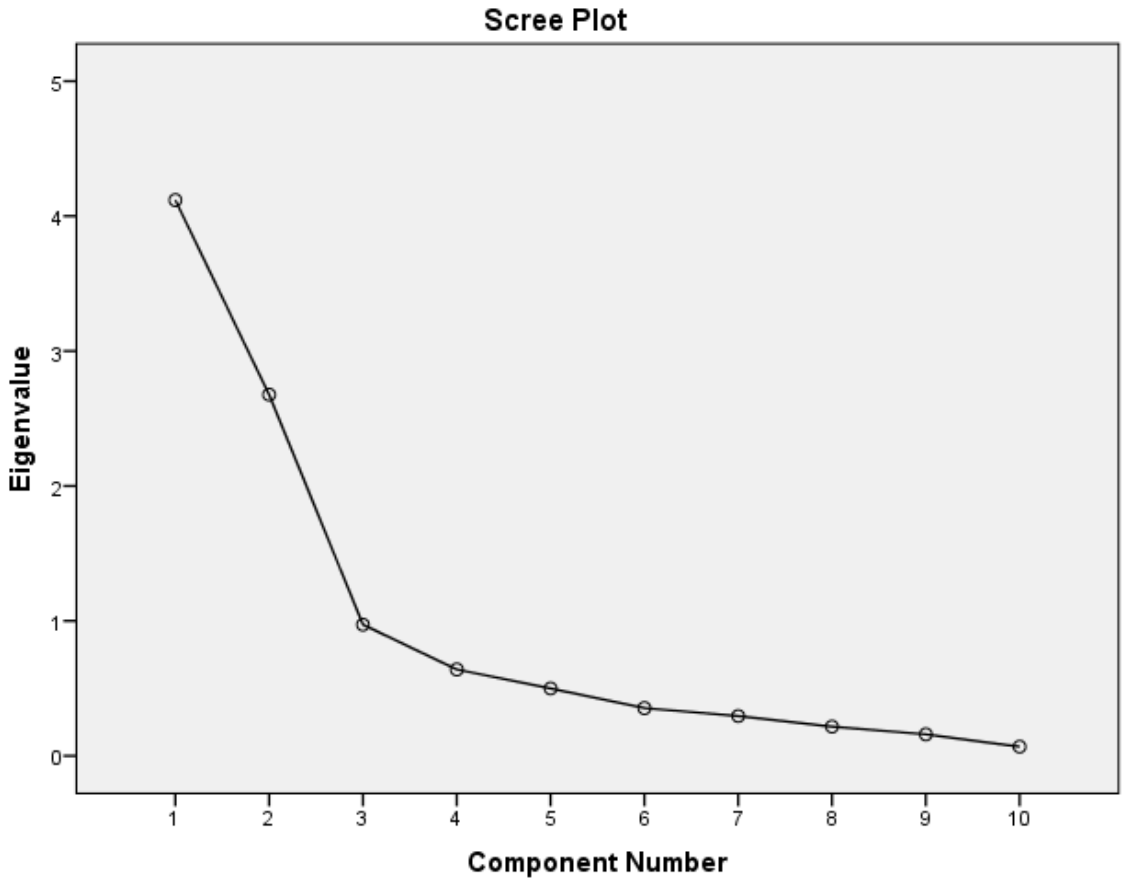

Figure 29 - Scree plot for Atlanta PCA.

Table 16 - Total variance explained by Atlanta components.

Component	Total	% of Variance	Cumulative %
1	4.118	41.183	41.183
2	2.677	26.766	67.949
3	0.972	9.723	77.672
4	0.64	6.401	84.073
5	0.5	4.996	89.069
6	0.354	3.539	92.609
7	0.295	2.953	95.562
8	0.217	2.166	97.728
9	0.159	1.593	99.321
10	0.068	0.679	100

To generate the PCA components, I ran the PCA procedure with 4 components using Varimax rotation to produce four statistically independent components. The component loadings are shown in Table 17. Each component is characterized by the indicators with an absolute value greater than 0.6, shown in bold in the table. The first component is highly correlated with sensitivity and adaptive capacity components, while the second contains both sensitivity and exposure. Component 3 is correlated exclusively with AC indicators, and component 4 is correlated with only living alone.

Table 17 - Rotated component loadings for Atlanta PCA.

	Component			
Indicator	**1**	**2**	**3**	**4**
NonWhite	**0.909**	0.105	0.123	-0.131
Living Below Poverty Line	**0.901**	-0.134	-0.126	-0.133
Less than High School Education	**0.868**	-0.015	0.259	-0.124
Diabetes	**0.836**	0.403	0.217	-0.097
Over 65	0.148	**0.893**	0.087	0.076
Over 65 and Living Alone	-0.044	**0.806**	0.253	0.355
Land Surface Temperature (°F)	0.024	**-0.734**	-0.378	0.387
No AC Access	0.178	0.14	**0.886**	0.085
No Full AC Access	-0.089	-0.334	**-0.717**	0.227
Living Alone	-0.493	0.17	-0.092	**0.778**

Figure 30 and Table 18 below show the scree plot and total variance explained for Detroit. These show that for Detroit, five components are appropriate for the PCA before the marginal benefit drops off. Five factors cumulatively explain about 83% of the total variance in the dataset.

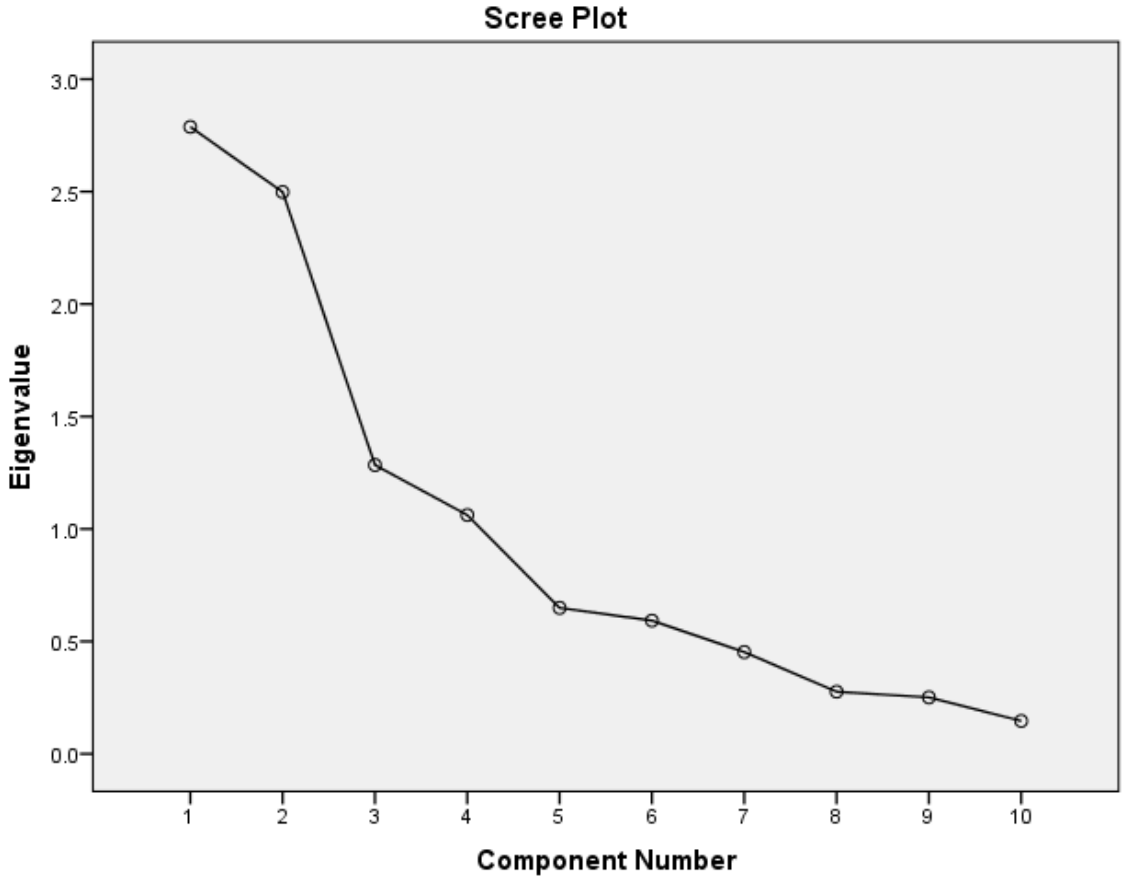

Figure 30 - Scree plot for Detroit PCA.

Table 18 - Total variance explained by Detroit components.

Component	Total	% of Variance	Cumulative %
1	2.788	27.877	27.877
2	2.498	24.981	52.858
3	1.284	12.842	65.701
4	1.062	10.62	76.321
5	0.649	6.49	82.811
6	0.593	5.925	88.736
7	0.453	4.528	93.264
8	0.276	2.762	96.026
9	0.251	2.511	98.538
10	0.146	1.462	100

The rotated component loadings for Detroit are shown in Table 19 below. For Detroit, the first component is correlated with exposure and adaptive capacity, while components 2 and 3 are associated with sensitivity. Component 4 is associated with sensitivity and adaptive capacity, and component 5 is entirely adaptive capacity.

Table 19 - Rotated component loadings for Detroit PCA.

	Component				
Indicator	**1**	**2**	**3**	**4**	**5**
No Full AC Access	**0.876**	-0.135	0.135	-0.053	0.008
No AC Access	**-0.802**	0.017	-0.151	-0.139	-0.155
Land Surface Temperature (°F)	**0.67**	0.13	-0.079	-0.329	0.201
Living Alone	-0.053	**0.911**	-0.001	0.2	-0.117
Over 65 and Living Alone	-0.016	**0.842**	0.358	-0.013	-0.054
Diabetes	0.142	0.057	**0.808**	0.332	0.364
Over 65	0.167	0.41	**0.789**	0.01	-0.285
NonWhite	-0.072	0.134	0.33	**0.856**	0.079
Less than High School Education	0.054	-0.134	0.126	**-0.721**	0.568
Living Below Poverty Line	0.246	-0.134	0.002	-0.051	**0.876**

Like Atlanta, four components were adequate for Phoenix as shown in the scree plot and total variance table below. Four components cumulatively explain about 80% of the total variance for the Phoenix dataset.

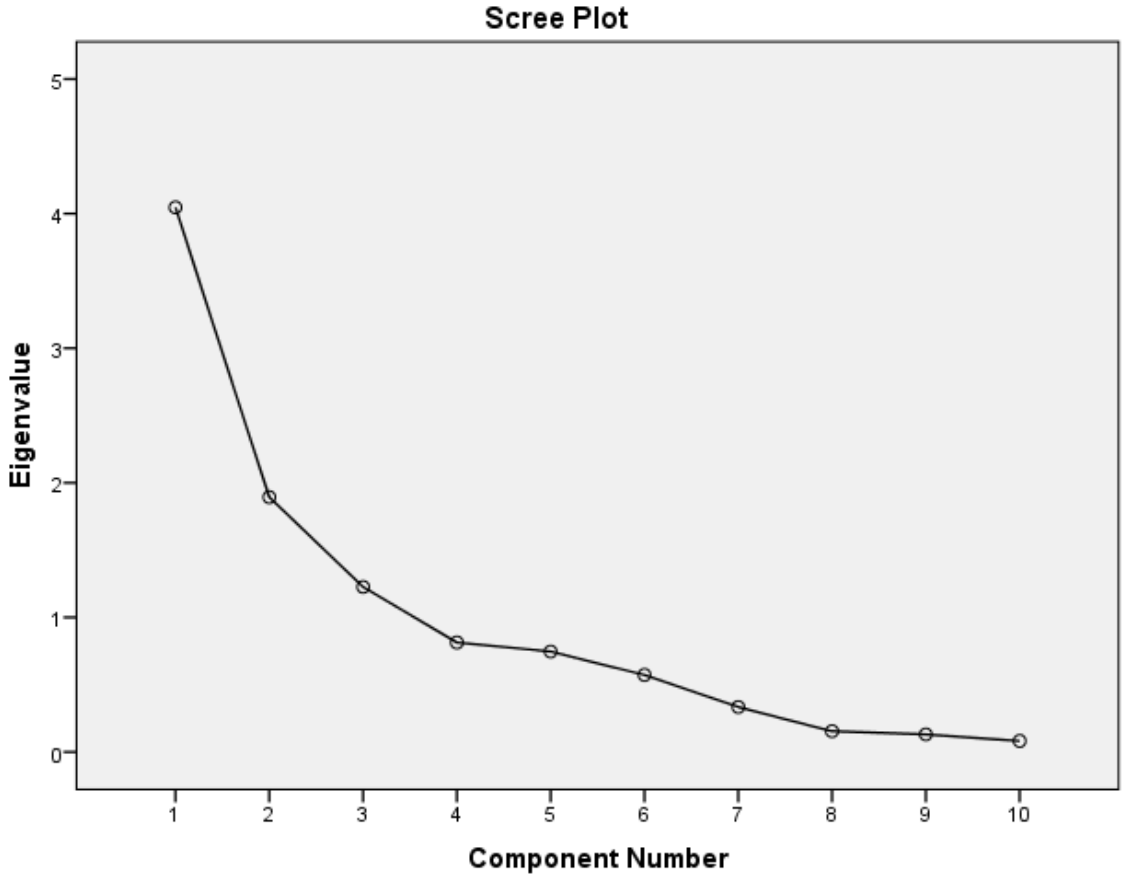

Figure 31 - Scree plot for Phoenix PCA.

Table 20 - Total variance explained by Phoenix components.

Component	Total	% of Variance	Cumulative %
1	4.046	40.459	40.459
2	1.894	18.936	59.396
3	1.226	12.264	71.66
4	0.814	8.136	79.796
5	0.746	7.465	87.261
6	0.572	5.723	92.984
7	0.334	3.343	96.327
8	0.154	1.542	97.87
9	0.131	1.311	99.181
10	0.082	0.819	100

As shown in Table 21 below, the first component was strongly associated with sensitivity and adaptive capacity indicators including elderly and isolated populations. The second component was strongly associated with sensitivity and adaptive capacity, while component 3 was correlated with only adaptive capacity indicators involving AC. The fourth component was associated with only LST, and NonWhite was not strongly associated with any of the components in Phoenix.

Table 21 - Rotated component loadings for Phoenix PCA.

	Component			
Indicator	**1**	**2**	**3**	**4**
Over 65 and Living Alone	**0.915**	-0.056	0.087	-0.148
Over Age 65	**0.878**	-0.093	-0.073	-0.13
Living Alone	**0.814**	-0.294	0.1	-0.159
NonWhite	-0.5	0.303	0.328	-0.152
Diabetes	0.016	**0.968**	0.009	0.094
Less than High School Education	-0.326	**0.88**	0.052	0.125
Poverty	-0.301	**0.813**	0.368	0.068
No Full AC Access	0.12	0.135	**0.794**	0.345
No AC Access	0.059	-0.07	**-0.788**	0.365
Land Surface Temperature (°F)	-0.276	0.177	-0.019	**0.815**

SPSS generated component scores for all census tracts in each city, which can then use the same HVI scoring scheme as Reid (2009). The component HVI scores were then summed to get a final PCA HVI score.

4.2.4 Spatial Statistical Attribution Model

In this section, I detail the data acquisition and processing for the spatial SAM model mortality estimates introduced in Section 3.4.2.

4.2.4.1 WRF Data Processing

All WRF data was provided by researchers in the 3HEAT study detailed in Section 3.3 as CSV files of daily average temperature over each day of the target period for each WRF cell in the city's domain (see Figure 17). Air temperature data was converted from Kelvin to Fahrenheit in Excel for use in this analysis. The WRF grid was created in ArcGIS using the Create Fishnet tool pinned to each corner of the WRF domain, with 156 rows and 156 columns, resulting in a 1-km fishnet grid across each city. WRF temperature datasets were joined to this grid using the FID of the final fishnet grid.

4.2.4.2 Baseline Mortality

All baseline mortality rates were downloaded from the CDC WONDER database (CDC) for the years 2008-2012, similar to the ACS data centered on the year 2010, for each study city's county. This data stratifies mortality rates for males and females for each of the following age cohorts separately: age 5-14, 15-24, 25-34, 35-44, 45-54, 55-64, 65-74, 75-84, and 85 and older. Ages 0-4 have been removed from this analysis to reduce infant mortality bias.

4.2.4.3 Gridded Population

All spatial SAM analyses were conducted at the WRF grid level, rather than the tract level. However, the ACS population cohorts are available at the census tract level. To match up these geographies, I needed to convert the tract population to a gridded population dataset.

The gridded population analysis was conducted spatially in ArcGIS using the following procedure:

1. Population is assumed to be evenly spread through each tract and is therefore be apportioned based on area.
2. Calculate tract area using the Calculate Geometry tool.
3. Split each WRF grid cell by tract boundaries using the Union tool to break the cells into segments that fit entirely within tract boundaries.
4. Calculate grid cell segments areas using the Calculate Geometry tool. All grid cell fragment areas add up to the total area of the tract in which they reside.
5. Convert grid cell segments to centroids using the Feature to Point tool.
6. Attribute a tract ID to each grid cell segment centroid using a spatial join assigning tract properties to each fragment centroid it contains.
7. Divide grid cell segment area by the tract area in which it resides to get an attributable proportion of the tract area for each cell fragment.
8. Multiply each tract population cohort by the attributable proportion for each grid cell segment to apportion the population to each grid cell fragment according to its proportional area.
9. Re-aggregate fragments into full grid cells using a spatial join from the cell segment back to the WRF grid cell geography. Use the sum of all grid cell segment centroids that fall within each WRF grid cell boundary.

Using this method, I am able to comprehensively apportion the tract population cohorts to each grid cell based on area. This method ensures that all WRF grid cells gain

population according to their proportional area of any tract with which they overlap. See Figure 32 below for an illustration of this procedure. The WRF grid cell in this image was split into segments along the boundaries of the three census tracts with which it overlaps. The segments were each assigned a tract ID and all associated tract population cohorts based on their centroid location, and population was apportioned based on each segment's areal attributable fraction. The segment population cohorts were then summed back to the WRF grid in which their centroid resides to get a final gridded population for each population cohort.

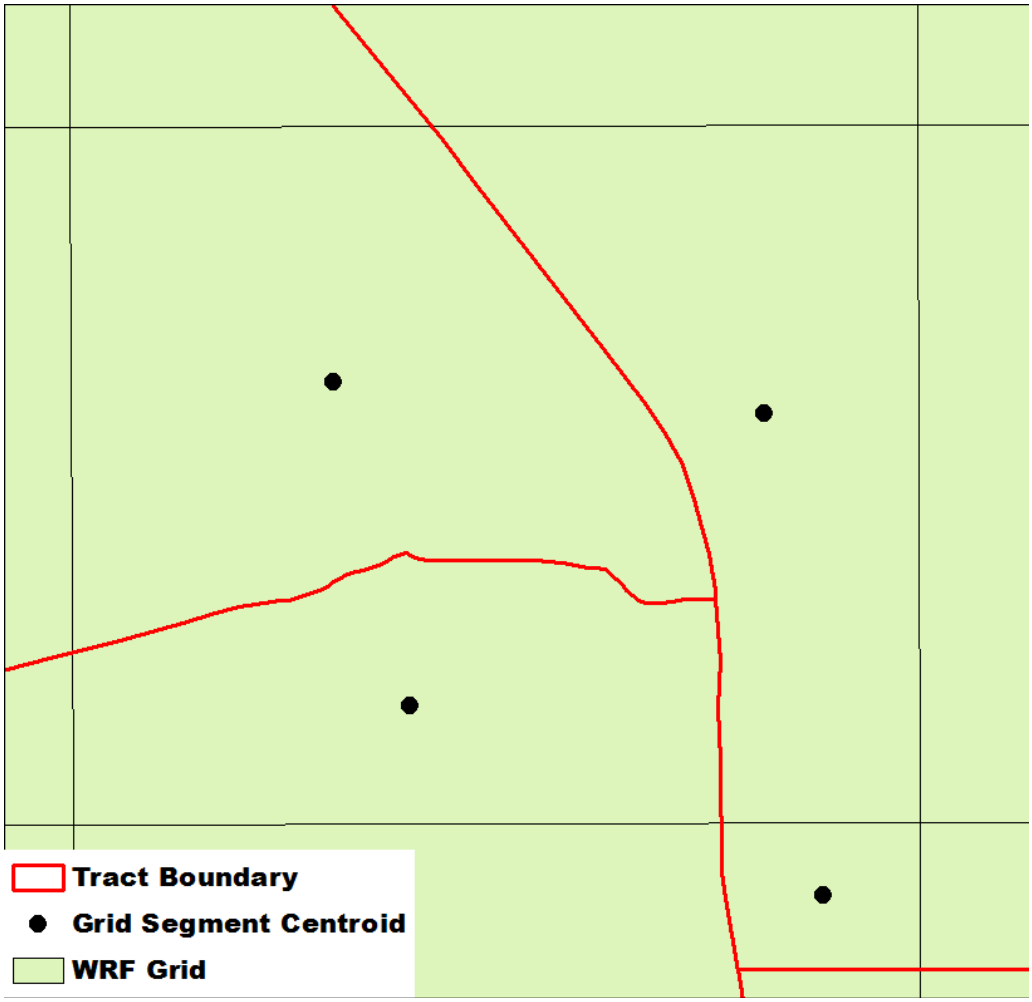

Figure 32 - Gridded population apportionment example.

4.2.4.4 Spatial SAM Script

To calculate the gridded mortality for each city, an R script was used to individually modify the baseline mortality of each population cohort obtained from CDC WONDER and multiply the adjusted mortality rates for each cohort by the population within each cohort. The procedure is illustrated in Figure 33 below.

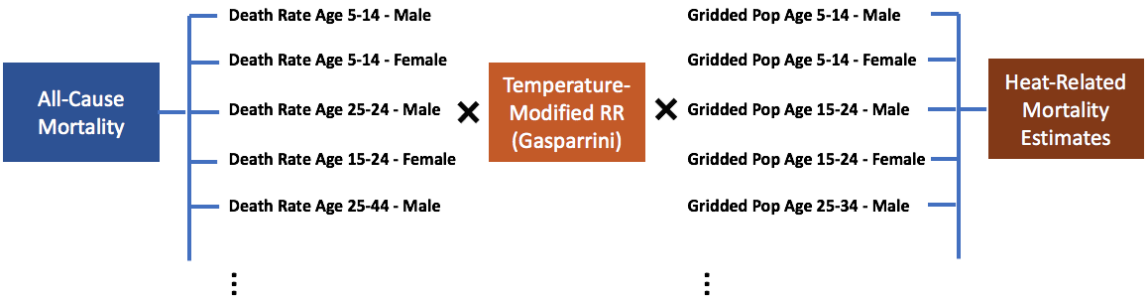

Figure 33 - Summary of response function applied to age and sex cohorts.

To accomplish this, the script referenced the Gasparrini (2015) relative risk curves for each city to look up the relative risk associated with each WRF grid cell's average daily mean temperature over the course of the modeled period for each city, then multiplied the baseline mortality rate for each age and sex cohort by that new relative risk to obtain a new baseline mortality unique to that age and sex cohort. This new mortality rate was multiplied by each respective cohort population to obtain an estimate of death rates for each grid cell. The script ensures that only heat-attributable mortality is counted by including only temperatures on the warm end of the relative risk curve (see Figure 34 below). This is defined as the inflection point for heat mortality, which is unique to each city. These inflection points are summarized in Table 22 below.

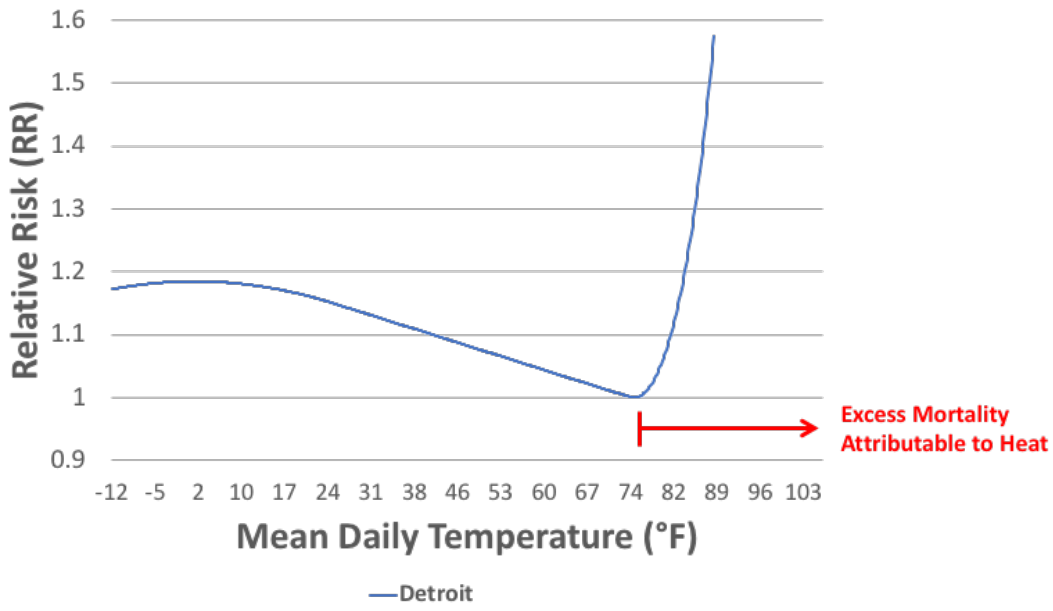

Figure 34 - Gasparrini (2015) relative risk curves used in R script.

Table 22 - Inflection points for heat-related mortality for all three cities.

	Atlanta	Detroit	Phoenix
Inflection (°F)	77.90	75.02	84.02

Once all the gridded mortality estimates were calculated, these data were joined back to the WRF grid in ArcGIS for aggregation to the census tract scale to compare to the HVI results. This followed a reversal of the procedure from section 4.2.4.3, as follows:

1. Calculate WRF grid cell area using Calculate Geometry tool.
2. Cut WRF grid cells into segments by census tract boundaries using the Union tool.
3. Calculate grid cell segment areas using the Calculate Geometry tool.
4. Divide grid cell segment area by total WRF grid cell area to get a proportion of total grid cell area for each segment.

5. Multiply gridded mortality by area proportion to get a fragment-level mortality count.
6. Convert each cell fragment to a centroid point using Feature to Point tool.
7. Aggregate to census tract geography using a spatial join. Use the sum of fragment mortality counts to add up all grid fragment centroids within each census tract to obtain a tract-level mortality.

4.2.5 HVI and Spatial SAM Comparison

Research questions 1, 1a, 1b, and 2 each use a different statistical comparison technique. These techniques are detailed in the sections below.

4.2.5.1 Research Question 1

RQ1: *To what extent can established HVI methods predict total heat-related mortality estimates as derived by the statistical attribution method?*

To answer this research question, I used a bivariate spatial regression between the HVI scores across all four construction methods and the total spatial SAM mortality for each census tract across the three cities. This analysis was conducted in GeoDa using a first-order queen contiguity spatial weights matrix. Since each HVI has a different HVI scale, the final HVI scores and spatial SAM totals were all converted to z-scores for a common scale across all comparisons. The R-Square for each regression shows the strength of the correlation between each HVI and the spatial SAM estimates.

4.2.5.2 Research Question 1a

RQ 1a*: Do different HVI construction methods within the same city produce statistically independent HVI scores?*

To test whether the HVI scores were statistically independent of one another, a paired t-test was run between each of the HVIs for each city. As with research question 1, the HVI scores were first converted to z-scores for a common scale between each HVI method. A statistically significant result at the $\alpha = 0.1$ level shows a statistically significant change between each HVI pair.

4.2.5.3 Research Question 1b

RQ 1b: *To what extent can HVI scores predict the top quartile of vulnerability as determined by the statistical attribution method?*

For this research question, I look at only the top quartile of each spatial SAM result as a binary variable, where a value of 1 is the top quartile, and 0 is below this threshold. These values were assigned to each tract in Excel using the Quartile function. This analysis uses a binomial logistic regression with the HVI score as the independent variable and the top quartile designation as the dependent variable. While the Hosmer-Lemeshow test may be used as a way to determine whether a binomial logistic regression is a good fit (Hosmer & Lemeshow, 1980), there is a more recent analog to the R-Square used in RQ1 proposed by Tjur (2009). Tjur's R-Square is derived by obtaining the probabilities from the binomial logistic regression for each observation, then subtracting the mean of the probabilities for which the dependent variable is 0 (event did not occur) from the mean of the probabilities

for which the dependent variable is 1 (event occurred). The theory is that for a perfect fit, the mean of the probabilities of an event occurring would be 1 (100% occurrence), subtracting out a 0% probability of occurring, or 0, gives a Tjur's R-Square of 1. While the results are not be directly comparable to each of the R-Square results from RQ1, they do provide a metric by which to compare each binary logistic regression fit.

4.2.5.4 Research Question 2

***RQ 2**: Which heat vulnerability indicators are significant predictors of heat-related mortality as derived by the statistical attribution method?*

For this research question, I run a multiple spatial regression between the individual HVI indicators and the spatial SAM mortality at the tract level. A statistically significant result at the $\alpha = 0.1$ level for any given indicator indicates a statistically significant relationship between that indicator and spatial SAM mortality. To avoid threats of multicollinearity, I have removed indicators that have a strong correlation with another variable. This includes over 65 and living alone, which is correlated with both over 65 and living alone, and no full AC access, which is correlated with no AC access.

4.3 Results

4.3.1 Total Heat-Related Mortality

The first result shown here is the total spatial SAM mortality across all tracts for the WRF-modeled period. Detroit was found to have the highest heat-related mortality, with 18.65 heat-attributable deaths and 0.0261 deaths per 1,000 people over the modeled period. Atlanta was found to have the lowest at only 2.23 heat-attributable deaths, and a

death rate of 0.0053 per 1,000 people. Phoenix was in the middle with 11.48 heat-attributable deaths and 0.0079 deaths per 1,000 people. These findings may be a result of Detroit's northern location and lower temperature threshold for heat-related deaths. The lower physiological acclimatization among the population makes heat a larger threat to Detroit than it does to the other cities. Atlanta is the smallest of the three cities by population, giving it a lower overall total heat-related death. Additionally, as a southern city, the relative risk curve for Atlanta is far less steep than a northern city like Detroit, as displayed in Figure 35 below. The threshold to heat-related mortality is much higher in warmer climates due to the population's physiological acclimatization to heat. This may explain why the death rate is also very low in Atlanta. While Phoenix is also a southern city with a warm climate, it has a much larger population, pushing the death total higher than Atlanta. But as shown in Figure 35, the relative risk curve remains stable until it increases sharply at very high temperatures. This may explain why the death rate for Phoenix remains only slightly above Atlanta.

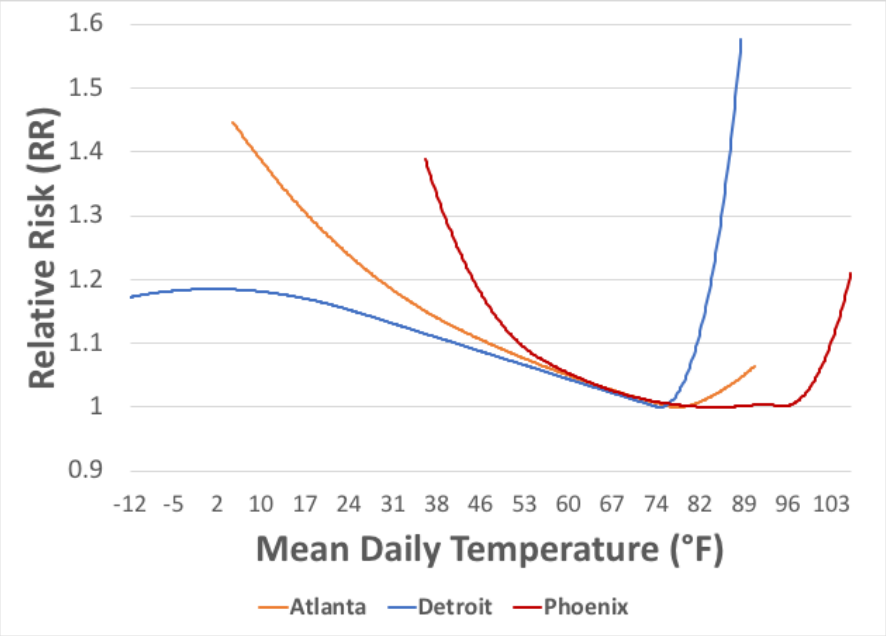

Figure 35 - Heat mortality relative risk curves for Atlanta, Detroit, and Phoenix (Gasparrini, 2015).

Table 23 – Summary of total heat-related mortality and death rate (WRF) over each city's target period.

	Atlanta	Detroit	Phoenix
Total	2.23	18.65	11.48
2010 Population	420,003	713,777	1,445,632
Death Rate (per 1,000 Population)	0.0053	0.0261	0.0079

4.3.2 HVI Results – Atlanta

The figures below show the HVI results for all four construction methods in Atlanta, followed by the spatial SAM results and the top quartile spatial SAM. For this analysis, all HVI scores are converted back to z-scores as a common metric for comparison

since each HVI method has a different range of possible scores. For mapping purposes, all HVI maps are displayed as quantiles rather than on a common scale to highlight relative prioritization. The results for each HVI show some consistency in results, mostly highlighting similar central and western tracts. However, the simplified HVI appears to show the greatest difference, highlighting mostly central tracts in the urban core.

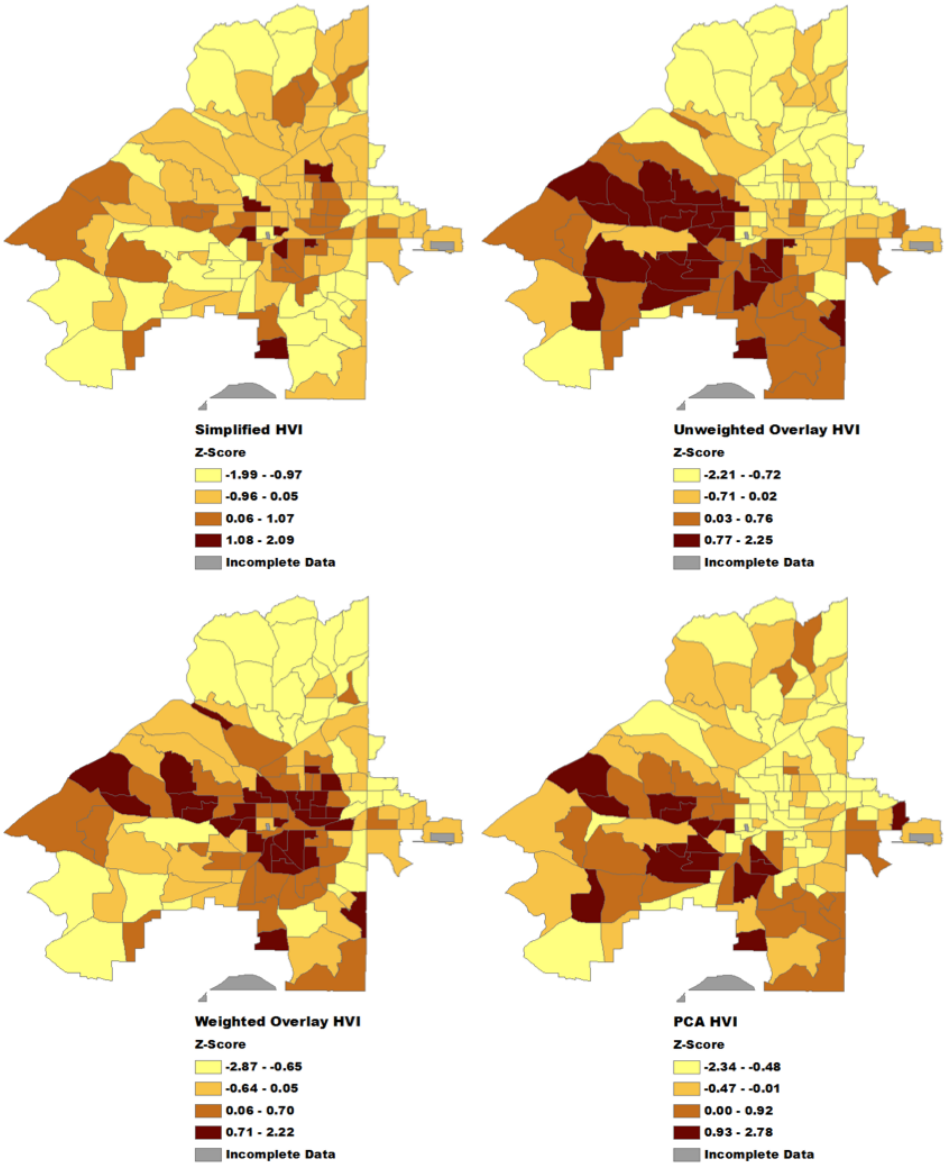

Figure 36 - Atlanta HVI results for all four HVI construction methods, tract-level z-scores

Figure 37 below shows the relationship between Atlanta's gridded population distribution, air temperature, and spatial SAM results at the grid cell level. Here we can see that the spatial SAM follows closely with the population distribution. Additionally, the spatial SAM appears to be modified further by the distribution of elderly population in the west-central portion of the city (see Figure 38). As this population has a particularly high baseline mortality rate, the spatial SAM reflects a sharp increase in mortality in these areas even if total population is relatively low. Figure 39 shows the total spatial-SAM mortality estimates aggregated to the tract level, as well as a death rate per 1,000 population to account for tract size.

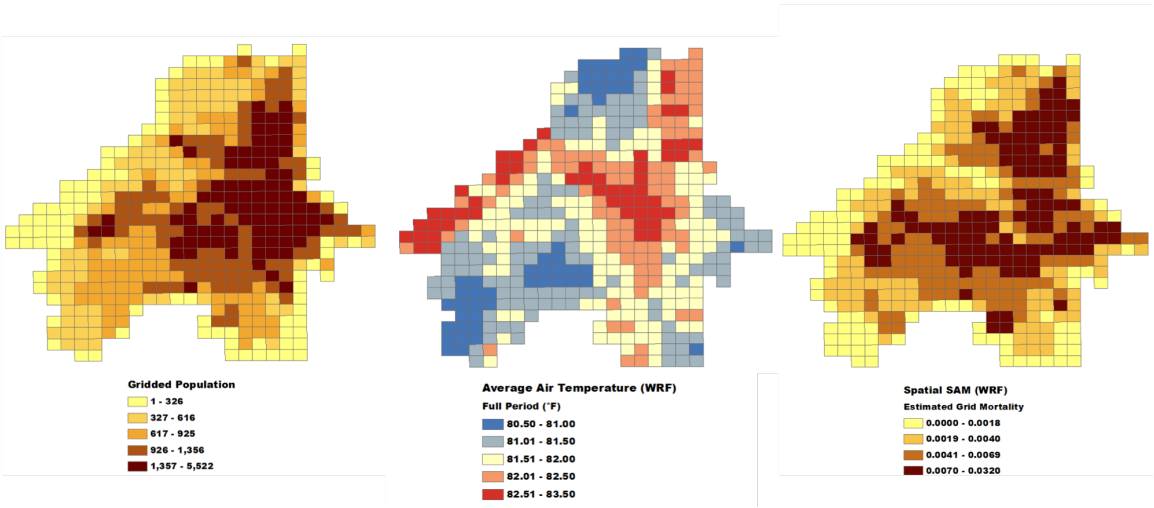

Figure 37 - Atlanta gridded population, WRF temperature, and spatial SAM mortality.

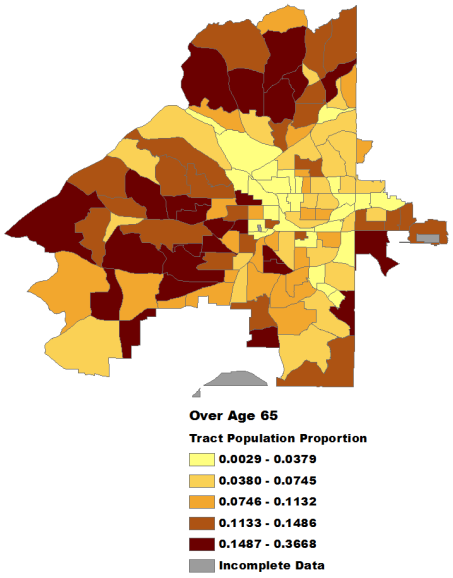

Figure 38 - Atlanta elderly population proportion at the tract level, quantile breaks.

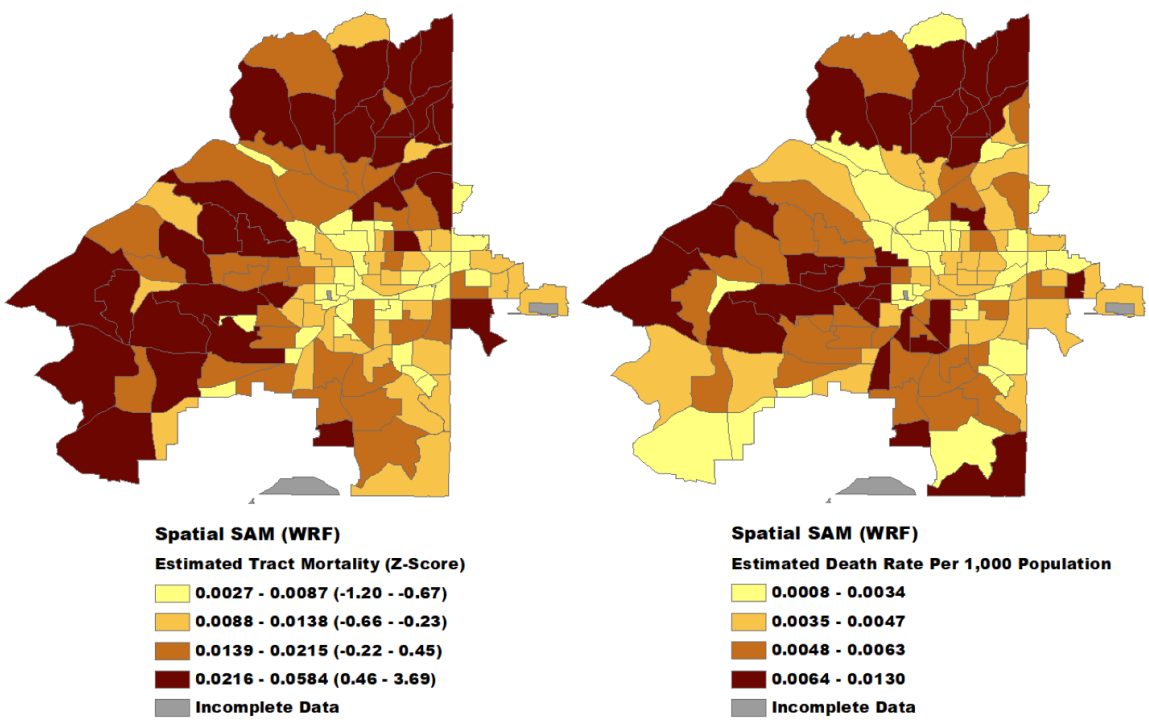

Figure 39 - Atlanta spatial SAM results using WRF inputs, tract-level mortality and death rate per 1,000 population.

The spatial SAM results for Atlanta appear to visually differ from the HVI results, highlighting mostly western and northern tracts away from the urban core. This is further emphasized in the top quartile map below, showing similar western tracts to some of the HVIs, but also some northern tracts that were generally low vulnerability in the HVI results. Figure 40 below shows a side-by-side comparison of the Simplified HVI and the spatial SAM. Though visually much different, the Simplified HVI was found to have the strongest statistical relationship with the spatial SAM results (see Table 24 for full results).

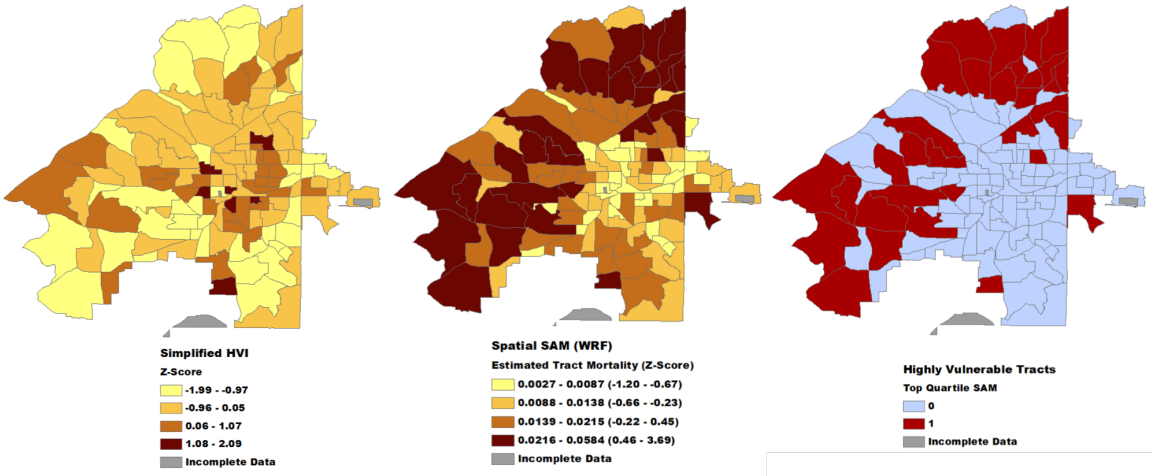

Figure 40 - Atlanta Simplified HVI (left), spatial SAM results (center), and top quartile spatial SAM mortality highlighted (right).

4.3.3 HVI Results – Detroit

The Detroit HVI results also display similarities between each method, mainly highlighting central and eastern tracts near the urban core. However, the spatial SAM again differs from the HVI results, focusing mainly on north-western tracts away from the urban core, with a few high-mortality tracts in the core along the Detroit River.

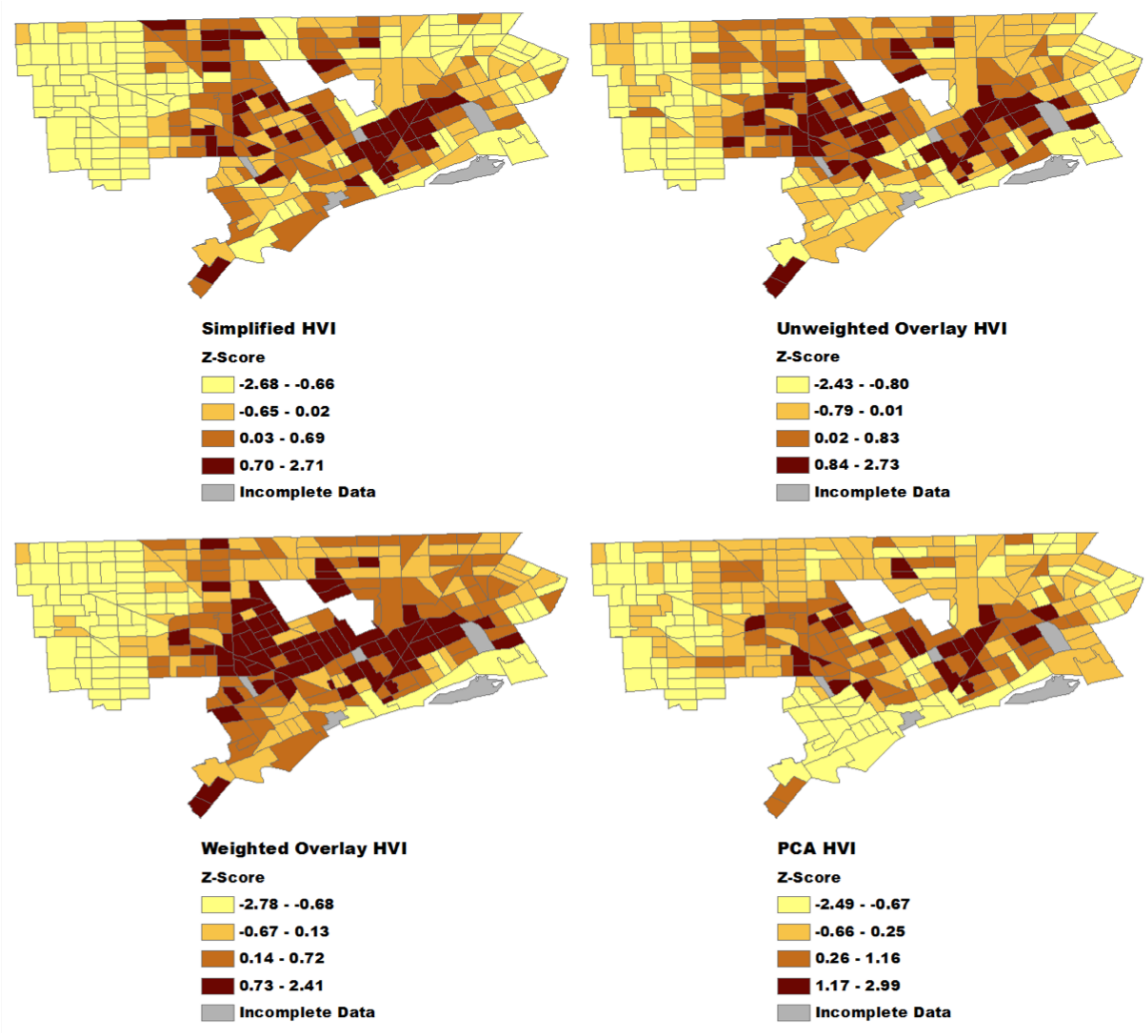

Figure 41 - Detroit HVI results for all four HVI construction methods, tract-level z-scores

Figure 42 below shows the relationship between gridded population, air temperatures, and spatial SAM results at the grid cell level. Similar to Atlanta, the Detroit spatial SAM appears to be mostly driven by the population distribution. However, the effect of temperature is more apparent with a larger area in the west side of the city where air temperatures are warmest.

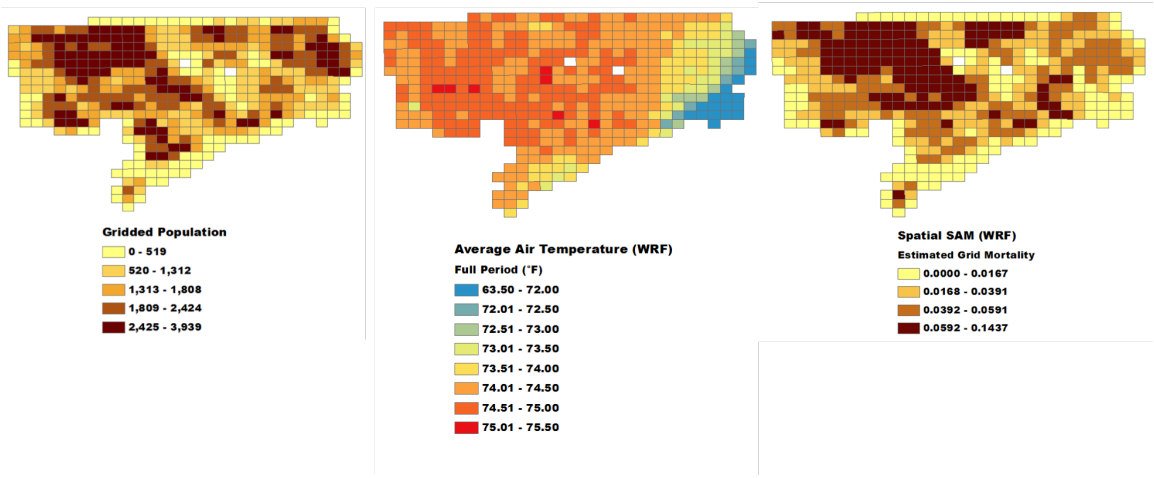

Figure 42 - Detroit gridded population, WRF temperature, and spatial SAM mortality.

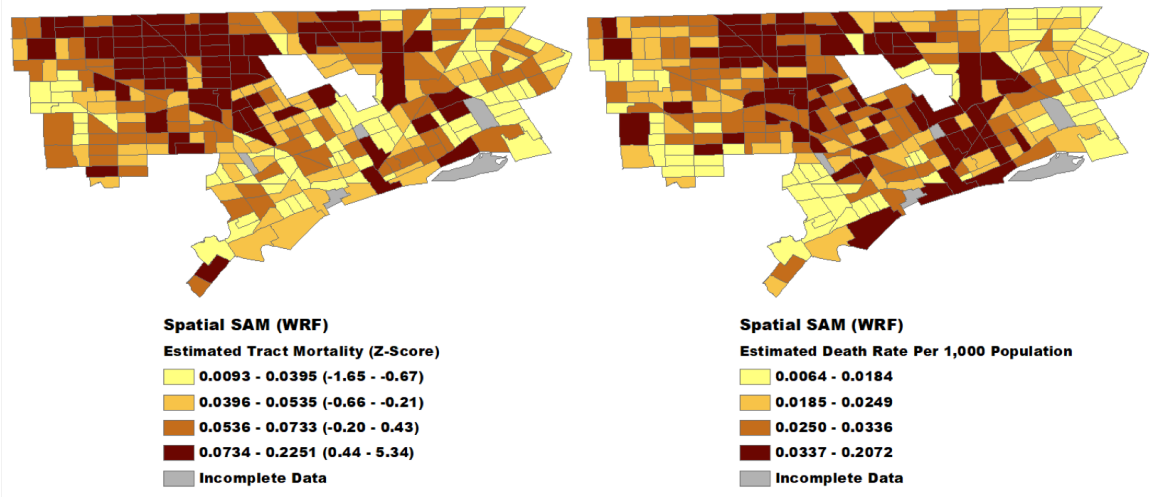

Figure 43 - Detroit spatial SAM results using WRF inputs, tract-level mortality and death rate per 1,000 population.

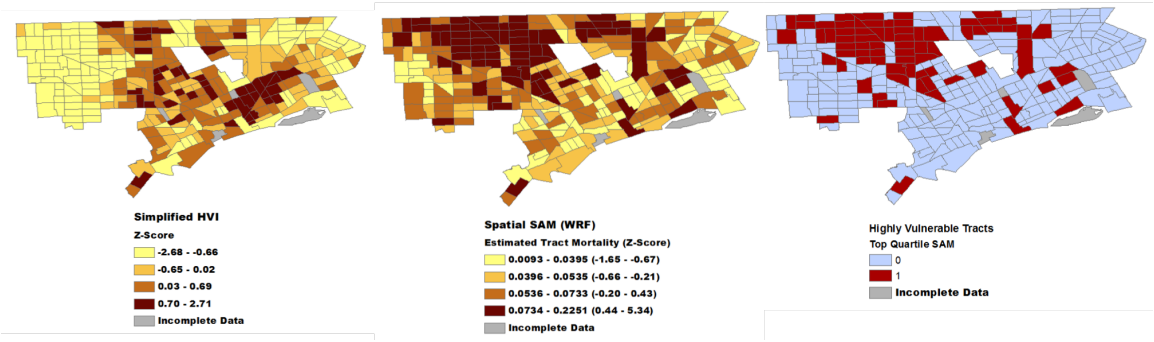

Figure 44 - Detroit Simplified HVI (left), spatial SAM results (center), and top quartile SAM mortality highlighted (right).

4.3.4 HVI Results – Phoenix

The HVI results for Phoenix show some visual similarities, mainly finding highest relative vulnerability in the northern and southern outskirts of the urban core. The Simplified HVI again shows some deviation from the others in highlighting more of the northern tracts than the other three HVI methods. Conversely, the spatial SAM displays the highest mortality in the urban core and in the far south.

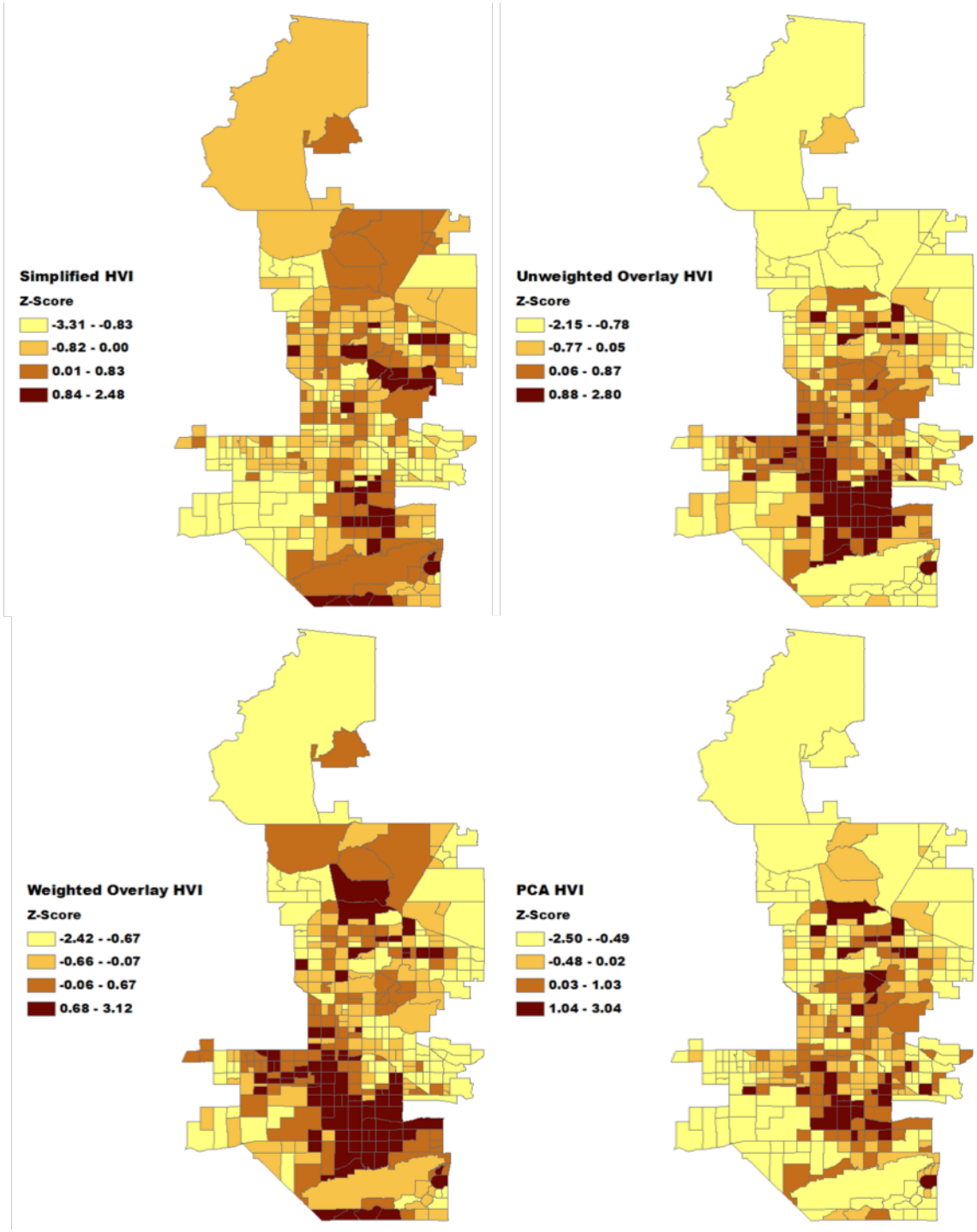

Figure 45 - Phoenix HVI results for all four HVI construction methods, tract-level z-scores

The Phoenix spatial SAM results track very closely with both population and temperature, which are themselves closely related in this case. The cooler northern section and park in the south both accurately reflect the lower vulnerability we would expect from a lower temperature and population. However, once aggregated to the tract level, we see some unexpected results as the park in the south picks up population from nearby grid cells, thereby elevating the spatial SAM results at this scale. This result highlights the significance of the scale of the analysis, as there may be some misleading results depending on the geographies chosen for aggregation.

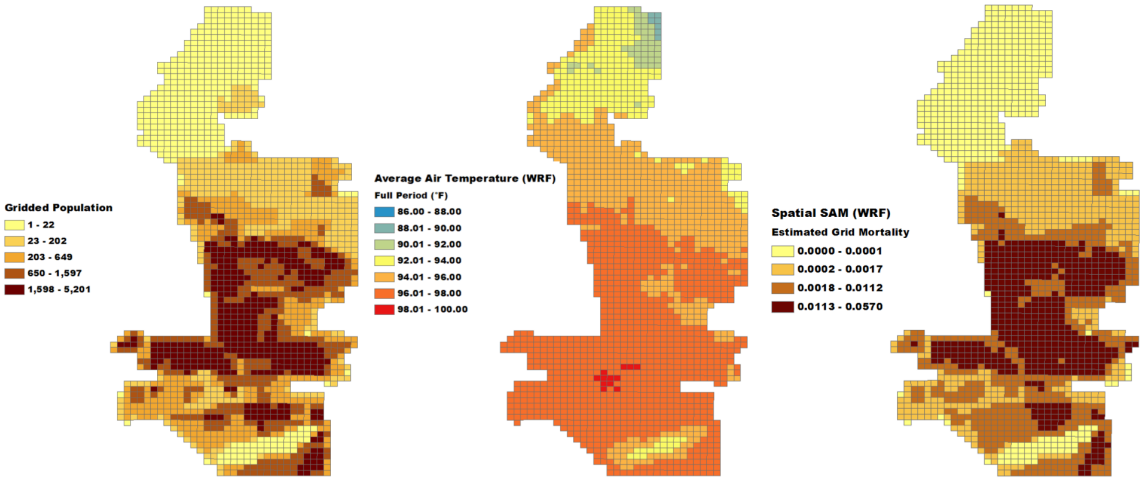

Figure 46 - Phoenix spatial SAM results using WRF inputs, tract-level z-score

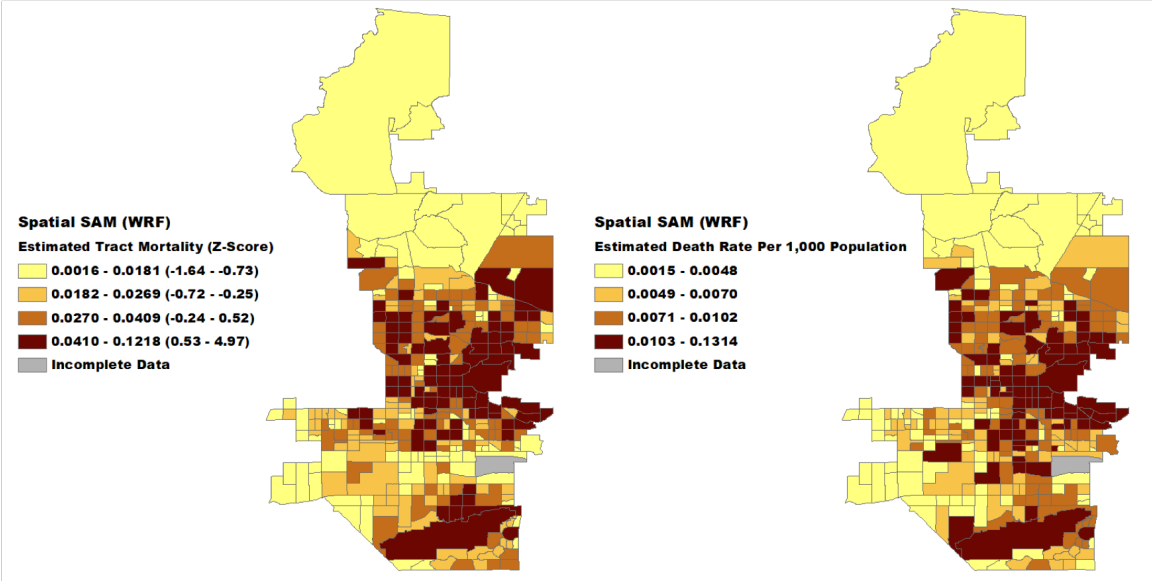

Figure 47 - Phoenix spatial SAM results using WRF inputs, tract-level mortality and death rate per 1,000 population.

For Phoenix, the Unweighted Overlay HVI was most highly correlated with the spatial SAM mortality estimates. Figure 48 below displays a comparison of the HVI and spatial SAM results side-by-side.

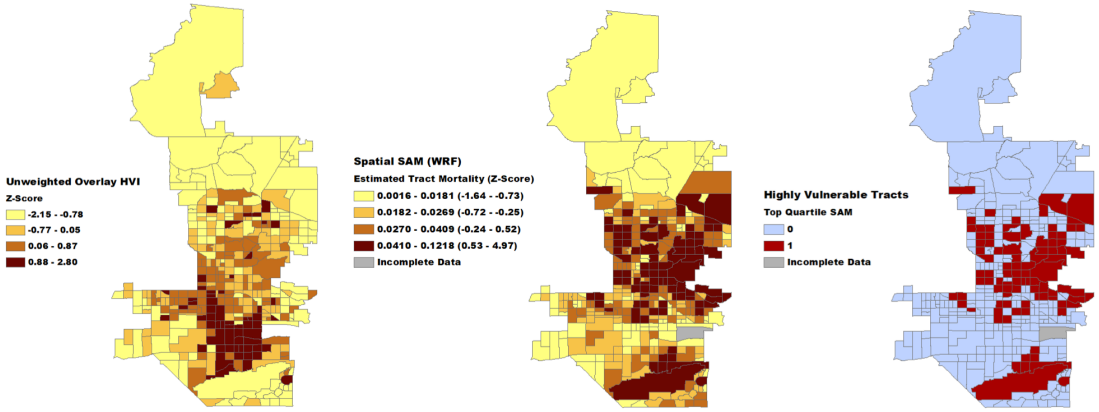

Figure 48 - Phoenix Unweighted Overlay HVI (left), spatial SAM results (center), and top quartile SAM mortality highlighted (right).

4.4 Research Question 1 Results

This section addresses the results of research question 1: *To what extent can established HVI methods predict total heat-related mortality estimates as derived by the statistical attribution method?* The table below shows the R-Square between each HVI construction method and the spatial SAM-derived heat mortality estimates using WRF air temperatures. The numbers in bold highlight the greatest correlation for each city. The Atlanta and Detroit results indicate that construction method does not greatly differ in predicting heat-related mortality. In fact, while the results were close, the simplified HVI using only population over age 65 and land surface temperature appears to have stronger predictive power than the more complex HVI construction methods in Atlanta, and the simplified HVI R-Square matched the PCA R-Square as the highest in Detroit. In the case of Phoenix, the unweighted overlay had the greatest predictive power, and R-Square decreased with the more complex construction methods.

Table 24 - R-Square between HVI methods and WRF spatial SAM mortality.

HVI Construction Method	Atlanta	Detroit	Phoenix
Simplified HVI	**0.43**	**0.40**	0.34
Unweighted Overlay	0.41	0.39	**0.42**
Weighted Overlay	0.41	0.39	0.28
Principal Components Analysis	0.42	**0.40**	0.29

4.5 Research Question 1a Results

Research question 1a asked*: Do different HVI construction methods within the same city produce statistically independent HVI scores?* The results below show results of a paired t-test analysis between each HVI method for each city. With a p-value of 1 for

each of the paired t-tests, these results indicate that the HVI score distributions across each city are not statistically independent across HVI construction models. This further supports the evidence from RQ1 that the HVI construction method does not significantly impact the distribution of HVI scores across the city.

Table 25 - p-value of paired t-test between each HVI z-score for Atlanta.

	Simplified	Unweighted	Weighted	PCA
Simplified				
Unweighted	1			
Weighted	1	1		
PCA	1	1	1	

Table 26 - p-value of paired t-test between each HVI z-score for Detroit.

	Simplified	Unweighted	Weighted	PCA
Simplified				
Unweighted	1			
Weighted	1	1		
PCA	1	1	1	

Table 27 - p-value of paired t-test between each HVI z-score for Phoenix.

	Simplified	Unweighted	Weighted	PCA
Simplified				
Unweighted	1			
Weighted	1	1		
PCA	1	1	1	

4.6 Research Question 1b Results

Research question 1b asked: *To what extent can HVI scores predict the top quartile of vulnerability as determined by the statistical attribution method?* The table below shows Tjur's R-Square between each HVI z-score and the top quartile of SAM mortality in the binary logistic regression. While these R-Square values are much lower than the R-Square results in RQ1, they do allow for a comparison between each model. In this analysis, the correlation between HVI score and top quartile spatial SAM differed for each model between the three cities. The Weighted Overlay showed the strongest for Atlanta, while the PCA was the strongest in Detroit, and the Simplified HVI was strongest in Phoenix.

Table 28 - Tjun R-Square between each HVI z-score and top quartile SAM mortality.

	Atlanta	Detroit	Phoenix
Simplified	0.0007	0.0019	**0.0510**
Unweighted	0.0052	0.0060	0.0082
Weighted	**0.0093**	0.0055	0.0087
PCA	0.0001	**0.0117**	0.0069

4.7 Research Question 2 Results

Research question 2 explores the relationship between individual indicators of vulnerability used in the HVI and the WRF-derived spatial SAM mortality estimates. This question asked: *Which heat vulnerability indicators are significant predictors of heat-related mortality as derived by the statistical attribution method?* The tables below show the multiple spatial regression results for the individual vulnerability indicators and the spatial SAM mortality at the tract level for each city. The p-values less than 0.1 are displayed in bold.

Table 29 - Atlanta regression results for HVI indicators and spatial SAM mortality.

Variable	B	Std.Error	z-value	p-value
W	**0.4214**	**0.1011**	**4.1657**	**<0.001**
Constant	0.0297	0.0379	0.7823	0.4340
Diabetes	-0.0149	0.0316	-0.4726	0.6365
No AC Access	0.1168	0.6274	0.1862	0.8523
Over Age 65	**0.0754**	**0.0171**	**4.4102**	**<0.001**
NonWhite	0.0007	0.0052	0.1437	0.8858
Less than High School Education	-0.0025	0.0125	-0.1982	0.8429
Poverty	-0.0108	0.0079	-1.3643	0.1725
Living Alone	-0.0037	0.0179	-0.2043	0.8381
Land Surface Temperature	-0.0002	0.0004	-0.6596	0.5095

Table 30 - Detroit regression results for HVI indicators and spatial SAM mortality.

Variable	B	Std.Error	z-value	p-value
W	**0.5320**	**0.0632**	**8.4223**	**<0.001**
Constant	-0.0379	0.0920	-0.4118	0.6805
Diabetes	0.0485	0.0727	0.6669	0.5048
No AC Access	0.7186	0.5091	1.4113	0.1582
Over Age 65	**0.1104**	**0.0365**	**3.0264**	**0.0025**
NonWhite	0.0139	0.0134	1.0335	0.3014
Less than High School Education	-0.0056	0.0169	-0.3314	0.7404
Poverty	**-0.0357**	**0.0131**	**-2.7273**	**0.0064**
Living Alone	-0.0572	0.0462	-1.2362	0.2164
Land Surface Temperature	-0.0002	0.0006	-0.3900	0.6965

Table 31 – Phoenix regression results for HVI indicators and spatial SAM mortality.

Variable	B	Std. Error	z-value	p-value
W	**0.3468**	**0.0619**	**5.6056**	**<0.001**
Constant	0.0227	0.0272	0.8327	0.4050
Diabetes	0.0389	0.0586	0.6644	0.5064
No AC Access	-0.0177	0.2833	-0.0626	0.9501
Over Age 65	**0.2075**	**0.0231**	**8.9808**	**<0.001**
NonWhite	**0.0137**	**0.0071**	**1.9366**	**0.0528**
Less than High School Education	0.0048	0.0098	0.4946	0.6209
Poverty	-0.0114	0.0090	-1.2686	0.2046
Living Alone	-0.0384	0.0282	-1.3637	0.1727
Land Surface Temperature	-0.0002	0.0002	-0.8763	0.3808

Across all three cities, elderly population appeared to be the most significant indicator of heat-related mortality. In Atlanta, this was the only significant indicator of heat-related mortality. In Detroit, poverty was found to be a significant predictor of heat-related mortality, and in Phoenix, nonwhite was also a significant predictor. Surprisingly, Land Surface Temperature was not a significant indicator in any of the three cities. However, this could be due to the inclusion of the lag term, W, in the spatial regression. This term includes the effects of each adjacent tract when using first-order queen contiguity. The significance of W could mean that it is picking up a strong temperature signal that is multicollinear with the individual tract's temperature value due to the overall smoothness of the variable. With the exception of stark land cover differences like land to water, adjacent tracts are likely to display similar LST. This effect of the spatial regression may be why LST was not found to be significant.

To explore this lack of LST significance further, I conducted an additional bivariate regression analysis between the WRF-derived average air temperatures and the MODIS-derived land surface temperatures averaged to the same WRF grid for each city. The differences between the two datasets are illustrated in the figures below. Both maps use quantile breaks to highlight relative differences in temperature distribution across the city. The results of the regression analysis are shown in Table 32 below.

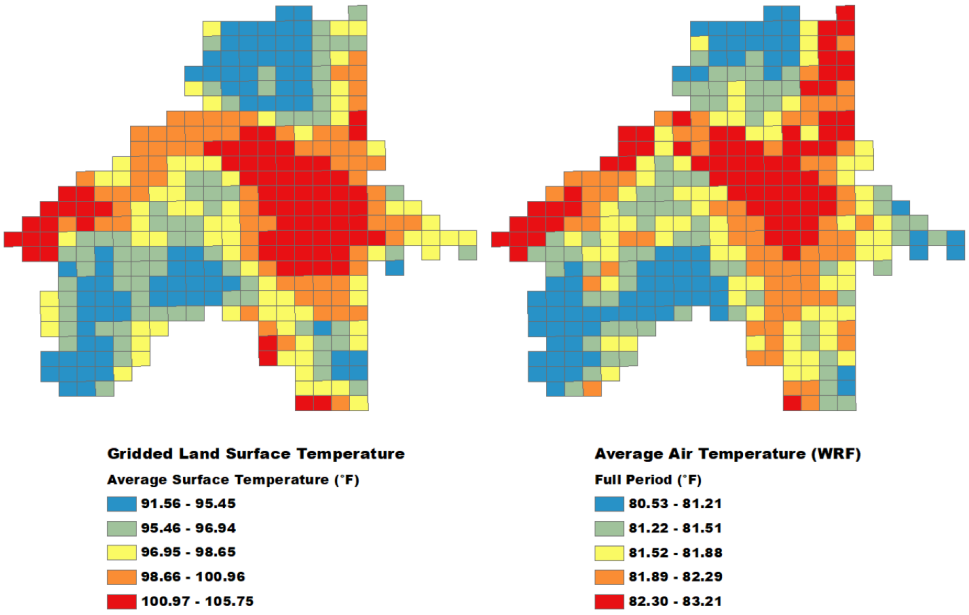

Figure 49 – Comparison of Atlanta LST (left) and WRF air temperature (right).

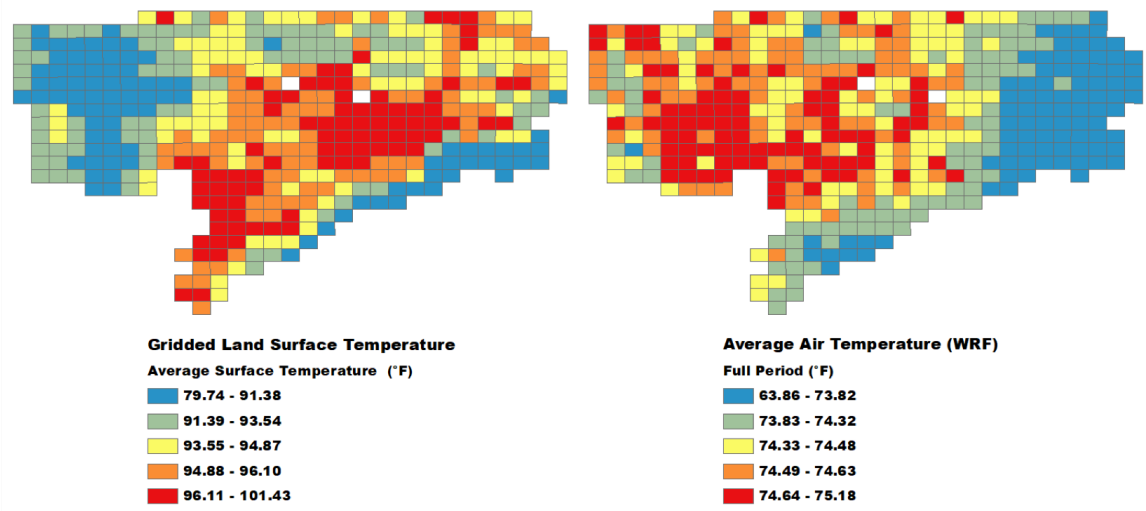

Figure 50 - Comparison of Detroit LST (left) and WRF air temperature (right).

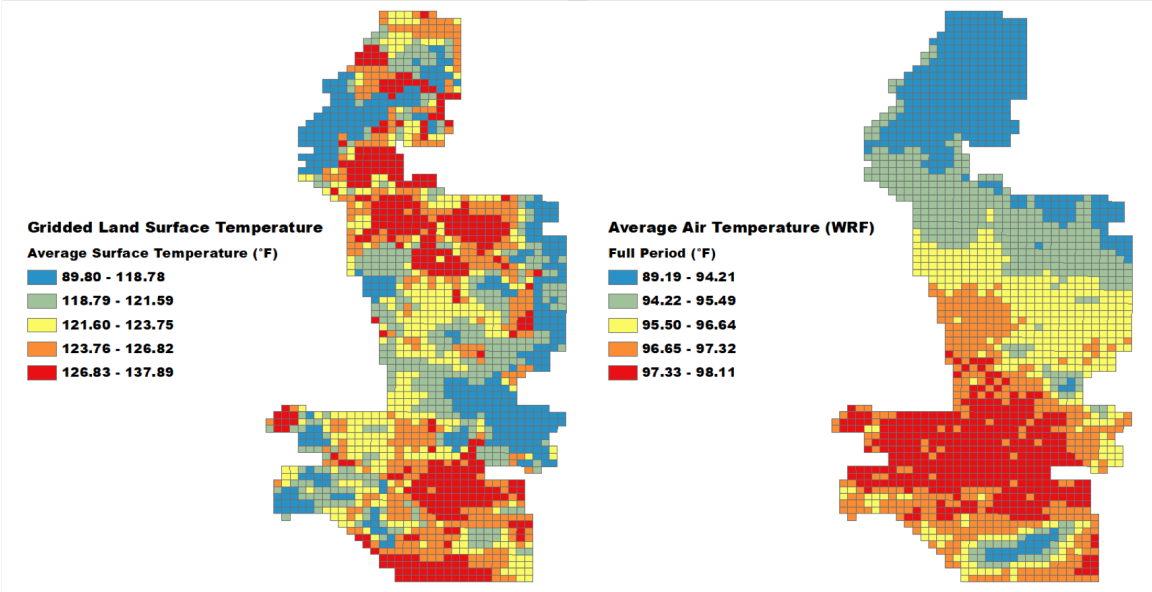

Figure 51 - Comparison of Phoenix LST (left) and WRF air temperature (right).

Table 32 - R-Square between gridded LST and WRF-derived average air temperature.

	Atlanta	Detroit	Phoenix
R-Square	0.5777	0.1387	0.0024

These results indicate that the relationship between LST and WRF-derived air temperature vary widely by city. Though not significant in the final analysis, Atlanta's LST distribution matches fairly well with the air temperature. However, this relationship is far weaker in Detroit. Here the LST is much higher near the urban core by the Detroit River in the east, while the air temperatures are more moderate in this area, and generally warm up as distance from the river increases. In Phoenix, the unique land cover dynamics of the desert environment result in a very weak relationship between LST and air temperature. Here, land surface temperatures are much warmer in the north where air temperatures are much cooler. The R-Square here is simply an indication of the strength of the relationship between LST and air temperature. However, this relationship may not be linear. But it is

clear that the spatial distribution does not match well between the two variables, particularly in Detroit and Phoenix. From an HVI perspective, this relative distribution is more important than the precise relationship between the two variables.

4.8 Discussion

The results of these analyses show that the choice of using an HVI or a spatial SAM as a decision support tool can influence the result, thereby influencing the resultant policy and investment of a city to address heat vulnerability. While the results of RQ1a indicate that no HVI construction method is statistically distinct from another, there are minor differences between each result. This was most readily apparent in the Simplified HVI results for Atlanta and Phoenix, which showed some notably distinct spatial patterns in the highest vulnerability tracts as compared to the other three methods. More importantly, no HVI construction method explained more than 43.3% of the variation in spatial SAM outcomes. This indicates that HVI methods may not adequately predict statistically attributed mortality across a city. In all three cities, the HVI outcomes produced patterns of high vulnerability that differed greatly from the spatial SAM. Furthermore, from the results of RQ1b, no HVI method showed a high correlation with the top quartile of spatial SAM outcomes. If cities are indeed using these decision support tools to identify the areas of highest priority, then the choice of model has shown to be influential in determining those outcomes. This has major implications on the utility of HVI methods as a decision support tool to protect the most vulnerable populations from heat risk.

Additionally, the results of RQ1 suggest that highly complex HVI methods are less likely to predict spatial SAM outcomes. In all three cities, simpler models actually

performed better in general than the more complex models when compared to the spatial SAM. This result is likely due to the influence of elderly population in both the Simplified HVI and the spatial SAM, as the baseline mortality rates are highest among that age cohort. A Simplified HVI composed of elderly population and population density would also have likely correlated well with the spatial SAM, as the mortality estimates tracked closely with the population distribution within each city. The top quartile analysis in RQ1b showed more mixed results, with no strong trend in which model fit best, but the fact that the two least complex HVI methods performed best in all three cities suggests that complex statistical models like PCA may be obscuring the true vulnerability with unnecessary confounding indicators.

In RQ2, it was found that very few indicators significantly predict statistically attributed mortality. Heat sensitivity and adaptive capacity indicators were found to be more significant predictors of heat-related mortality than the primary exposure variable. However, this may be due to the observed low correlation between LST and air temperature observed here and corroborated in the literature (Ho et al., 2016; Weng, 2009). This analysis further indicates that LST may not be an adequate predictor of air temperatures, which are more relevant to human health outcomes. LST is all the more problematic as an HVI indicator in locations such as Phoenix, where sparsely populated desert landscapes display much warmer surface temperatures than the vegetated urban areas. However, Jenerette et al. (2012) found that it is primarily wealthy residents with high adaptive capacity who can afford to establish and maintain vegetation in Phoenix, known as the "luxury effect." The urban areas without vegetation and thus higher LST may also have more vulnerable residents with lower adaptive capacity.

One limitation of this analysis is that the HVI is not as sensitive to population as the spatial SAM. An area with low population can still have high vulnerability if the population, housing, and built environment characteristics of that tract indicate high vulnerability. But from a planning and policy perspective, cities strive to optimize the cost effectiveness of their heat response strategies, protecting the most people with the least amount of public investment. Thus, the spatial SAM's sensitivity to both temperature and population is appropriate in identifying the locations where the greatest quantities of people will be impacted by heat. While not used in this study, it may be useful to modify HVI outcomes by population or include population density as a vulnerability indicator in the HVI to better replicate the spatial SAM outcomes and prioritization.

4.9 Conclusion

This chapter explained the methods and findings for Research Questions 1, 1a, 1b, and 2. The findings of these analyses suggest that in the end, HVI methods may not adequately predict statistically attributed heat mortality to justify public investment guidance. The results of Research Question 2 also suggest that complex HVI methods may include more indicators than are necessary to identify relative spatial priority similar to the spatial SAM outcomes. These findings would suggest that a spatial SAM may be a more appropriate method to guide investment to protect the most vulnerable population centers. But given the high complexity and cost of running WRF, it is a difficult choice for cities to move forward with the analysis. In the following chapter, I explore the potential to replace WRF with more accessible air temperature datasets.

CHAPTER 5. SPATIAL SAM EXPOSURE SOURCE ANALYSIS

5.1 Introduction

This chapter primarily deals with Research Question 3 on improving the accessibility of the spatial SAM model. As detailed in Chapter 2, one major strength of HVI studies is that they primarily focus on publicly available datasets such as the US Census or remotely sensed data for ease of construction. This makes HVI methods generally accessible tools for the average urban planning or public health practitioner by leveraging common skills and training in GIS. However, no similar attempt has been made to improve the accessibility of the spatial SAM method by using publicly available datasets as the air temperature input. This chapter seeks to address that gap by replacing the WRF temperature inputs with airport weather station data and the Daymet air temperature model.

5.2 Method Details

In this section, I explain the data acquisition and processing for the publicly available air temperature datasets as alternative inputs to the spatial SAM model, including airport weather stations and Daymet modeled air temperatures.

5.2.1 Airport Temperature

For the airport data, I used the same GHCND dataset detailed in section 4.2.2.4 on the MODIS data acquisition procedure. For this analysis, I replaced the WRF gridded temperature uniformly with the daily average temperature readings from the airport weather station in each city for each day in the target period. The spatial SAM R script was

then run using the same population cohort data, but with a weather station period average temperature.

5.2.2 Daymet Temperature

For a slightly more complex model, I used the Daymet V3 Daily Gridded Surface Data, available at 1km resolution across all of North America from the Oak Ridge National Laboratory (Turner et al., 2006). See Thornton et al. (1997) for more information on the creation of this dataset. This data was downloaded from the NASA EarthData tool. The data is available in NetCDF format for daily minimum temperature and daily maximum temperature. For the purposes of this analysis, I averaged the Tmin and Tmax to generate a daily average temperature for use in the spatial SAM.

As the data is only available for an entire year at a time, for the entire domain of North America, further processing was necessary to reduce it to a manageable size for this analysis. The data was processed in R using the "raster" library to identify only the relevant dates to match the target period and XY coordinates of each city's local domain. The Daymet dates are recorded as DOY, or "Day of Year" rather than the date, so I used the following indices for each city:

Table 33 - Dates indices used in Daymet analysis.

	Atlanta	**Detroit**	**Phoenix**
Start Date	8/5/95	6/8/94	7/11/06
End Date	8/25/95	6/26/94	8/1/06
Start DOY	217	159	192
End DOY	237	177	213

As both the Daymet dataset and WRF grids use the Lambert Conformal Conic (meters) projection, I was able to identify the coordinates of the bounds, or the extent, on each WRF grid layer in ArcGIS. In the R script, I was able to extract Daymet data only within the bounds of space and time for each city's location and target period for Tmin and Tmax, then average these two to create a daily average temperature for each city over the target period.

To match the Daymet data with the WRF grid, I first plotted the Daymet data as XY points in ArcGIS. I then used a spatial join to attribute all of the Daymet data to the nearest WRF grid cell centroid. In the spatial SAM script, I used an average of the entire target period for each city as the input temperature in place of the WRF-derived air temperatures.

5.2.3 Model Comparison

To compare the three different spatial SAM models, I ran the spatial SAM R script with each separate temperature model input using the same population cohort data for each. I then aggregated each gridded mortality estimate to the tract level using the procedure detailed in section 4.2.4.4. Once all spatial SAM mortality data were aggregated to the tract level, I used a paired t-test to test for statistical independence between the model results, similar to the procedure for RQ1a detailed in Section 4.2.5.2.

5.3 Results

In this section, I present the results of the air temperature model analysis, answering Research Question 3: *to what extent can the WRF-driven statistical attribution method be replicated using publicly available data sources?*

5.3.1 Air Temperature Results

First, I begin by showing the differences between each air temperature model over the target period for each study city, including both a full period average and a heat wave-only version to show how the datasets perform between the different temperature regimes. All temperature maps are displayed using common air temperature break points to highlight the differences between each model.

5.3.1.1 Atlanta

The figures below show Atlanta's average air temperature over the full period as well as the heat wave period alone. In the case of Atlanta, the airport was relatively cool as compared to the WRF model but was warmer than much of the Daymet model. While Daymet was generally cooler than the WRF model, it does show the outline of some temperature differentiation in the west side of the city. However, the model does not capture the extremes of the urban heat island as well as the WRF model. During the heat wave period, the airport was generally much warmer than the Daymet model, but again not as warm as the hotter urban areas of Atlanta shown in the WRF model. This shows how volatile the airport station can be depending on temperature regime, which when applied

to the entire city can result in much warmer and much cooler temperatures as compared to WRF.

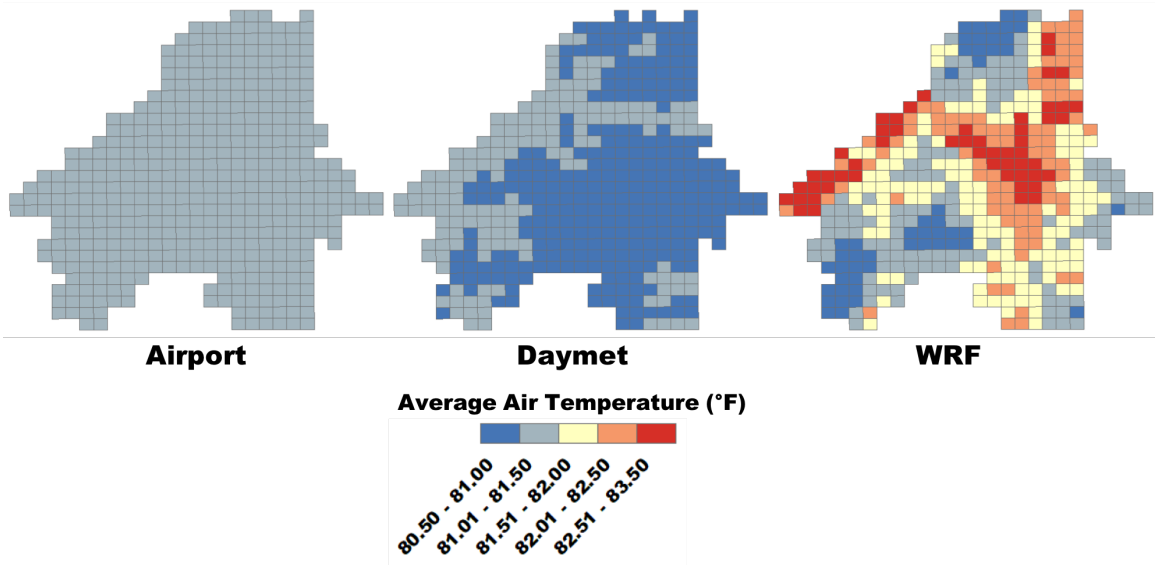

Figure 52 - Comparison of Atlanta air temperatures for Airport, Daymet, and WRF (full period average)

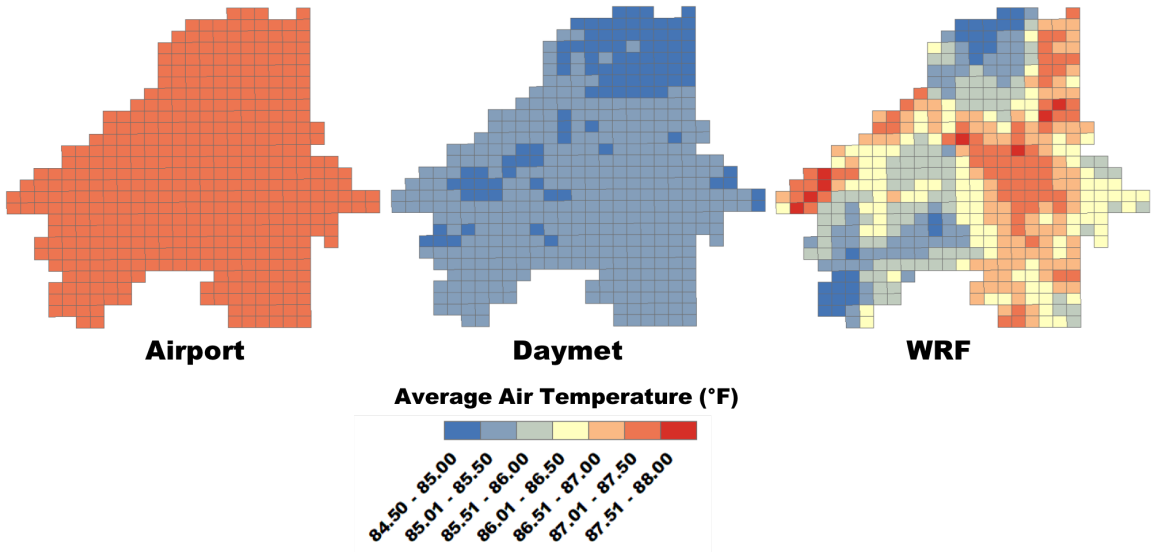

Figure 53 - Comparison of Atlanta air temperatures for Airport, Daymet, and WRF (heat wave period average)

5.3.1.2 Detroit

Detroit displays some clear temperature trends across the city. In general, the airport was very warm compared to the rest of the city. This case highlights how the airport may not be a good representation of an entire city, as it has landcover that does not necessarily reflect the landcover of the rest of the city. There is also a clear gradient across the city for both the Daymet and WRF datasets, but in different directions. While the full period Daymet average shows a north-south gradient, the WRF model shows more of an east-west gradient with cooler temperatures by the Detroit River and increasing temperatures further from the water. However, this trend seems to be well represented in the heat wave period for both Daymet and WRF.

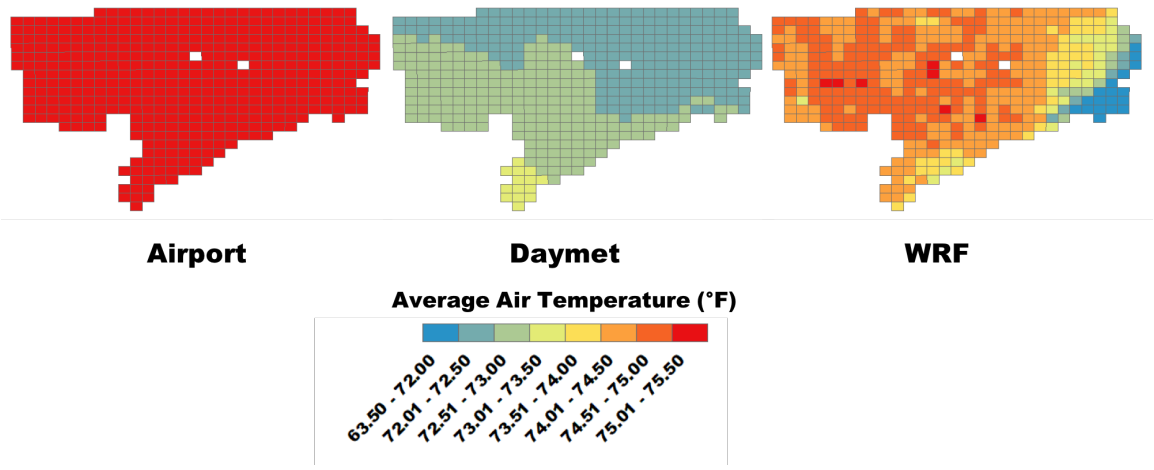

Figure 54 - Comparison of Detroit air temperatures for Airport, Daymet, and WRF (full period average)

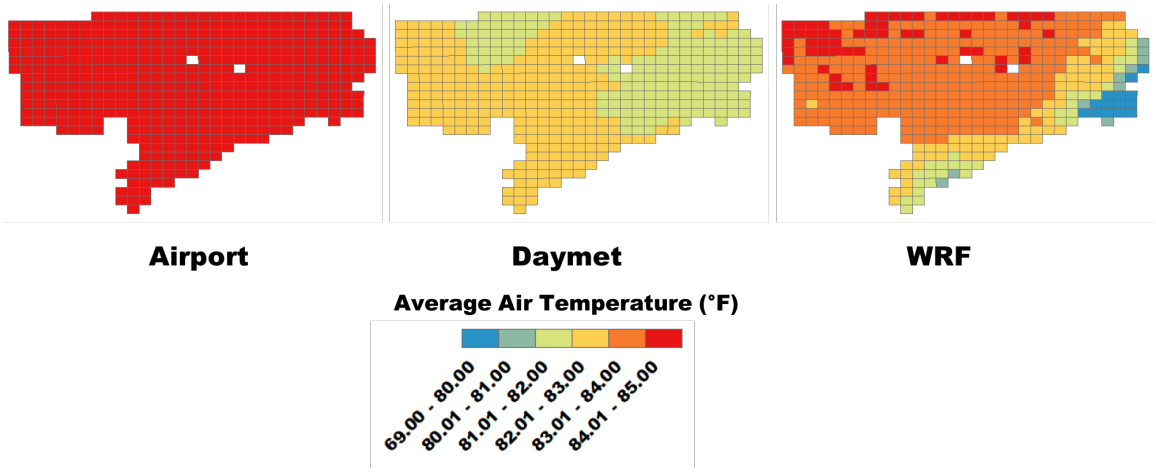

Figure 55 - Comparison of Detroit air temperatures for Airport, Daymet, and WRF (heat wave period average)

5.3.1.3 Phoenix

For Phoenix, the airport fell on the warmer end of the scale, but not as extreme as the Detroit case. Daymet appears to perform much better in Phoenix than in the other two cities. This may be due to the large size of Phoenix as compared to the other two, providing more opportunities for heterogeneity in land cover such as topography. The relatively cool areas in the south and north ends of Phoenix, apparent in both Daymet and WRF, are actually mountains. The north cool spot is the Phoenix Sonoran Preserve, while the cool spot in the south is the South Mountain Park and Preserve. This shows that Daymet may perform fairly well over large areas where there is stark difference in topography, but may not perform well in relatively flatter, more homogeneous areas like Atlanta.

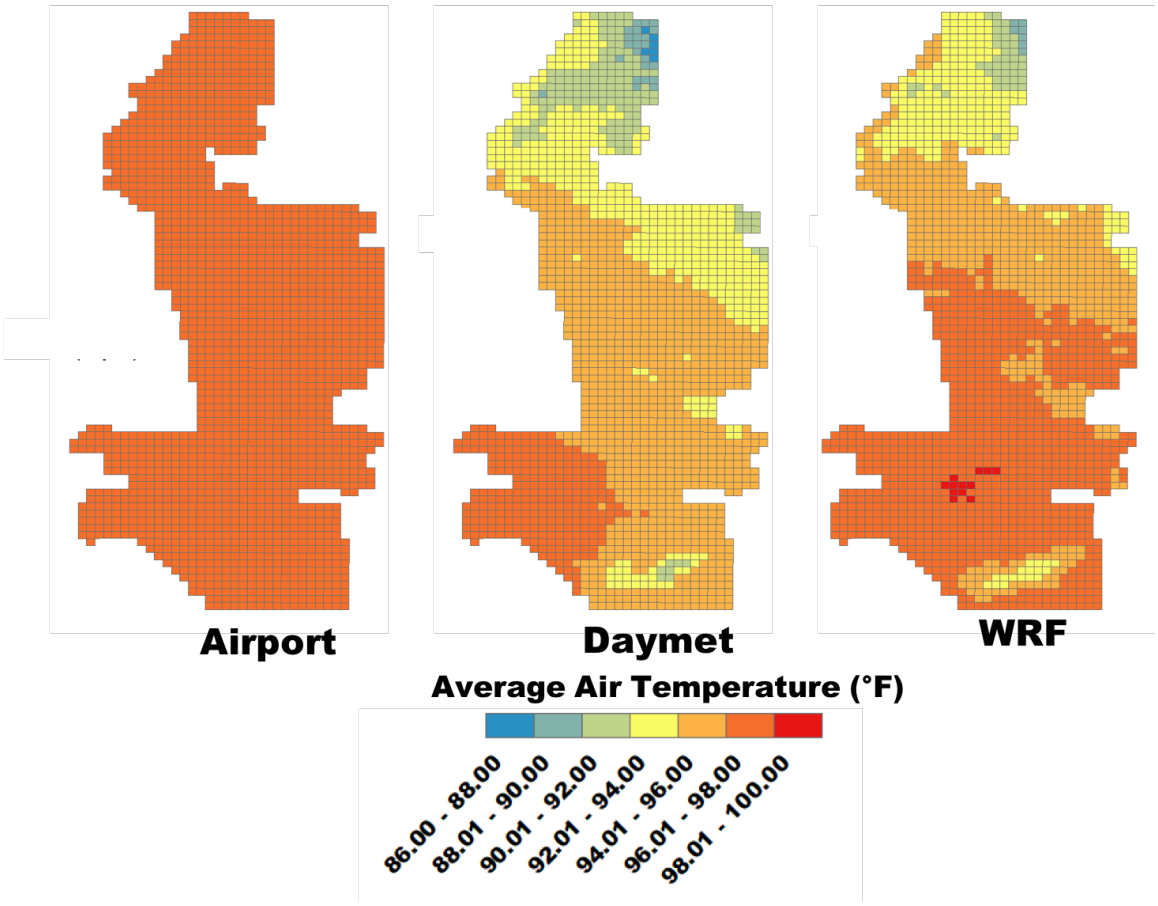

Figure 56 - Comparison of Phoenix air temperatures for Airport, Daymet, and WRF

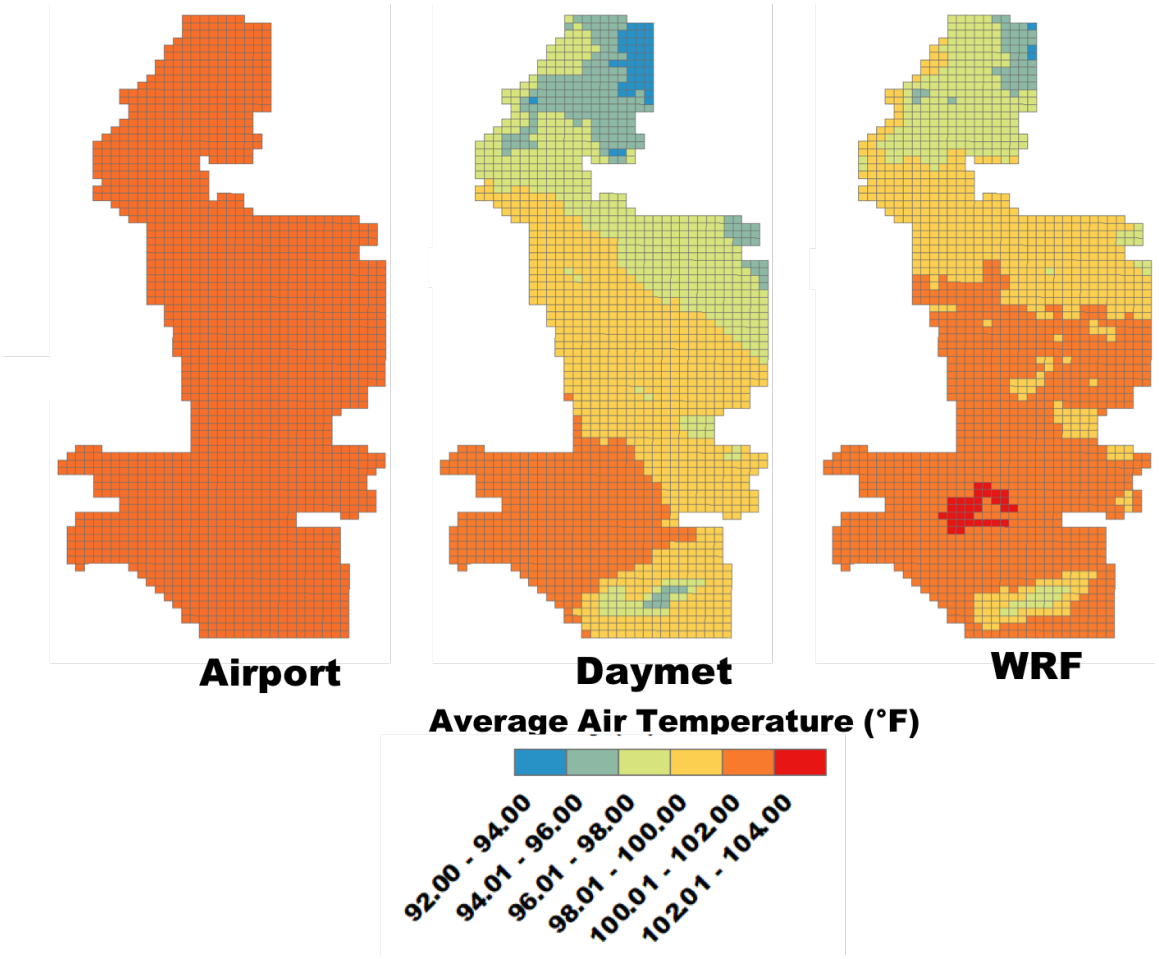

Figure 57 - Comparison of Phoenix air temperatures for Airport, Daymet, and WRF (heat wave period average)

5.3.2 Spatial SAM Results

Table 34 below shows the total spatial SAM mortality across each air temperature dataset for the target period. These results show that the temperature model can lead to large differences in the total mortality, particularly if the model resulted in large temperature differences. The airport data resulted in large deviations from the WRF model for Detroit and Phoenix, as it was generally warmer than the rest of the city. As shown in section 5.3.2.2, the Detroit Airport was much warmer than the rest of the city, and as a result, inflated the spatial SAM mortality for the city. The same result was found in

Phoenix. Daymet was generally the coolest model of the three and under-estimated the total spatial SAM mortality as compared to WRF. Table 34 below shows the total spatial SAM mortality estimates across each city and temperature dataset. In parentheses are listed the percentage change from WRF for both the airport and Daymet datasets.

Table 34 - Total spatial SAM mortality for each air temperature dataset in each city and percentage change from WRF-derived mortality estimates.

	Atlanta	Detroit	Phoenix
WRF	2.23	18.65	11.48
Daymet	1.76 (-21.08%)	14.78 (-20.75%)	7.05 (-38.59%)
Airport	2.47 (+10.87%)	23.70 (+27.08%)	16.74 (+45.82%)

5.3.2.1 Atlanta Spatial SAM Comparison

In this section, I present the mortality results for the three temperature models to compare the results visually. The results are presented as quartiles for a clear comparison of relative risk. In the tract maps, the spatial SAM is reported as both total tract mortality and tract z-score. The end of each section includes the gridded 2010 population for convenient comparison, as the spatial SAM model has been shown to be highly sensitive to population distribution as well as temperature.

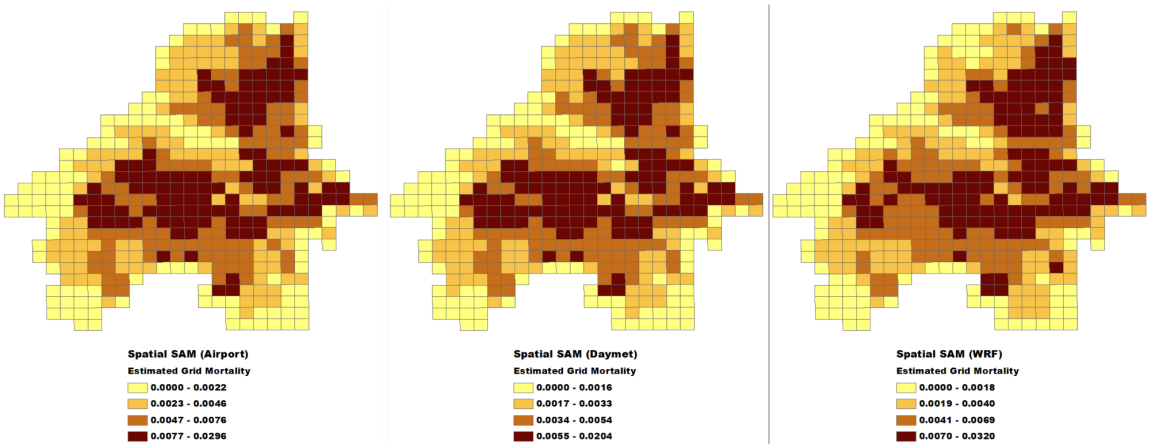

Figure 58 - Atlanta gridded spatial SAM results for Airport, Daymet, and WRF temperature inputs.

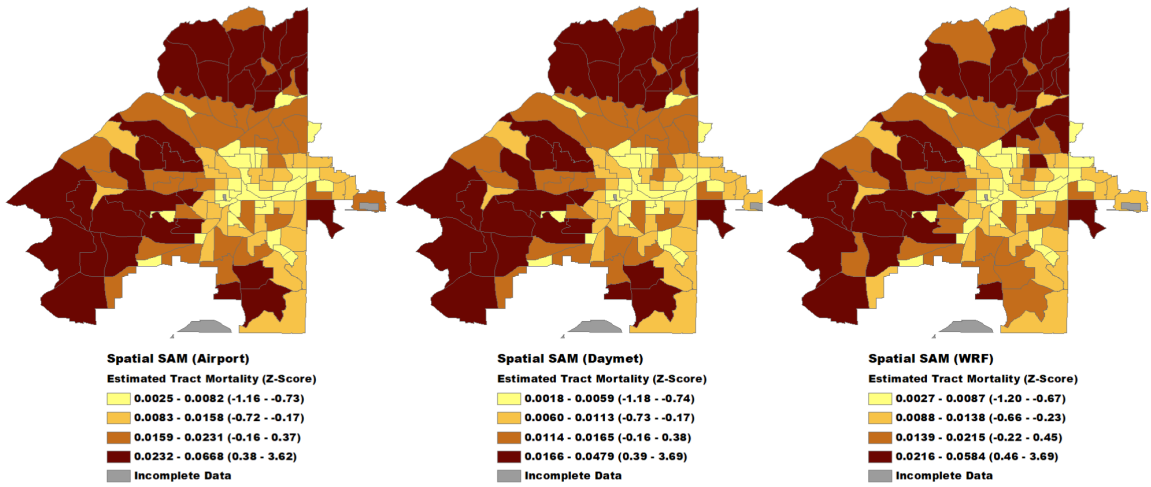

Figure 59 - Atlanta spatial SAM results for Airport, Daymet, and WRF temperature inputs, tract level mortality.

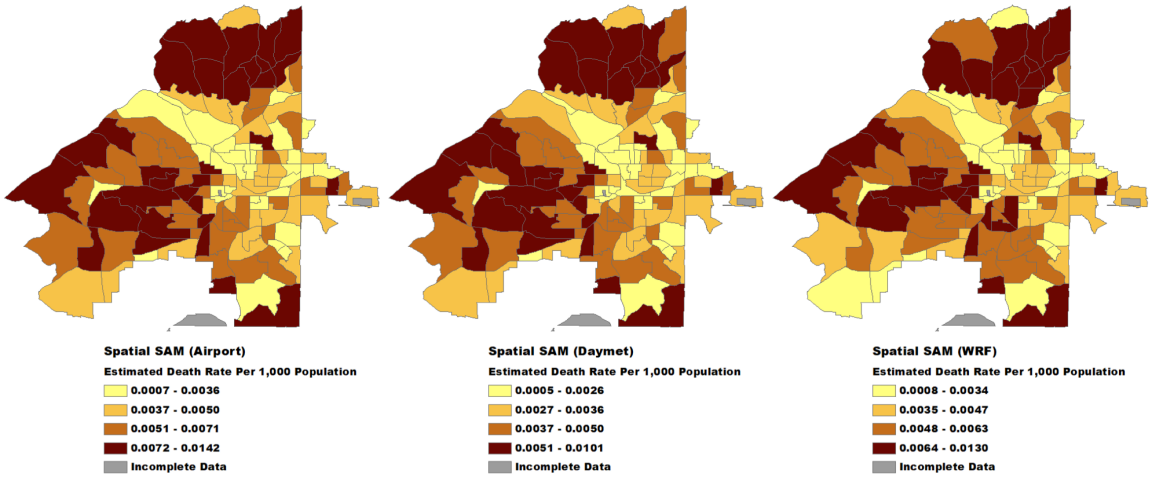

Figure 60 - Atlanta spatial SAM results for Airport, Daymet, and WRF temperature inputs, normalized to deaths per 1,000 population in tract.

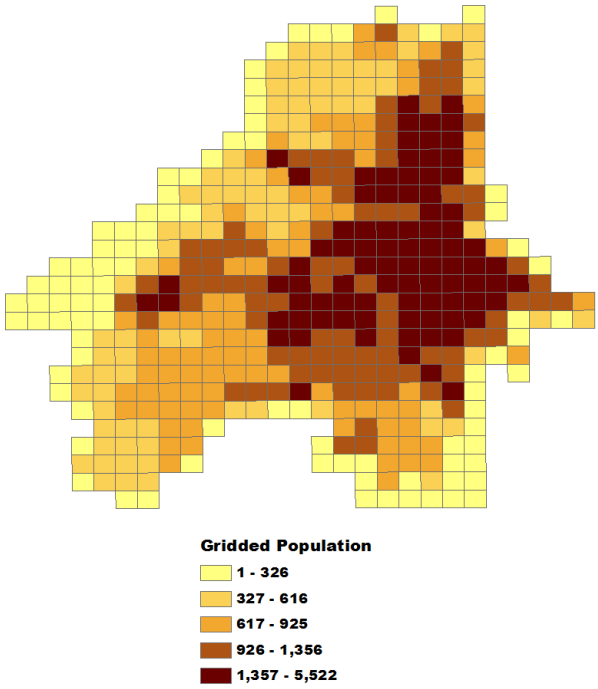

Figure 61 - Atlanta 2010 gridded population.

Visually, the trends between all three cities are very similar. Each model highlights similar areas of the city, with only small variations in gridded and tract priority. Even

applying the airport temperatures uniformly across a city still shows heterogeneous distribution in mortality, as the model is also sensitive to population centers across the city.

5.3.2.2 Detroit Spatial SAM Comparison

Like Atlanta, the spatial distribution of mortality appears similar between the three temperature models in Detroit at both the gridded and tract scale, with only minor variations between the models.

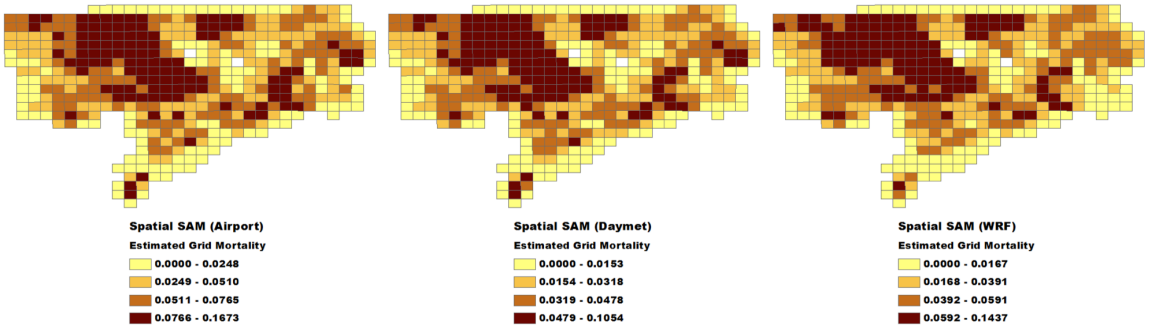

Figure 62 - Detroit gridded spatial SAM results for Airport, Daymet, and WRF temperature inputs.

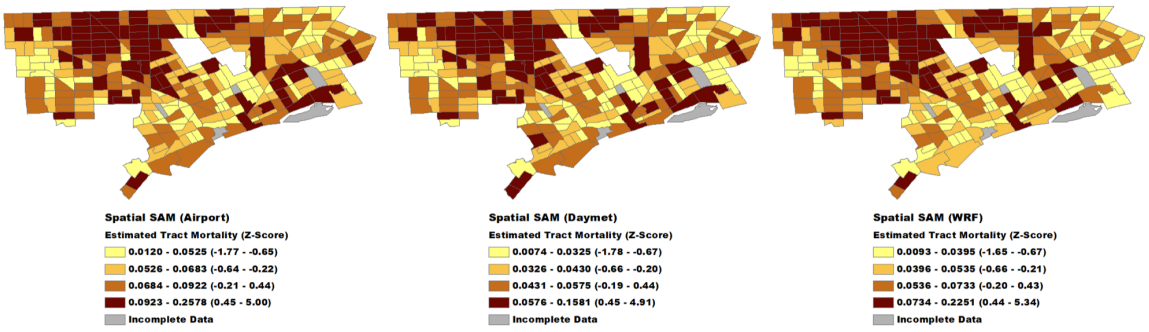

Figure 63 - Detroit spatial SAM results for Airport, Daymet, and WRF temperature inputs, tract level mortality.

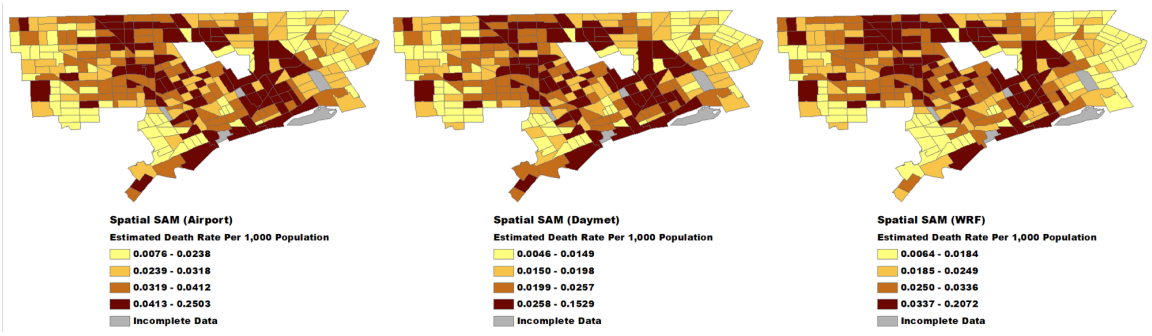

Figure 64 - Detroit spatial SAM results for Airport, Daymet, and WRF temperature inputs, normalized to deaths per 1,000 population in tract.

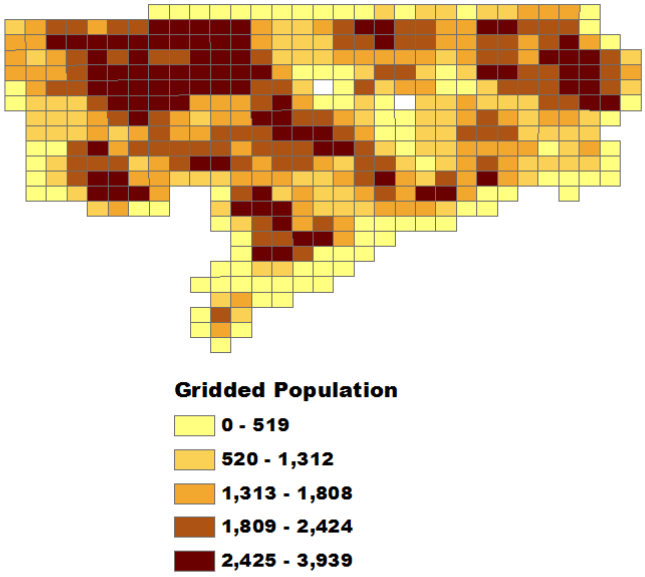

Figure 65 - Detroit 2010 gridded population.

5.3.2.3 Phoenix Spatial SAM Comparison

Phoenix also shows similar relative prioritization between the three temperature models at both the grid and tract scale. However, unlike Atlanta and Detroit, there do appear to be more differences between the tract-level models between the three datasets,

particularly in the northern end of the city. The airport inflated temperatures far above the WRF model in the north, which identified these areas as much cooler than the rest of the city. When applied uniformly to the whole city, the airport temperatures inflated mortality in these areas far above what is estimated from the WRF and Daymet models despite having a low population.

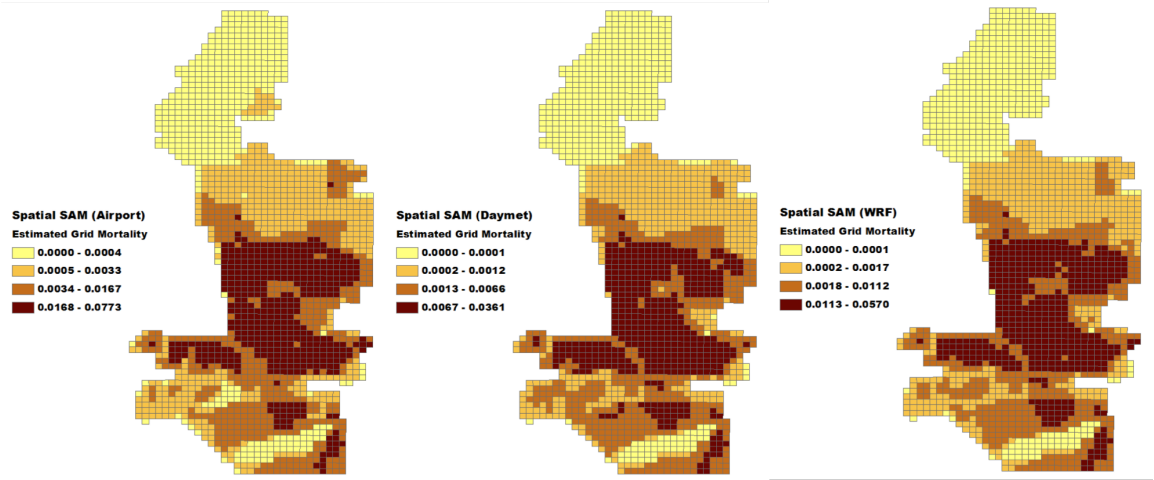

Figure 66 - Phoenix gridded spatial SAM results for Airport, Daymet, and WRF temperature inputs.

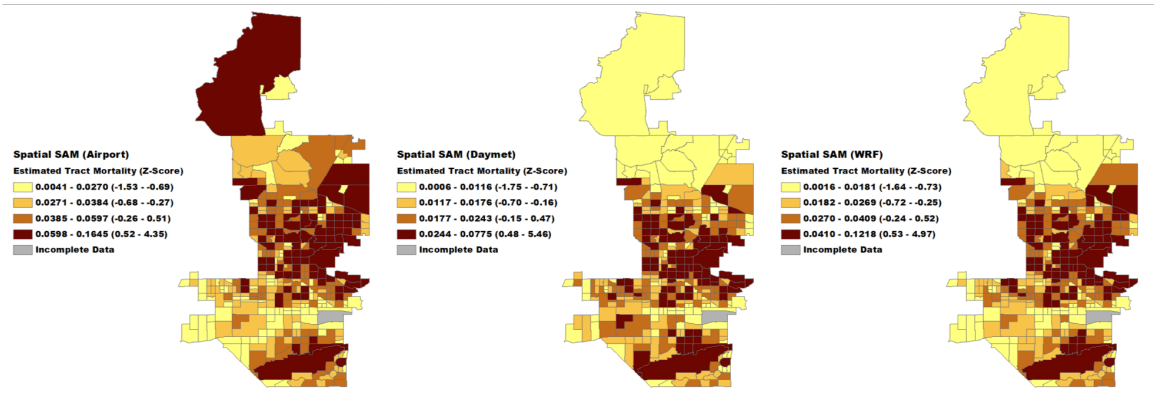

Figure 67 - Phoenix spatial SAM results for Airport, Daymet, and WRF temperature inputs, tract level mortality.

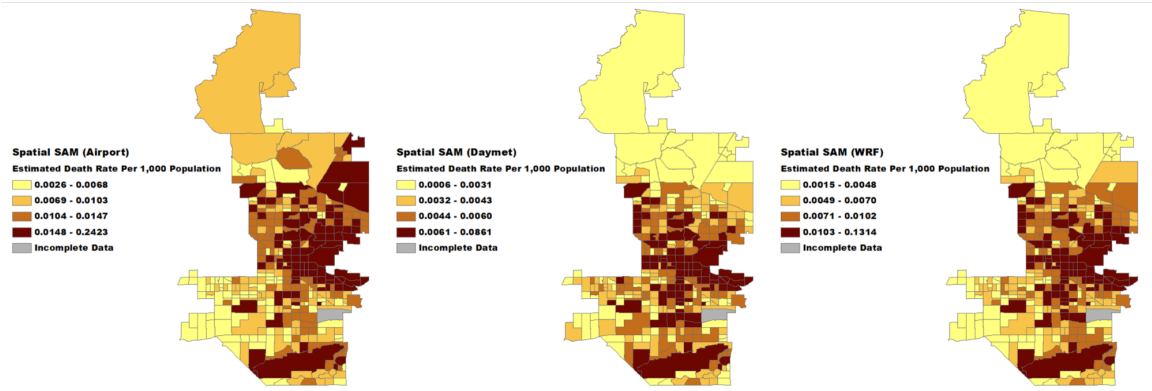

Figure 68 - Phoenix spatial SAM results for Airport, Daymet, and WRF temperature inputs, tract level z-scores, normalized to deaths per 1,000 population in tract.

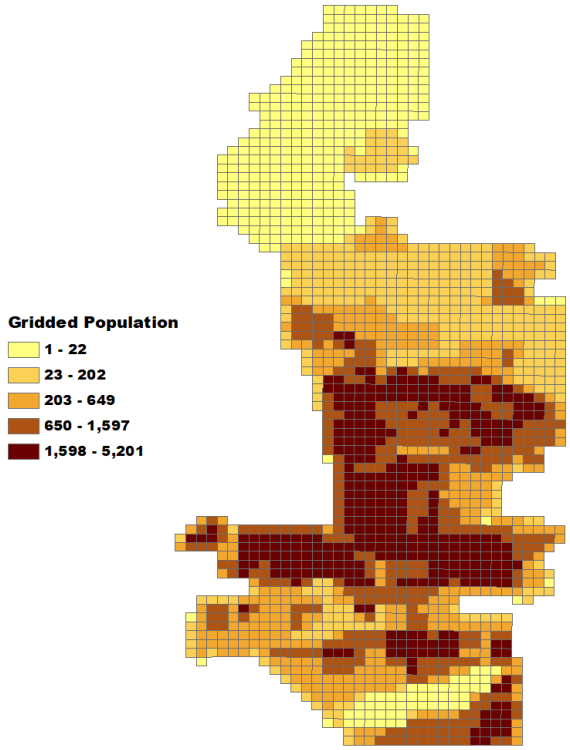

Figure 69 - Phoenix 2010 gridded population.

5.3.2.4 Spatial SAM Statistical Comparison

When comparing the results statistically using a paired t-test at the census tract level, the results appear to show greater differences in absolute spatial SAM mortality than

the maps suggest visually. The tables below show the p-value of the two-tailed paired t-tests between each mortality model result. These results show that consistently across each city and model the results are statistically independent. So, as the total mortality across each city in Table 34 suggest, the differences in spatial SAM mortality are statistically distinct. However, if viewed exclusively as an exercise in relative spatial prioritization, the maps appear to show great similarity between the models and may be adequate substitutes for one another in some cases.

Table 35 - p-values from paired t-test in Atlanta spatial SAM comparison.

	Airport	Daymet	WRF
Airport			
Daymet	< 0.001		
WRF	< 0.001	< 0.001	

Table 36 - p-values from paired t-test in Detroit spatial SAM comparison.

	Airport	Daymet	WRF
Airport			
Daymet	< 0.001		
WRF	< 0.001	< 0.001	

Table 37 - p-values from paired t-test in Phoenix spatial SAM comparison.

	Airport	Daymet	WRF
Airport			
Daymet	< 0.001		
WRF	< 0.001	< 0.001	

5.4 Discussion

The results of the previous chapter suggested that the spatial SAM method may provide greater utility to cities as a heat vulnerability decision support tool as compared to the HVI by protecting more vulnerable populations. The results detailed in this chapter also suggest that the distribution of population is a major driver of spatial SAM outcomes. While spatial SAM results were influenced by air temperature, these results suggest that relative spatial priority does not greatly differ when using a less complex air temperature dataset like. However, when calculating total mortality over a heat event, the results did vary greatly between the temperature inputs.

The paired t-test analysis suggests that total spatial SAM mortality estimates can significantly differ between temperature model input sources. However, the maps visually do not differ greatly in Atlanta or Detroit for any model and are also similar in Phoenix for both the Daymet and WRF models. If vulnerability mapping is viewed as an exercise in relative spatial prioritization meant primarily to determine where to direct resources, then Daymet may be an adequate and more accessible replacement for WRF-derived air temperatures in a spatial SAM analysis.

But if vulnerability mapping and more specifically mortality modeling are used as a justification for heat management planning as a priority for the city deserving of capital investment, then the choice of air temperature input will make a statistically significant impact on the estimated severity of the issue. As shown in the Phoenix results, using the airport resulted in an increase in total mortality of roughly 46% compared to WRF, while Daymet resulted in a reduction by almost 39% compared to WRF. From this perspective,

it is important to get an accurate assessment of total heat-related mortality for the purposes of communicating risk and justifying public expenditure. These results imply that neither the airport nor Daymet are reliable replacements for WRF, as they can result in a wide range of total mortality across the modeled event.

It is also important to note that WRF has the added benefit of scenario modeling and simulation to test the impacts of landcover change. Several studies have used WRF to model the temperature impacts of land cover change, such as adding additional trees or green roofs, or by adjusting albedo to simulate white roof implementation (Stone et al., 2010; Stone et al., 2019; Urban Climate Lab, 2017; Zhou et al., 2010). So, while WRF may not be necessary in the spatial SAM analysis modeling current conditions, it does provide added utility in simulating the impacts of planning strategies and policies that cities are interested to adopt. If a city has the financial capacity to pursue WRF modeling in its planning efforts, then it may still be the best option to provide useful information to inform heat risk evaluation and response.

One important caveat to this recommendation is that the spatial SAM method, regardless of temperature input, still requires several other complex inputs. This research was fortunate to build upon the work of Gasparrini (2015), who provided pre-processed temperature exposure-response functions and relative risk curves necessary for the analysis. The spatial SAM process used in this dissertation also included several complex steps using ArcGIS data processing and spatial assignment of both population and temperature datasets. The process also included use of an R script to generate the spatial SAM outcomes. Given these challenges, it may be unreasonable to expect the average urban planning office to be able to reproduce this process by scratch. However, with access

to the relative risk curves or guidance on how to create them in house using publicly available datasets like CDC WONDER and the Global Historical Climatology Network (GHCN), along with the R script used to process this data, it is reasonable that an urban planner trained in GIS analysis could reproduce the spatial SAM procedure for their own city. A yet more accessible spatial SAM analysis will require further study.

5.5 Conclusion

This chapter explained the methods and findings for Research Question 3. The findings of this analyses highlight the two uses of the spatial SAM: to model heat-related mortality across a city, and to determine relative spatial prioritization for planning initiatives and investment. These findings suggest that replacing WRF modeled air temperatures with Daymet may be adequate to address the relative spatial prioritization, but not to accurately represent mortality across the city. In the end, the recommendation to use one method over another falls to how the planner chooses to use these tools in the planning process. Given proper funding, WRF-derived spatial SAM may still be the most appropriate method to guide heat management policy with the added benefit of scenario modeling to test potential strategies in the local context. In the next chapter, I synthesize the findings from all of the central research questions in this study to provide recommendations for policy.

CHAPTER 6. RECOMMENDATIONS FROM STUDY FINDINGS

6.1 Introduction

In chapter 4, I tested three central research questions exploring the relationship between Heat Vulnerability Indices and spatial Statistical Attribution Models in Atlanta, Detroit, and Phoenix. Chapter 5 explored the potential to enhance spatial SAM method accessibility by analyzing the impact of alternative temperature models on the spatial SAM outcomes. Through this research, I have found that the complexity of HVI construction methods do not have a statistically significant influence on HVI score distribution, and in fact, simpler HVI methods generally correlated more strongly with spatial SAM mortality estimates. This research also shows that not all vulnerability indicators typically used in HVI analyses significantly predict heat-related mortality as estimated by a spatial SAM, suggesting that not all indicators are appropriate to include in the index. Finally, I found that while changing the air temperature model may create statistically distinct spatial SAM estimates, the relative spatial prioritization does not greatly change between spatial SAM temperature inputs.

This final chapter addresses the implications of this research for practice. In particular, I detail three main recommendations: 1) prioritize spatial SAM methods over HVIs to inform heat mitigation policy when possible 2) tailor response strategies to specific vulnerabilities, and 3) enhance public outreach and education on matters relating to heat risk and personal adaptations.

6.2 Recommendation 1: Prioritize Spatial SAM Methods Over HVI

The primary purpose of this dissertation was to examine to what extent commonly accessible HVI methods can predict much more complex and less accessible statistically attributed mortality estimates. Across all three cities and four HVI construction methods, the statistical relationship between HVI score and spatial SAM mortality estimates never exceeded an R-Square of 0.43. This study also further highlights the subjectivity of HVI methodology in analyzing heat vulnerability. The literature review conducted for this dissertation found a wide variety of HVI construction methods and combinations of vulnerability indicators. Conlon et al. (n.d.) found that even swapping out different measures of heat exposure can greatly influence the HVI score, thereby identifying entirely different neighborhoods as relatively high vulnerability. In this research, while the HVIs were not found to be statistically distinct in a paired t-test, each HVI construction method did show the potential to highlight different sets of neighborhoods as high priority areas for intervention.

Another major finding from this study was that more complex HVI methods were found to be less correlated with spatial SAM mortality than the more complex methods. Additionally, when compared to each other, the HVI construction methods did not prove to be statistically distinct in a paired t-test. This indicates that there is little added benefit in using more complex HVI methods like PCA. Wolf et al. (2015) surveyed authors of HVI studies and found that their studies did not appear to be significantly influencing policy. This could be a result of information lost along the way in constructing more complex HVIs. As HVIs increase in the number of indicators or statistical methods, they can increasingly obscure *why* an area is vulnerable. Losing this information makes it much

more difficult to address the issue in an efficient and effective way using targeted strategies tailored to the specific vulnerability.

Similarly, in answering Research Question 2 (*Which heat vulnerability indicators are significant predictors of heat-related mortality as derived by the statistical attribution method?*) this study found that very few of the individual indicators significantly predicted spatial SAM mortality in each city. This implies that some of the indicators may not be necessary to include in the HVI analysis. In fact, over age 65 was shown to significantly predict spatial SAM mortality in all three study cities. Conversely, LST was not significant for any of the three cities. This is evidence that even the Simplified HVI consisting of only these two variables may be misleading if used as a single score, as the LST is relatively less important in predicting mortality.

Furthermore, LST has been shown to be an unreliable indicator of heat exposure, as it is air temperature that humans experience (Ho et al., 2016; Weng, 2011). From a mapping standpoint, LST was also found to be a problematic indicator of relative heat exposure across the city, as LST and air temperature were not found to be strongly correlated in either Detroit or Phoenix. This relationship was particularly low in Phoenix, where LST was found to be highest even in areas where the air temperature was low. If LST is used in an HVI analysis for a city like Phoenix, the heat exposure distribution would be misleading. This could direct public funds into neighborhoods where there would be less marginal benefit from heat management interventions. Despite this discrepancy, LST continues to be a common indicator of heat exposure due to its comprehensive spatial coverage and ease of access. Until more accessible air temperature datasets become

available, urban planners and policymakers should be aware of the potential risks of relying on LST for relative spatial prioritization in heat management.

It is also important to consider local context when selecting HVI indicators. Consider the effect of nonwhite population in cities like Atlanta and Detroit, where the nonwhite populations are 63% and 89% respectively (see Appendix B). In many HVIs, this indicator is included as a "minority" status. But in these cities, the white population is the minority. For these cities in particular, given the demographics, it may be less likely that nonwhite residents are necessarily more vulnerable to heat risk than white residents.

These results suggest that an a-priori HVI score alone should not be used to guide policy on heat mitigation. The spatial SAM method is a more objective, observation-driven approach that accounts for both reliable heat exposure (air temperature) and vulnerable populations. The spatial SAM has been shown to closely track population centers, and additionally accounts for elderly population vulnerability due to the higher baseline mortality among that age cohort. Therefore, I recommend that cities pursue spatial SAM vulnerability assessments when possible over HVI methods.

It is important to recognize that this recommendation also comes with the challenge of obtaining reliable and spatially comprehensive air temperature datasets. WRF-derived air temperature datasets are technically and computationally intensive and are generally inaccessible to the average urban planner without investment in a consultation partnership. As this dissertation analysis has shown, replacing WRF with airport or Daymet data can also have a statistically significant impact on total mortality estimates. But as a relative spatial prioritization exercise, it may still be viable to explore alternative temperature

datasets. While spatially comprehensive sensor networks are rare, cities could potentially utilize networks like Weather Underground to expand on the single airport weather station model and create locally distinct temperature zones across the city. Additionally, new alternatives to WRF are beginning to emerge that could provide greater accessibility to the spatial SAM procedure. An example of which is The Air-temperature Response to Green/blue-infrastructure Evaluation Tool (TARGET), created by Broadbent et al. (2019). This model is designed to be a publicly accessible, user-friendly air temperature model that utilizes skills more common to the average urban planner such as land cover analysis and GIS. In its current state, it will likely still require some consulting or other external guidance to set up the model for a planning office or firm to run the model successfully. However, it is evidence that efforts are ongoing to create an accessible model for use in planning and policy design.

Additionally, the spatial SAM method requires more than just a temperature dataset. In order to successfully run the spatial SAM analysis, planners will need to work closely with the public health community to acquire or construct relative risk curves for heat mortality that reflect the unique heat sensitivity and acclimatization of the local population. The necessary data inputs are available from public datasets like CDC WONDER and GHCN, but a public health practitioner or biostatistician may be necessary to provide the expertise to construct the relative risk curve. However, once the components are assembled, the population allocation procedure and the R script used in this dissertation can provide guidance on completing the procedure for a successful spatial SAM analysis. Further research should formalize this procedure in an accessible format alongside efforts like TARGET to make this method a realistic goal for city planning departments.

6.3 Recommendation 2: Tailor Response Strategies to Specific Vulnerabilities

While I have recommended the spatial SAM procedure over HVIs to direct heat mitigation policy, there is still much work to be done to ensure this is a realistic goal for cities to achieve. It is important for cities to begin heat mitigation planning as soon as possible to protect vulnerable populations from the ongoing threat of extreme heat exposure in the urban environment. As such, HVIs can play an important role in mitigating heat vulnerability. However, I recommend that cities pursuing HVIs as a tool for heat vulnerability assessment keep their methods simple, such that they do not obscure meaningful results with unnecessary or misleading aggregation.

Much of the challenge of using complex HVI methods like PCA comes from the potential to lose the message of *why* an area is vulnerable. Because it consists of so many inputs, a high composite HVI score does not immediately imply a specific response. Even the Simplified HVI consisting of only one sensitivity and one exposure indicator could reduce its vulnerability score through *either* reduced sensitivity or exposure. For example, this could mean either cooling strategies like green infrastructure or social programs that inform and protect elderly populations during extreme heat events would lower the HVI score. This challenge becomes all the more complex with each new vulnerability indicator and statistical processing method.

Therefore, in any heat vulnerability mapping exercise, I recommend mapping individual vulnerability indicators or components of vulnerability (sensitivity, exposure, and adaptive capacity) separately, rather than aggregating to a composite HVI score, as each unique vulnerability implies a different response strategy. Furthermore, research

question 2 found that not all indicators were significant predictors of heat-related mortality estimates as derived by the spatial SAM method. To avoid an overwhelming amount of information, planners should select indicators carefully, using only ones they can clearly connect to an implied strategy response. Figure 70 below shows over age 65 and LST for Atlanta as separate HVI indicators side by side. But As also indicated in Atlanta's Simplified HVI, there is little overlap between these two indicators. Elderly populations tend to live outside the urban core, where it is more heavily canopied and much cooler as a result (see also Figure 27 for satellite imagery). Conversely, the LST is most extreme in the dense urban core where there are very few elderly residents. These two distinct vulnerabilities require two distinct response strategies. These maps imply that the City of Atlanta should focus long-term greening strategies to mitigate temperatures in the urban core while building short-term emergency response strategies like checking on elderly populations or opening cooling centers around the outskirts of the city during extreme heat events in which elderly residents are at much higher risk of mortality. To plant more trees in the urban periphery near elderly populations may be a misguided effort, as they are not the areas in greatest need of heat mitigation according to the LST map.

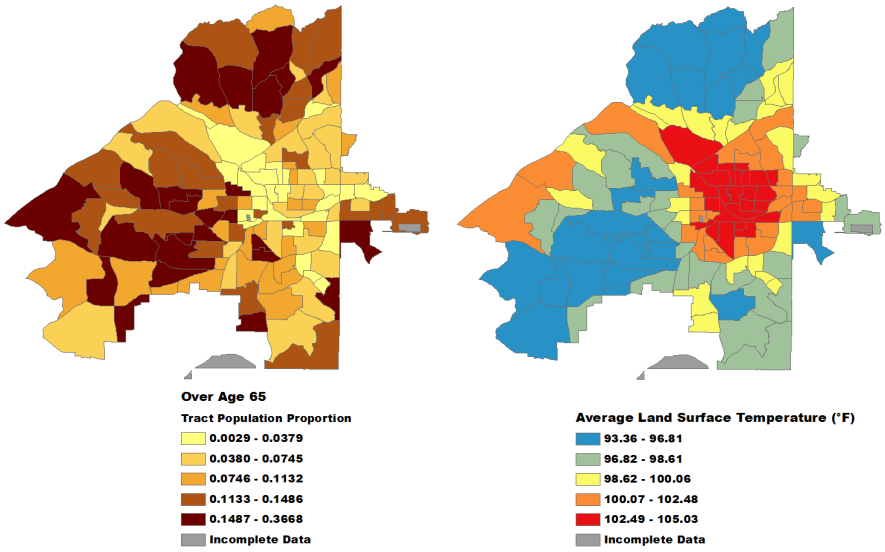

Figure 70 - Over age 65 (left) and LST (right) as distinct Atlanta HVI indicators.

As discussed in chapter 4, LST was shown to be an unreliable predictor of air temperature in Detroit and Phoenix. As such, it is important to carefully consider which indicators to include in the vulnerability assessment. Since lack of vegetation and impervious materials are major drivers of the urban heat island (Stone, 2012), it may be more appropriate to utilize datasets like the National Land Cover Database impervious surface cover or canopy cover, or Landsat-derived normalized difference vegetation index (NDVI) to highlight areas in need of intervention in cities.

One decision support tool model I would recommend is the Chicago Heat Vulnerability Tool (Wilson et al., 2017). This tool allows the user to select individual heat exposure and sensitivity indicators for instant mapping exploration in Chicago. This allows the user to observe only the indicators they find most relevant without other indicators confounding the overall message. See Figure 4 for an illustration of the user interface. But more broadly, any urban planner with access to Social Explorer can similarly map heat

sensitivity and adaptive capacity indicators at any census geography on the fly. Online data portals like NASA Earth Explorer or Google Earth Engine make it increasingly simple for users to look up heat exposure metrics on-demand as well, further enhancing the accessibility of such methods to the average planning practitioner. All of this can be completed even without access to ArcGIS or statistical software to run PCA analysis.

Based on the findings in Chapter 4, I suggested that the spatial SAM may be the better decision support tool to protect the most vulnerable populations. But it is important to consider how planning and public health practitioners will use the spatial SAM outcome, even if it is more accessible. While the spatial SAM does highlight spatial prioritization that is sensitive to both temperature and population centers, this method itself may be missing important information that could influence the resultant planning initiatives. The findings of Research Question 3 indicated that while the total mortality is sensitive to temperature inputs, they did not greatly influence the spatial patterns of vulnerability.

In this way, I would recommend that for cities interested in heat vulnerability assessment could start with a spatial SAM analysis using the best available temperature inputs for a sense of relative spatial prioritization. The planners should then follow this analysis with consideration of the individual indicators of vulnerability that could influence response strategy design. For example, proportion of population living below the poverty line could add some nuance to the response. An area with high temperature and population, but also wealthy residents may not need to use a cooling center as often as a similarly hot and populated area with high poverty rates. Using this method, planners can gain the benefits of both spatial SAM analysis and multi-indicator HVI while retaining information on exactly why an area is considered vulnerable.

6.4 Recommendation 3: Enhance Public Outreach and Education

This dissertation has largely found that Heat Vulnerability Indices may not be the most useful tool in assessing overall heat risk. But as described in Recommendation 2, they can be a useful to identify specific vulnerabilities individually and can be a useful public outreach and communication tool for these communities. Heat sensitivity and adaptive capacity are just as important as heat exposure when assessing heat vulnerability. For the areas at greatest risk of sensitivity and adaptive capacity-related vulnerability, planners and public health practitioners should enact protective response strategies to enhance local resilience to extreme temperatures when they occur. In particular, such strategies should encourage behavioral change and enhanced social capital during extreme heat events so residents can better protect themselves from dangerous heat exposure.

To accomplish this, I recommend that planning practitioners focus on public outreach and education on matters relating to heat risk and personal adaptations. Such strategies should be the particular focus of short-term emergency response plans during extreme heat events. Additionally, these public education efforts can encourage local residents to take responsibility and uphold grassroots initiatives to enhance local climate resilience through a distributed community effort. Such top-down and bottom-up approaches will be necessary to build resilience to each component of heat vulnerability.

6.4.1 Communicating Heat Risk

The vulnerability mapping in this dissertation can be used for identifying areas of a city that are at greatest risk of heat impacts, but it will take a mutual effort on the part of city officials and residents alike to adequately address the issue in these targeted areas and

populations. Heat-related illness and death is largely preventable as long as public health officials, government agencies, and the media continue to take proactive measures to address heat risks on unusually hot and humid days (Davis et al., 2003). In a warming climate, heat warnings are an increasingly necessary adaptation strategy to reduce heat-related mortality and morbidity. Toloo et al. (2013) reviewed 15 articles on the effectiveness of Heat Health Warning Systems (HHWS) and found that 6 studies explicitly reported reductions in expected heat-related deaths after implementation. Furthermore, a cost-benefit analysis of the heat warning system estimated that the cost of running the system was minimal, at roughly $210,000 per year compared to the estimated $468 million benefit of saving 117 lives (Toloo et al., 2013). Given the efficacy and cost-effectiveness of heat warnings, planners and public health officials should ensure vulnerable populations receive and understand heat warnings when they are issued so they may take appropriate action to reduce personal exposure.

Since vulnerable populations often lack resources to cope with extreme heat, the success of the warning depends on the individual actions and behaviors of these populations to reduce personal exposure, so it is important to prioritize behavior change, or personal adaptations, in the messaging. Sheridan (2007) studied the efficacy of cities' heat mitigation strategies in terms of providing awareness and evoking a response from their citizens. The study reviews heat mitigation plans of 4 cities and surveyed elderly residents in each city by phone within 7 days of a heat event inquiring about awareness and behavior change during the event. The study found that though awareness of a heat warning was high among these residents (roughly 90%), and that many had advance knowledge at least 1 day before the event, far fewer actually modified their behavior in response to the

warning. Less than 2% of survey respondents sought out cooler locations, and only 4% mentioned staying hydrated. Furthermore, some residents partook in potentially dangerous actions including running a fan in their home with the windows closed, which can rapidly enhance dehydration and inhibit radiative and conductive heat loss.

Several Weather Forecasting Offices (WFOs) simply use heat warnings and watches as part of their Weather Watch Advisory (WWA) products. This type of messaging alone may not be most effective in getting key information across to those who need it. The Sheridan (2007) study shows that while the message itself may get wide exposure, knowledge of the details of the message is far lower, and actual behavior change as a result is lower still. The author recommends several steps to enhance this messaging. The first is to increase advance training of the media on heat-related issues so they may communicate effectively. Second, the general public must be made aware that depending on the metric used, watches and warnings can be based on actual human health responses, and that they will be personally at risk unless proper actions are taken. Third, efforts must be expanded to relate people's vulnerability, specifically mentioning what conditions may place one at higher risk. Research shows that if an individual finds themselves personally at greater risk, they are far more likely to take preventative actions such as seeking out air conditioning, hydrating, dressing lightly, or avoiding strenuous activity (Toloo et al., 2013). Fourth, expand the explanation on the correct use of fans or other cooling mechanisms to ensure that they are not used incorrectly in potentially dangerous ways.

Hawkins et al. (2015) surveyed local WFOs, providing useful feedback on public outreach. Current messaging through media partners often results in a spatial mismatch, as the media's Designated Market Area is not often confined completely within a WFO's

County Warning Area, sometimes leading to warnings reaching those who don't need them, leading to some confusion and misunderstanding among the public. Instead, one respondent recommended a move toward "concise, attention-grabbing social media," and to "limit the messaging to the essentials: check on the kids, elderly, and other vulnerable populations. Filter out the rest." Others added "promote the use of social media to increase the delivery of heat awareness information that can be easily shared through graphics, videos and links." Vargo et al. (2015) recommends the use of "location-smart devices" with "animated visualizations of weather conditions describing recent historic and near future weather conditions with improved precision." This type of messaging can be specifically targeted to certain locations or populations via mobile weather applications like Weather Underground, which can also be used to crowdsource information through "hazard reports" (Vargo et al., 2015).

However, it is likely that those who are most vulnerable are also those who would not have regular access to social media and smartphone apps for alerts, such as the elderly and those living in poverty. For these populations, it is important to collaborate with health partners at the local level to gain more information on how to reach specific populations (Hawkins et al., 2015). Cities like Dayton and Philadelphia have specific measures in their heat mitigation plans to contact elderly residents via a "buddy system" to check in on them regularly, direct notification of nursing homes, and opening hotlines for heat-related health questions (Sheridan, 2007). Toronto additionally deploys "street patrols" to distribute bottled water to the public (Sheridan, 2007). Heat vulnerability mapping using these relevant indicators could highlight where to implement these strategies most effectively and efficiently, and kickstart the process of identifying local partners.

Additionally, it may be useful to partner with schools to educate children about the risks of heat exposure. Not only does this equip younger generations with useful knowledge to reduce personal heat risks, but they may also in turn educate their families at home. This type of communication can regard both long-term education goals of heat preparedness, personal adaptations and behavioral change, as well as short-term education goals of disseminating important information during heat warning days. Additionally, in the last 3 decades, obesity rates have tripled among children ages 6-11, with greater rates for African American and Hispanic children (Dannenberg et al., 2011). Not only does this hinder thermoregulation in the children, but it also places them at higher risk of type-II diabetes, with estimates as high as 30% of boys and 40% of girls developing it in their lifetimes (Dannenberg et al., 2011). These dual threats further exacerbate heat vulnerability, so it is extremely important to ensure these children understand the risks of extreme heat, as well as the benefits of a healthier lifestyle as they grow older so they can avoid heat-related illnesses.

Strategies like the above could specifically target vulnerable neighborhoods identified through the vulnerability mapping techniques detailed in the preceding chapters of this dissertation. This is one way to directly reach vulnerable areas with specific interventions tailored to their needs. While this takes far greater effort than a blanket "watch" and "warning" system at the WFO level, it is one that could ultimately save many lives.

6.4.2 Communicating the Need for Heat Mitigation Policy in a Changing Climate

Climate change is and will continue to be one of the most important factors influencing planning today. As the climate continues to warm, urban residents will be increasingly exposed to extreme heat. Unfortunately, planning for climate change adaptation is still an emerging responsibility for the urban planner. It involves a wide range of stakeholders with varying levels of engagement or even acceptance that it is something for which to plan at all. As highlighted in chapter 5, the spatial SAM method can provide useful evidence that heat mitigation planning is justified by quantifying risk in lives lost to extreme heat exposure. But the choice of temperature input can result in a wide range of total mortality estimates over the modeled period. The planner must not only be aware of the possible challenges of heat vulnerability modeling and associated uncertainties but must also use what information is available to make reasonable and pragmatic decisions to move a city toward greater resilience.

The first key consideration in this communication process is information gathering. When communicating the need for heat mitigation strategies, the planner should gather the best information possible on the risks of inaction and the benefits of proactive heat mitigation policy in a warming climate. As climate scientists are rarely in the realm of advocacy, it is often up to the planner to bridge the gap between the scientific field and the policy and planning fields that utilize this information for on-the-ground actions (Richardson, 2015). As highlighted in this dissertation, scientists do not always provide information that is easily interpreted or usable by planners, making it difficult for planners to get precise, locally relevant data for use in their plans (Biesbroek, 2013; Eliasson, 2000).

This information gap is commonly cited as a major barrier to climate change planning (Baker, 2012; Biesbroek, 2013; Measham et al., 2011; Moser, 2014).

But this information should not be used in isolation. Preston (2010) argues that planners tend to isolate the issue of climate change planning by not taking non-climatic factors into account. Planners must move beyond conventional risk-based approaches in order to account for "complex and dynamically evolving social-ecological systems," and must apply global or regional information to a local context (Kennedy et al., 2010). Jones & Preston (2011) recommend that planners should reframe climate change from purely climatic factors to broader issues of vulnerability and resilience. So, in this case, the risks of rising temperature alone may not be adequate in isolation as an argument for public investment in heat mitigation strategies. Instead, it must be connected to unique local vulnerabilities and concerns of residents. Such synthesis of potential impacts in the local context can be facilitated by the mapping techniques detailed in this dissertation.

For planners to gain a sense of local concerns, it is helpful to collaboratively co-produce climate knowledge with local stakeholders, residents, experts, and champions together (Stocker et al., 2012). This means planners should take an active role in knowledge production rather than rely solely on in-house assessments or consultants for information. If planners can take a strong coordinating role between scientists, community stakeholders and their own ongoing efforts, then this knowledge can be better applied to the local context to suit local needs. This procedure need not be an entirely new exercise, as planners often act collaboratively with the public. Following existing planning techniques like identifying community leaders can help disseminate information effectively while also devising

locally relevant solutions more likely to be upheld by the community rather than "one-size-fits-all" approaches (Preston et al., 2011).

When meeting with the public, Jones & Preston (2011) recommend that community-based methods be "easy to understand, procedurally simple, and culturally appropriate." This may be a difficult task considering the complex socio-ecological challenges of climate change. But keeping the conversation simple and clear will not overwhelm participants while still meeting goals of knowledge production, knowledge dissemination, identifying risks, and scoping community goals. Such meetings can help the planner gain a better understanding of where and how to implement the local strategies described in the section above, and how to better tie them in with ongoing local initiatives unrelated to climate change, such as targeted community safety and development initiatives or determining future tree planting locations. The mapping techniques detailed in this dissertation can be effective communication tools in this effort to co-develop heat mitigation policy.

Another key consideration when communicating the need for heat mitigation policy to both planners and the public is that it may be difficult to convince all parties that it is worthy of investment. Some stakeholders may be skeptical about the risks of heat or climate change, and others may be wary of spending public and private funds on heat planning initiatives if they do not recognize the risks of high urban temperatures. Thus, it may be useful to focus on the entire spectrum of co-benefits of such policies in order to make the argument that investing in them is a good idea regardless of climate change as a driving motivation.

For both planners and the public, the financial case for heat mitigation strategies like tree canopy expansion is clear. In terms of cooling energy use, studies have shown beneficial effects like energy savings with tree shading and green roof implementation. One study found that every 10% increase in shade coverage, a suburban residence can save 2% of daily energy use (Pandit & Laband, 2010). Scaling up, one study finds that a large park in Tokyo provides enough cooling potential to offset the equivalent of 2,600 air conditioning units (Sugawara et al., 2015). Research has also shown that green roofs can reduce annual building energy consumption for cooling by up to 60% depending on building insulation (Berardi et al., 2014).

In terms of stormwater control, trees, green roofs and other green infrastructure can greatly reduce runoff volumes, thereby reducing the associated costs of treatment to the city while enhancing urban water quality. Research shows that trees can reduce runoff by as much as 11.3 kL per tree per year with associated annual savings up to $48 per tree depending on the size of the tree and the costs of stormwater management (Mullaney et al., 2015). Green roofs have also been found to reduce runoff volumes up to 60% (Foster et al., 2011). Additionally, parks consisting of extensive areas of turf grass require supplemental irrigation and maintenance. However, adding trees to open parkland can reduce water consumption by as much as 50% (Shashua-Bar et al., 2009). This is a major incentive for the city but can also be a direct financial incentive to the public if Atlanta were to establish a stormwater utility.

Trees have also been associated with higher property values and business income (Burden, 2006; Donovan & Butry, 2010; McPherson et al., 2005; Pandit et al., 2010; Sander et al., 2010; Wolf, 2005), as well as social benefits ranging from crime reduction to

enhanced community engagement by residents (EPA, 2014; Mullaney et al., 2015). This provides yet another financial incentive by increasing the tax base for the city, increasing profits upon sale for homeowners, and making neighborhoods that implement such strategies more desirable.

Aside from heat reduction, urban vegetation can also have benefits for human health and well-being (Qin et al., 2013). Trees have been found to encourage physical activity, reduce physical and mental stress and fatigue, and even improve physical recovery from illness (Mullaney et al., 2015; Velarde et al., 2007). Vegetation can also reduce smog and other air pollutants directly linked to respiratory illnesses like asthma (Abhijith et al., 2015; Akbari, 2002; Nowak et al., 2006; Nowak et al., 2014; Scott et al., 1998; Tallis et al., 2011), which can be a great benefit to vulnerable communities identified in the knowledge-gathering and co-production phase.

Given this wide variety of benefits, the savings over the lifetime of the tree can outweigh the costs of planting and maintenance (Peper et al., 2007). In a study of assessed economic costs and benefits of tree planting in five medium-sized US cities, McPherson et al. (2005) found that the annual benefits of trees exceed costs by a factor of 1.4 to 3.1. Similarly, green roofs can cost more than conventional roofing by a factor of roughly 4 to 8, but the energy, stormwater and longevity benefits of the green roof can more than cover the additional costs of installation to make it an economically viable strategy in the long run (ASLA, 2011; Foster et al., 2011).

These benefits provide a strong argument in favor of capital investment in heat mitigation strategies like green infrastructure. In following with Recommendation 2, a

simplified heat vulnerability assessment approach using carefully selected, locally relevant vulnerability indicators can help planners identify vulnerable neighborhoods, potential local partners, and areas at risk of high heat exposure in need of intervention. A collaborative conversation between planners and the public using the framing detailed above can go a long way to enhancing local resilience by protecting the economic, social and ecological health and well-being of the city and its residents.

6.5 Conclusion

In a warming climate, it is increasingly important for cities to adopt strategic plans to protect our most vulnerable populations from heat-related morbidity and mortality. This study is the first of its kind to compare Heat Vulnerability Indices and statistically attributed heat mortality estimates as methods to guide heat mitigation policy. This information can help urban planners and public health officials improve their emergency response plans and communication strategies for greater heat resilience in urban areas by specifically targeting short and long-term responses by neighborhood. If a statistically significant correlation between the two methods can be determined, this study can provide planners with further insights into these useful tools to protect vulnerable populations in urban areas effectively and efficiently with minimal public funds. Along with traditional HVI techniques, a simplified statistical attribution method constructed using publicly available air temperature datasets could guide both greening policies for passive cooling as well as emergency heat response planning among sensitive populations.

This research utilizes the latest scientific methods to meet contemporary climate change planning needs and could advance the policies we use to adapt to a changing

climate. Extreme urban temperatures are a threat we already face today, and with anticipated increases in heat wave intensity, duration, and frequency, we must continue to develop anticipatory heat response planning methods to protect vulnerable populations and enhance local resilience. The findings and recommendations in this dissertation help equip urban planners, public health practitioners, and the general public with the decision support tools and rationale necessary to design and justify effective and efficient heat response strategies sensitive to local context.

APPENDIX A. HVI INDICATOR MAPS

A.1 Atlanta

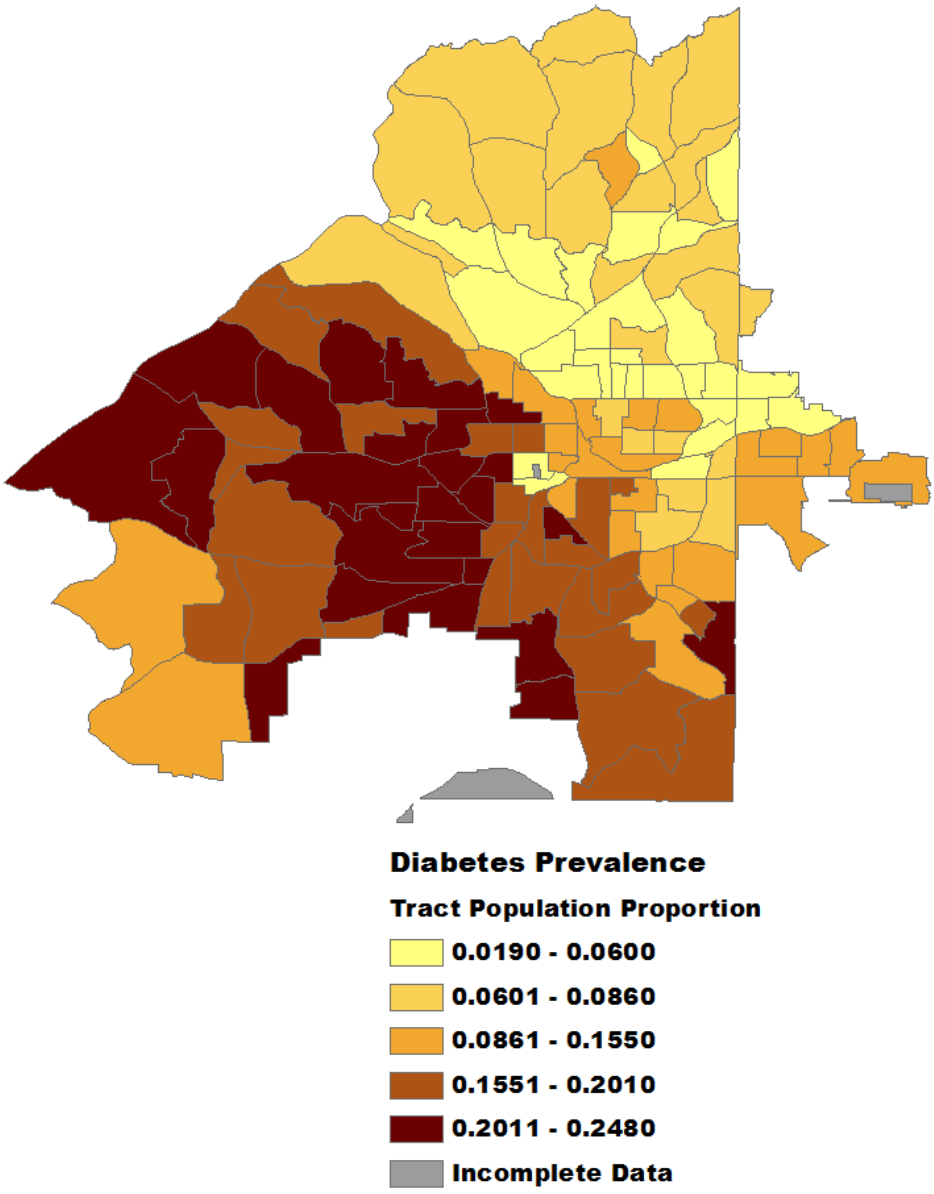

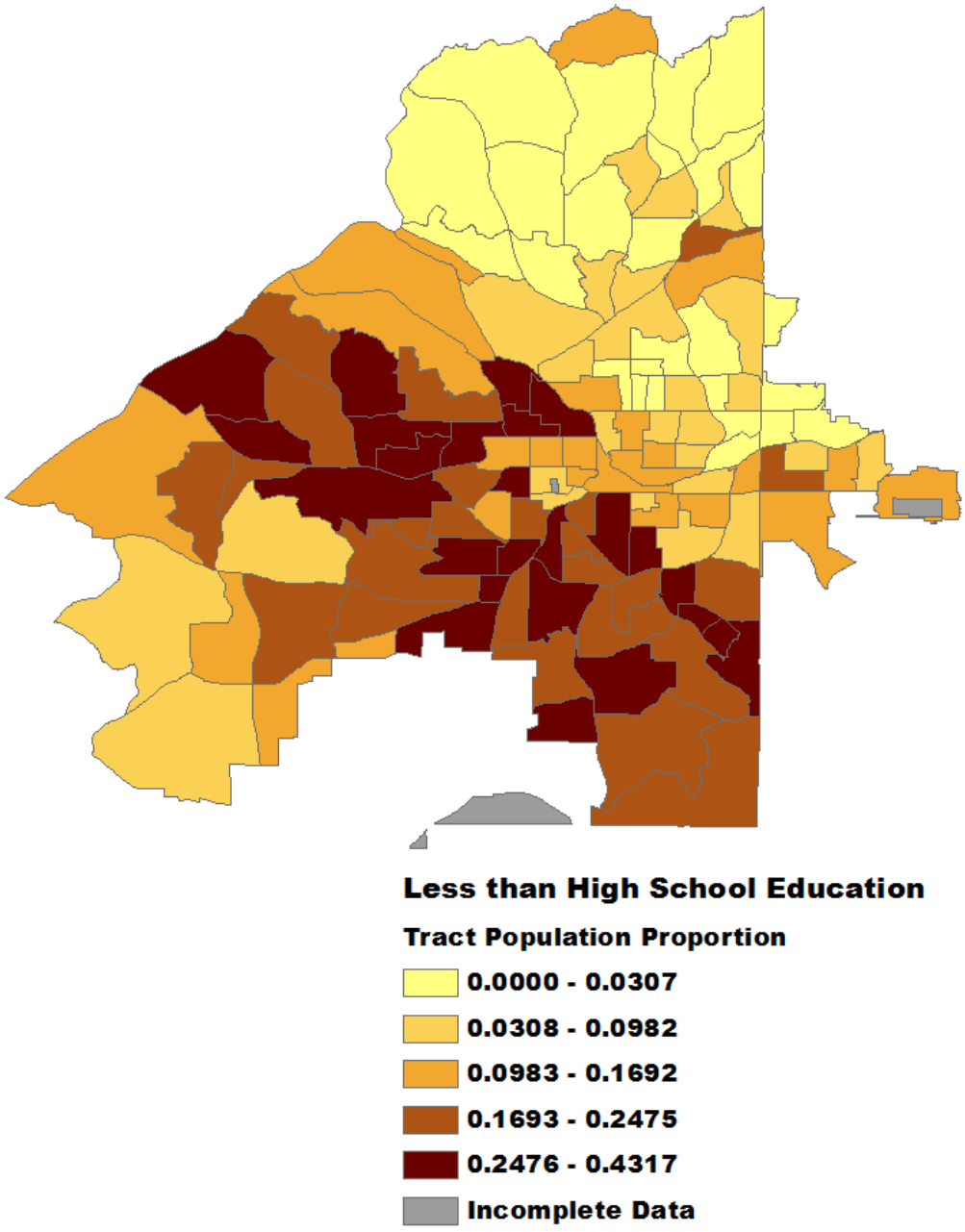
Less than High School Education
Tract Population Proportion
0.0000 - 0.0307
0.0308 - 0.0982
0.0983 - 0.1692
0.1693 - 0.2475
0.2476 - 0.4317
Incomplete Data

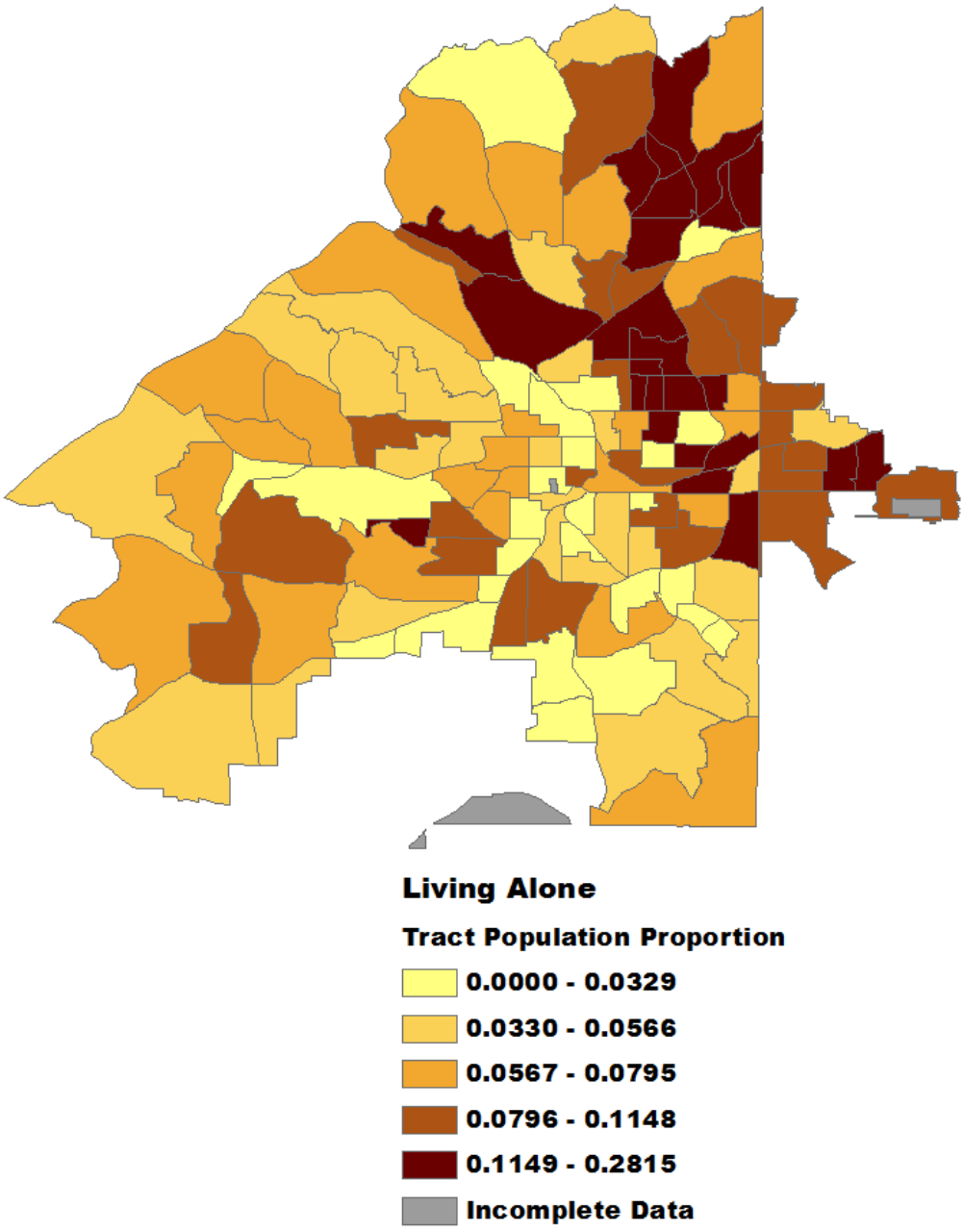
Living Alone
Tract Population Proportion
0.0000 - 0.0329
0.0330 - 0.0566
0.0567 - 0.0795
0.0796 - 0.1148
0.1149 - 0.2815
Incomplete Data

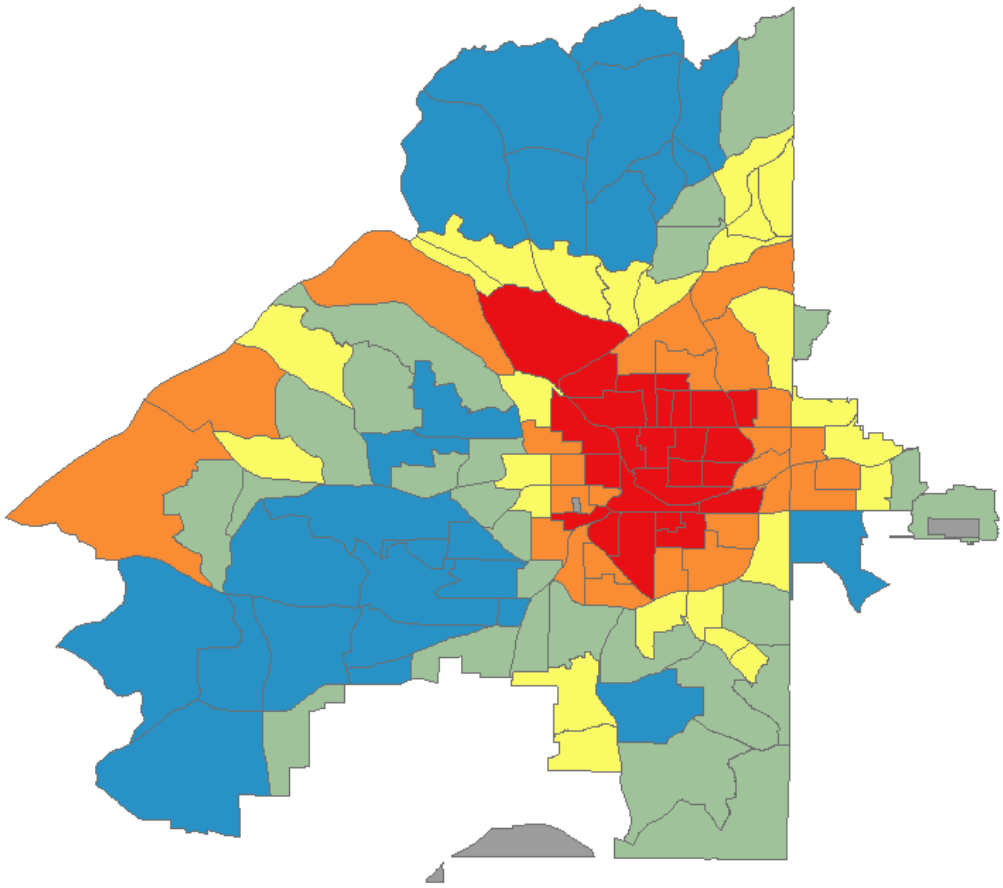

Average Land Surface Temperature (°F)

- 93.36 - 96.81
- 96.82 - 98.61
- 98.62 - 100.06
- 100.07 - 102.48
- 102.49 - 105.03
- Incomplete Data

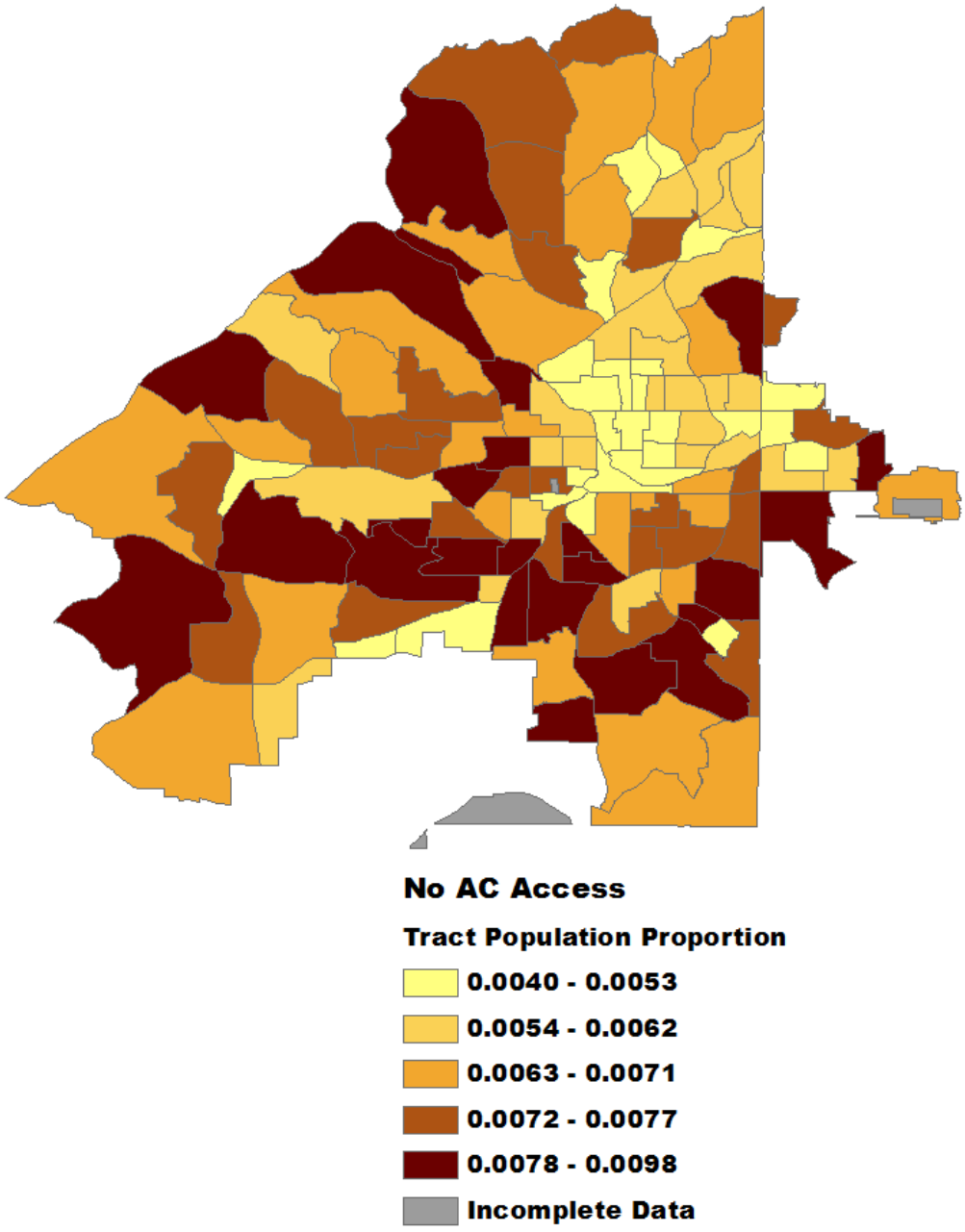
No AC Access
Tract Population Proportion
0.0040 - 0.0053
0.0054 - 0.0062
0.0063 - 0.0071
0.0072 - 0.0077
0.0078 - 0.0098
Incomplete Data

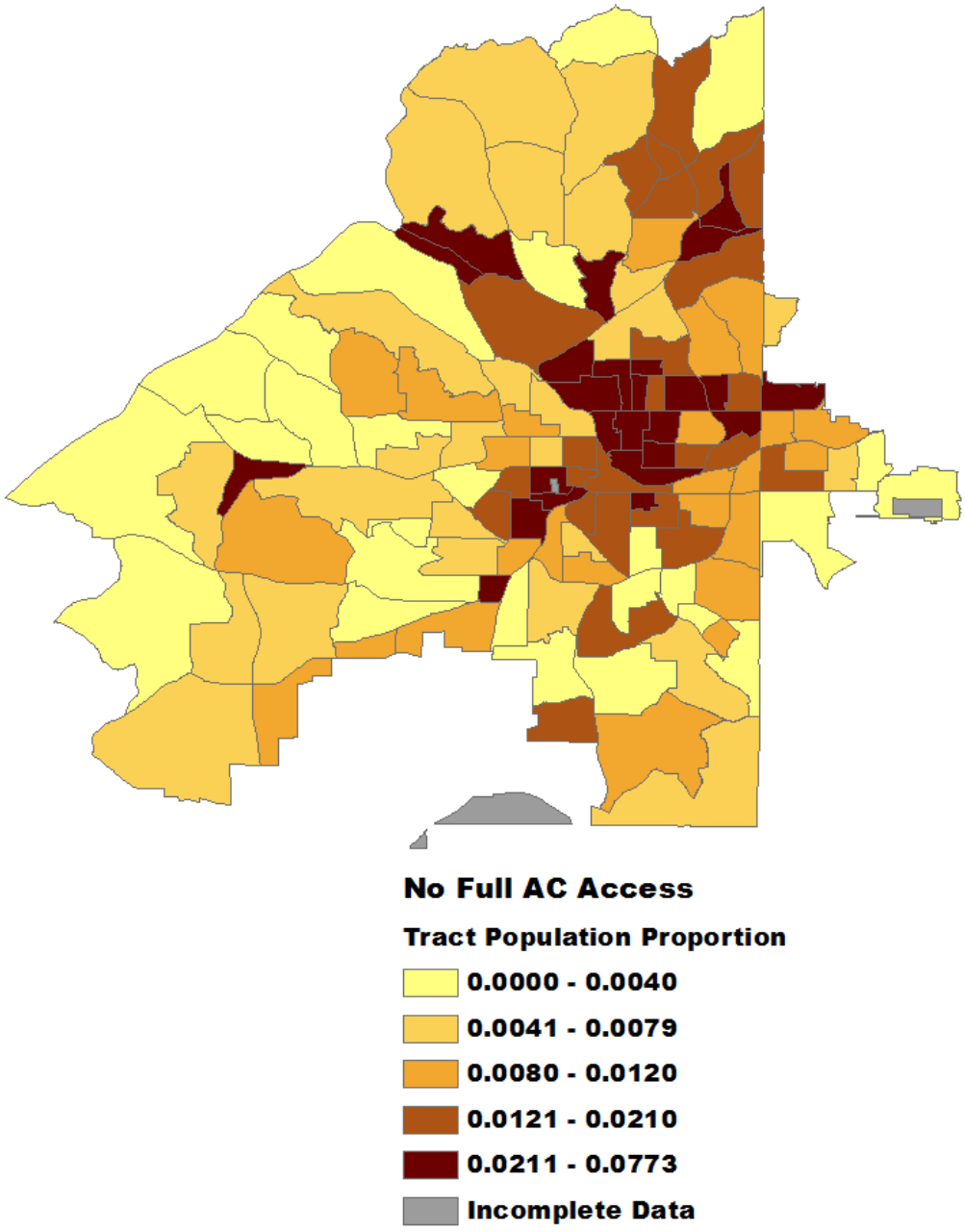
No Full AC Access
Tract Population Proportion
0.0000 - 0.0040
0.0041 - 0.0079
0.0080 - 0.0120
0.0121 - 0.0210
0.0211 - 0.0773
Incomplete Data

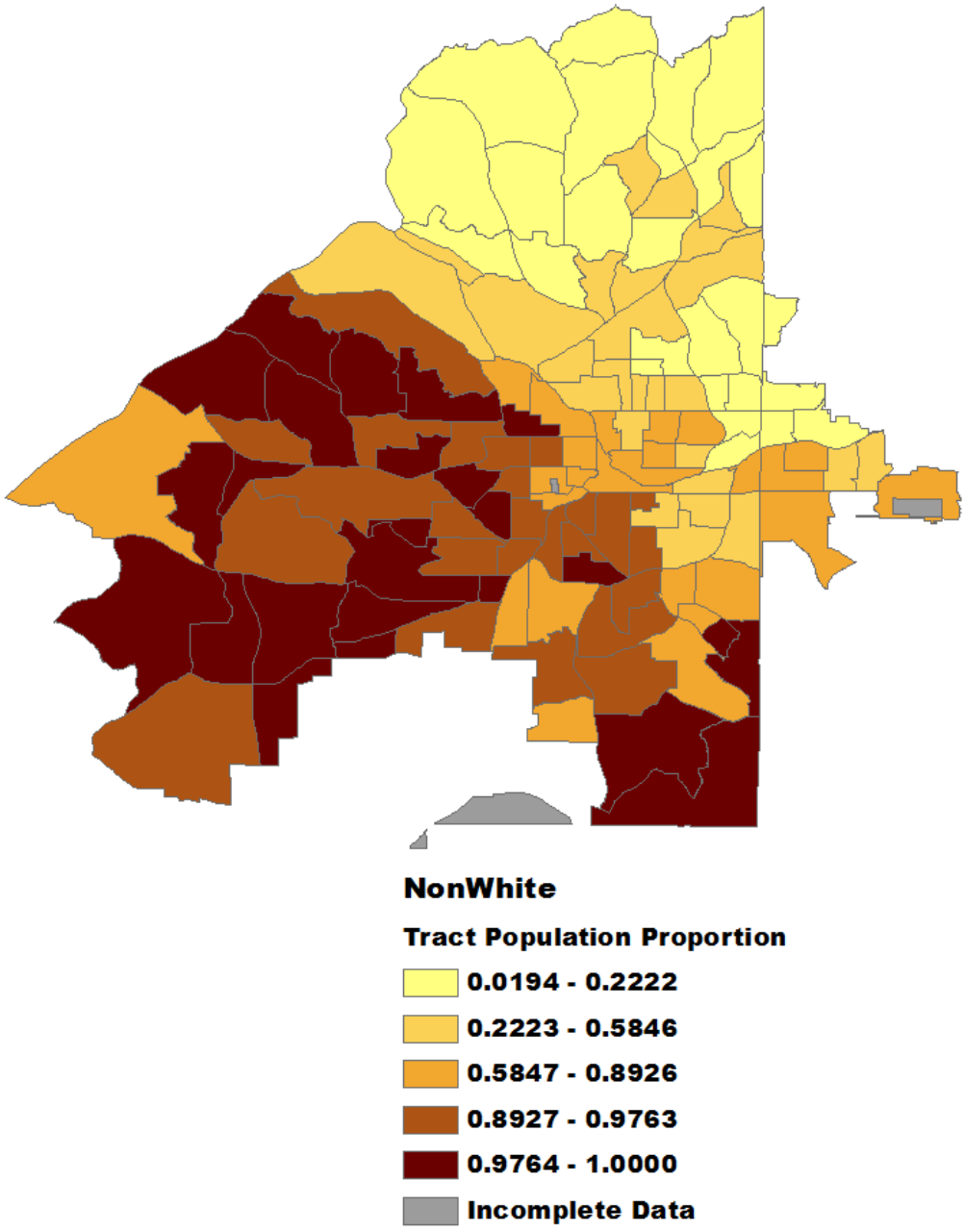
NonWhite
Tract Population Proportion
0.0194 - 0.2222
0.2223 - 0.5846
0.5847 - 0.8926
0.8927 - 0.9763
0.9764 - 1.0000
Incomplete Data

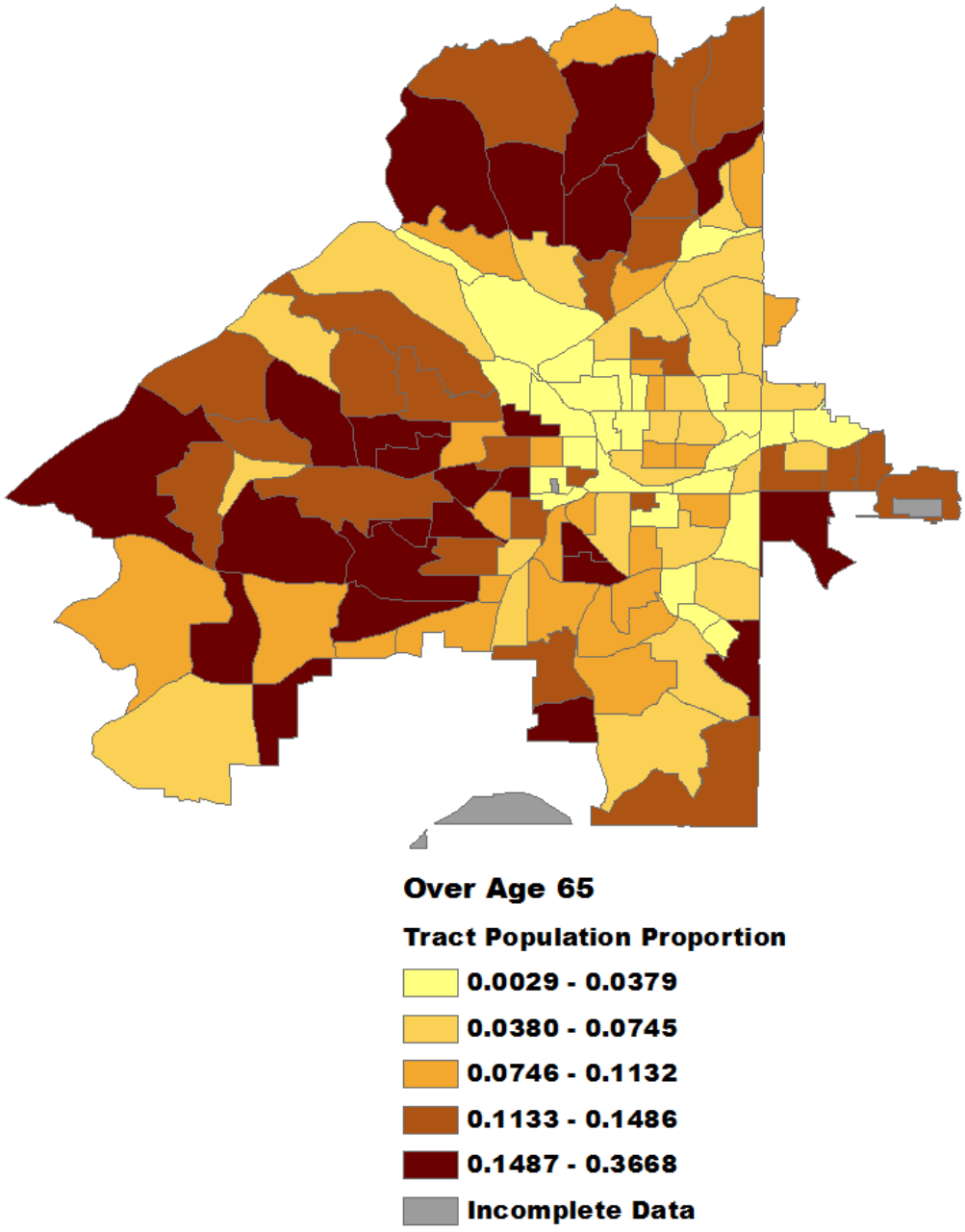
Over Age 65
Tract Population Proportion
0.0029 - 0.0379
0.0380 - 0.0745
0.0746 - 0.1132
0.1133 - 0.1486
0.1487 - 0.3668
Incomplete Data

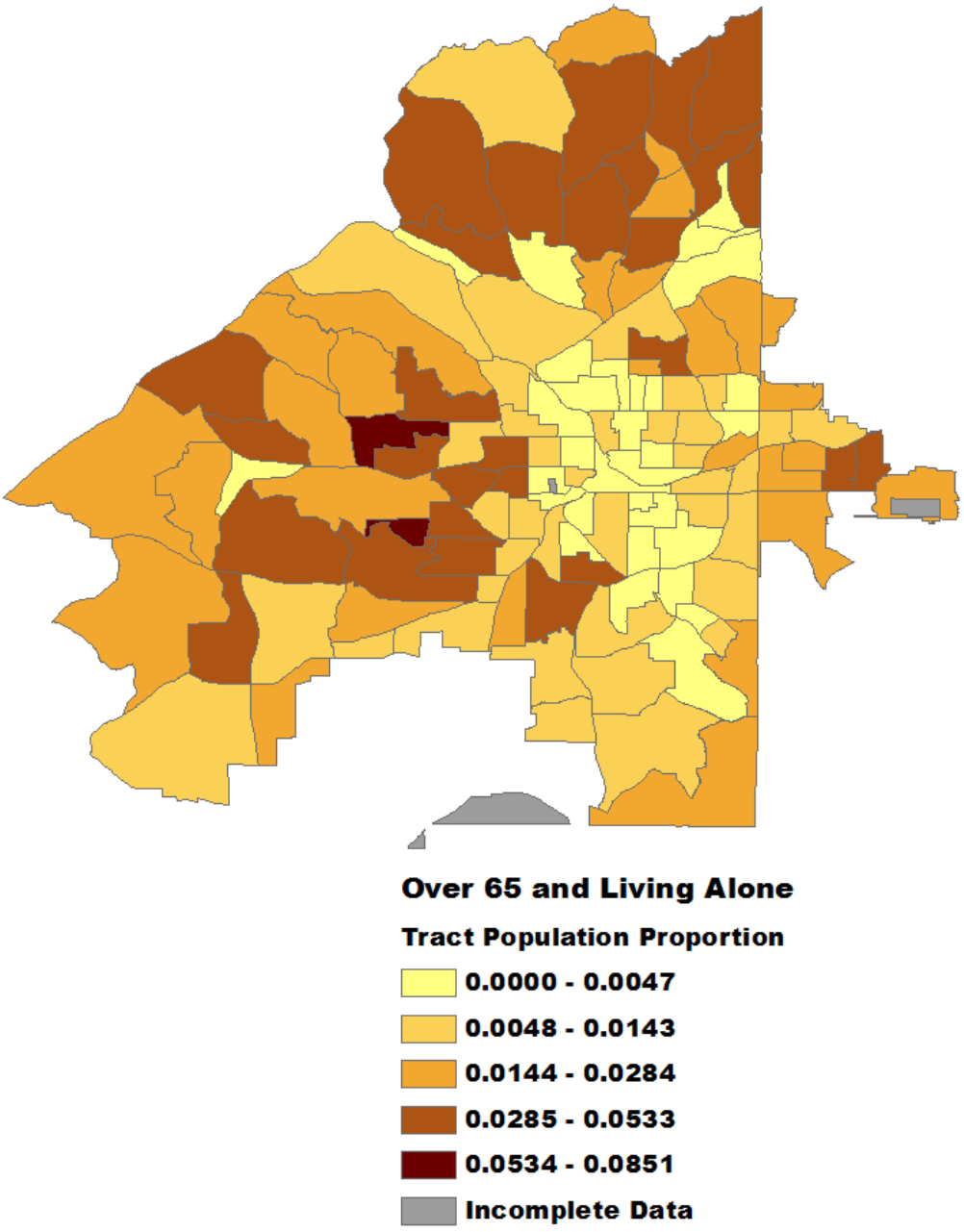
Over 65 and Living Alone
Tract Population Proportion
0.0000 - 0.0047
0.0048 - 0.0143
0.0144 - 0.0284
0.0285 - 0.0533
0.0534 - 0.0851
Incomplete Data

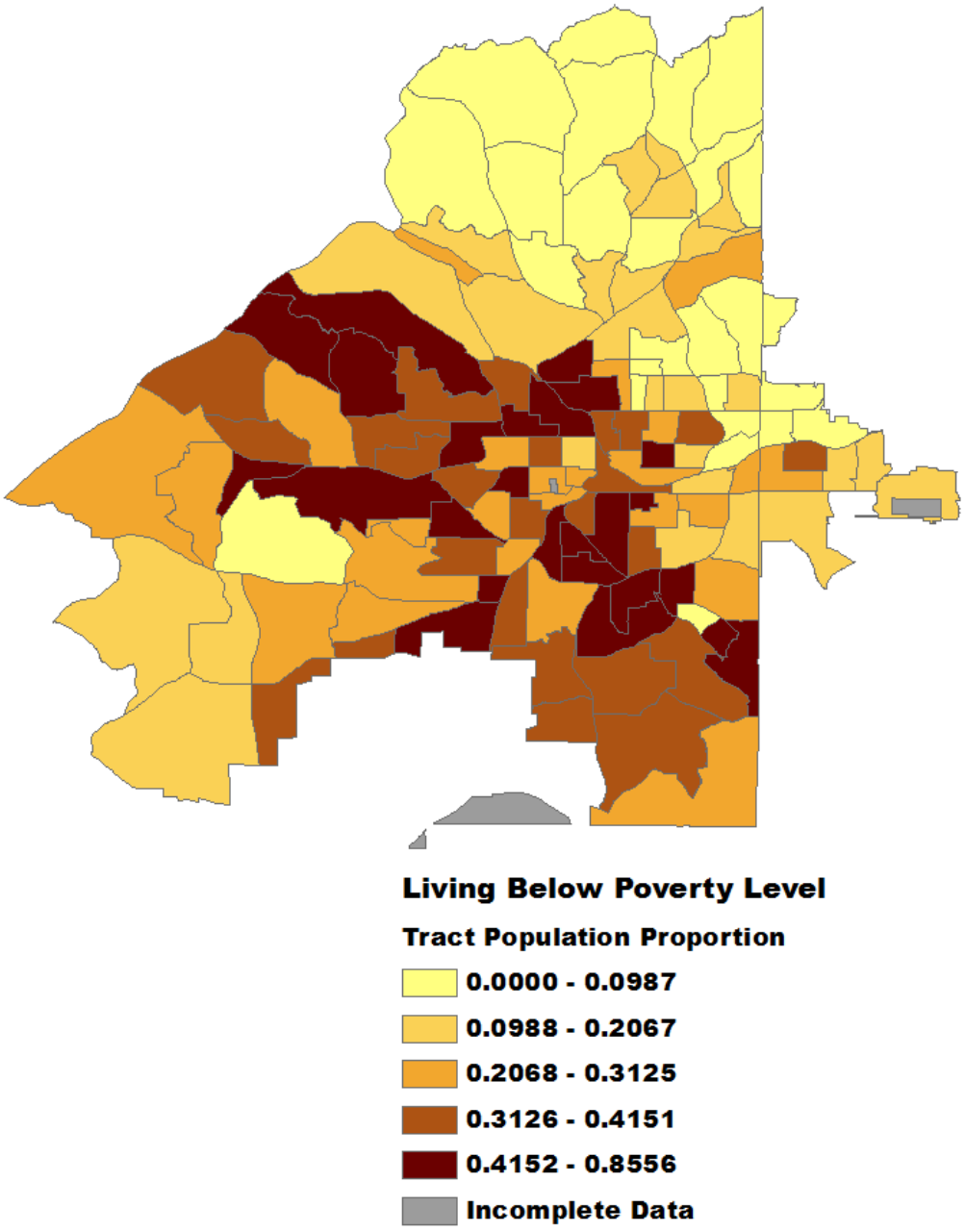
Living Below Poverty Level
Tract Population Proportion
0.0000 - 0.0987
0.0988 - 0.2067
0.2068 - 0.3125
0.3126 - 0.4151
0.4152 - 0.8556
Incomplete Data

A.2 Detroit

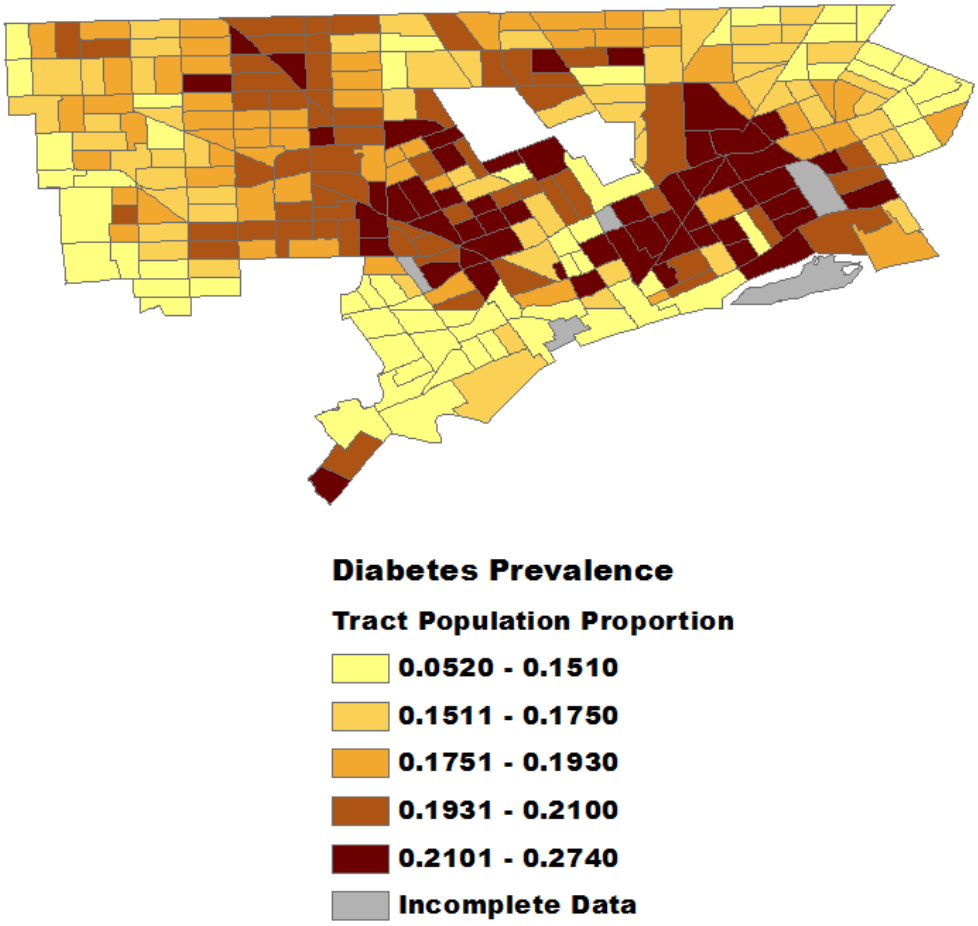
Diabetes Prevalence
Tract Population Proportion
0.0520 - 0.1510
0.1511 - 0.1750
0.1751 - 0.1930
0.1931 - 0.2100
0.2101 - 0.2740
Incomplete Data

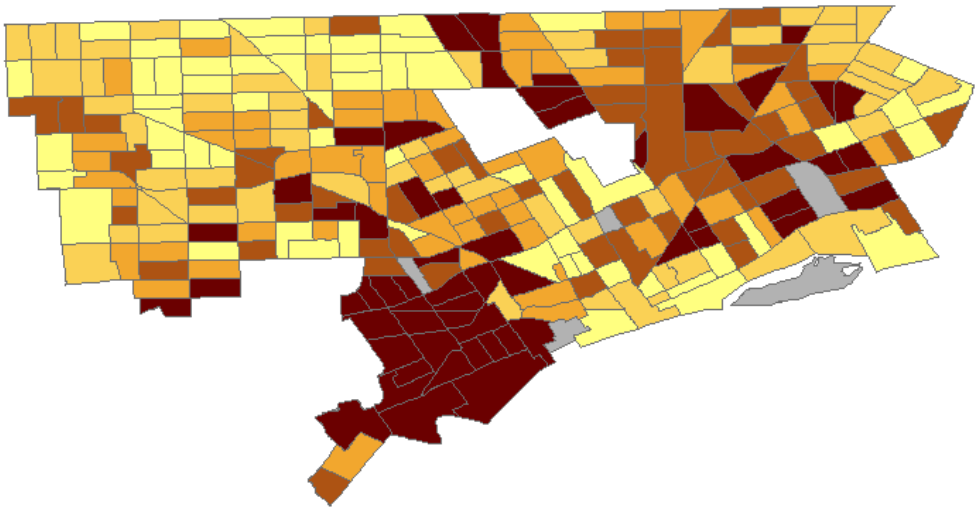
Less than High School Education
Tract Population Proportion
0.0192 - 0.1420
0.1421 - 0.1961
0.1962 - 0.2517
0.2518 - 0.3085
0.3086 - 0.6709
Incomplete Data

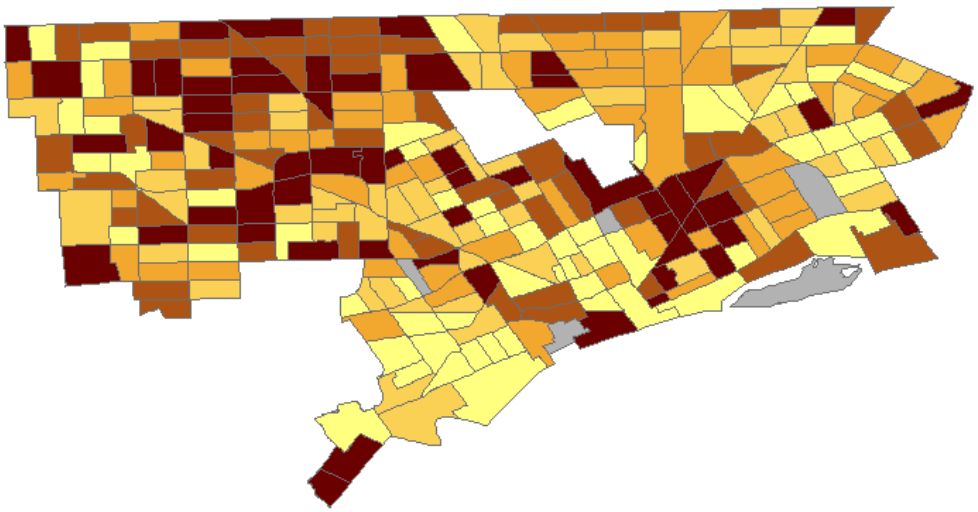
Living Alone
Tract Population Proportion
0.0000 - 0.0388
0.0389 - 0.0529
0.0530 - 0.0690
0.0691 - 0.0856
0.0857 - 0.2509
Incomplete Data

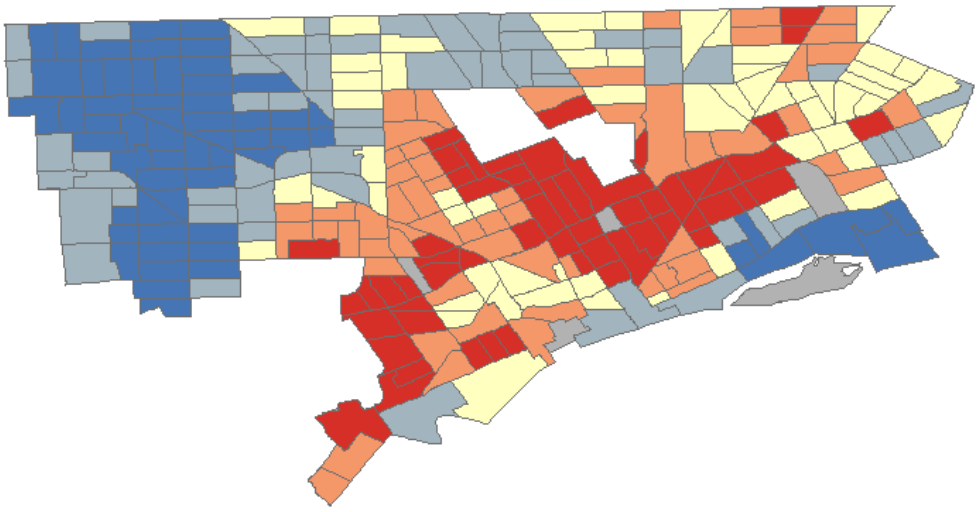

Average Land Surface Temperature (°F)

- 83.92 - 91.40
- 91.41 - 93.93
- 93.94 - 95.05
- 95.06 - 95.96
- 95.97 - 98.00
- Incomplete Data

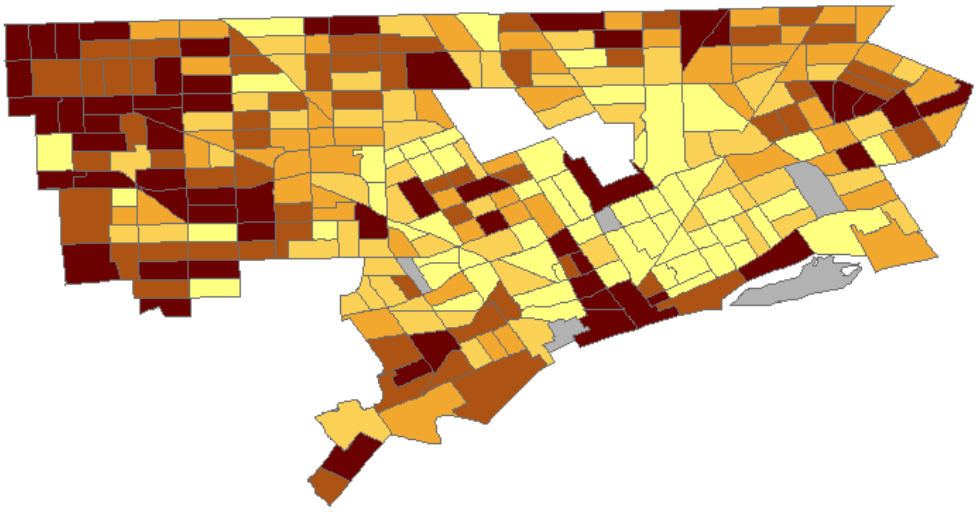
No AC Access
Tract Population Proportion
0.0884 - 0.1004
0.1005 - 0.1021
0.1022 - 0.1035
0.1036 - 0.1045
0.1046 - 0.1069
Incomplete Data

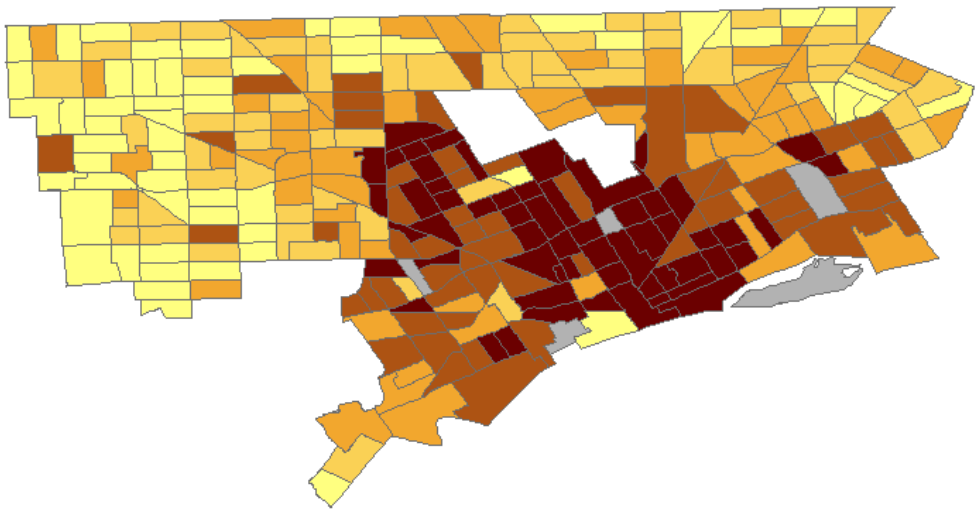
No Full AC Access
Tract Population Proportion
0.0000 - 0.0125
0.0126 - 0.0289
0.0290 - 0.0566
0.0567 - 0.1013
0.1014 - 0.3092
Incomplete Data

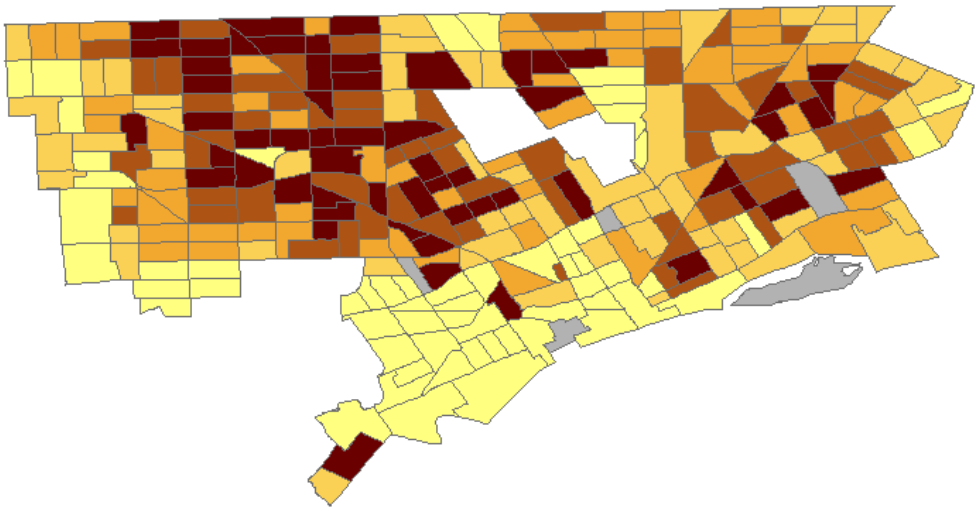
NonWhite
Tract Population Proportion
0.1930 - 0.8238
0.8239 - 0.9399
0.9400 - 0.9720
0.9721 - 0.9899
0.9900 - 1.0000
Incomplete Data

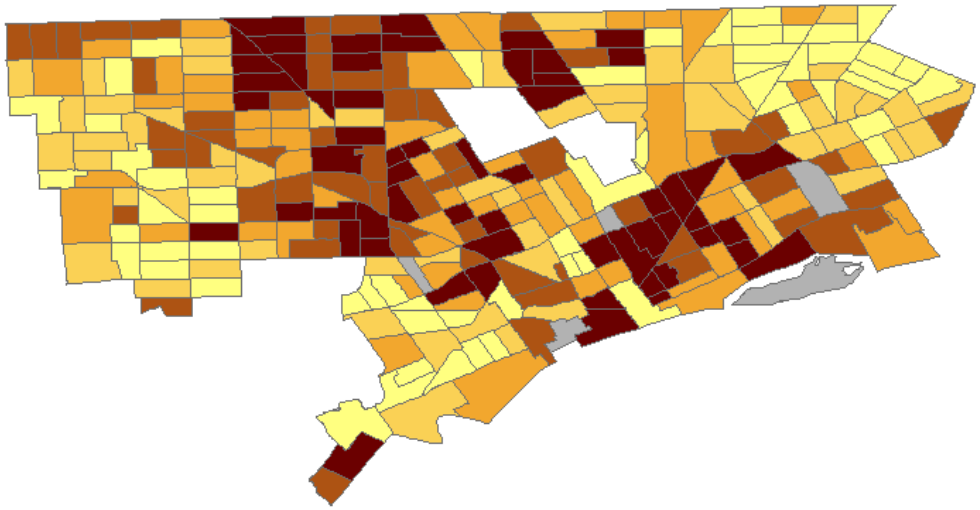

Over Age 65

Tract Population Proportion

- **0.0000 - 0.0718**
- **0.0719 - 0.1006**
- **0.1007 - 0.1268**
- **0.1269 - 0.1660**
- **0.1661 - 0.3842**
- **Incomplete Data**

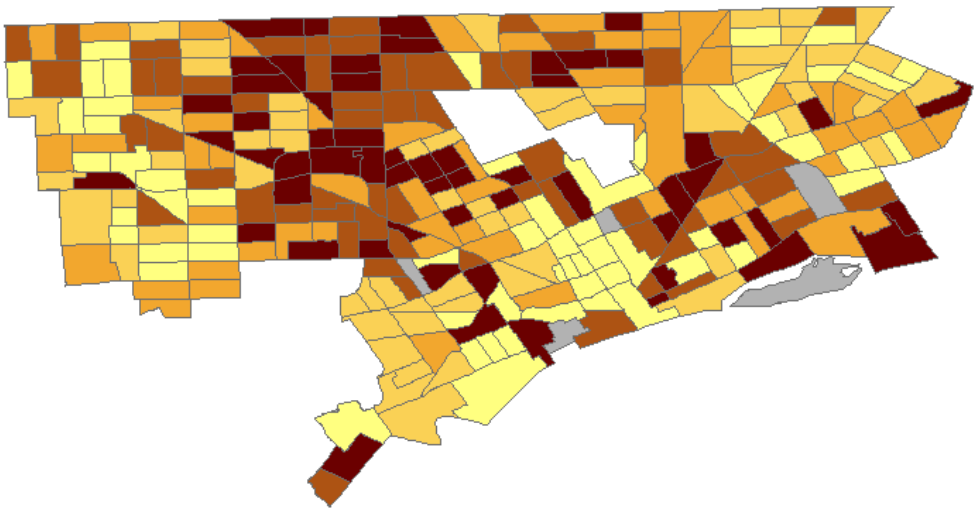
Over 65 and Living Alone
Tract Population Proportion
0.0000 - 0.0097
0.0098 - 0.0180
0.0181 - 0.0264
0.0265 - 0.0362
0.0363 - 0.1746
Incomplete Data

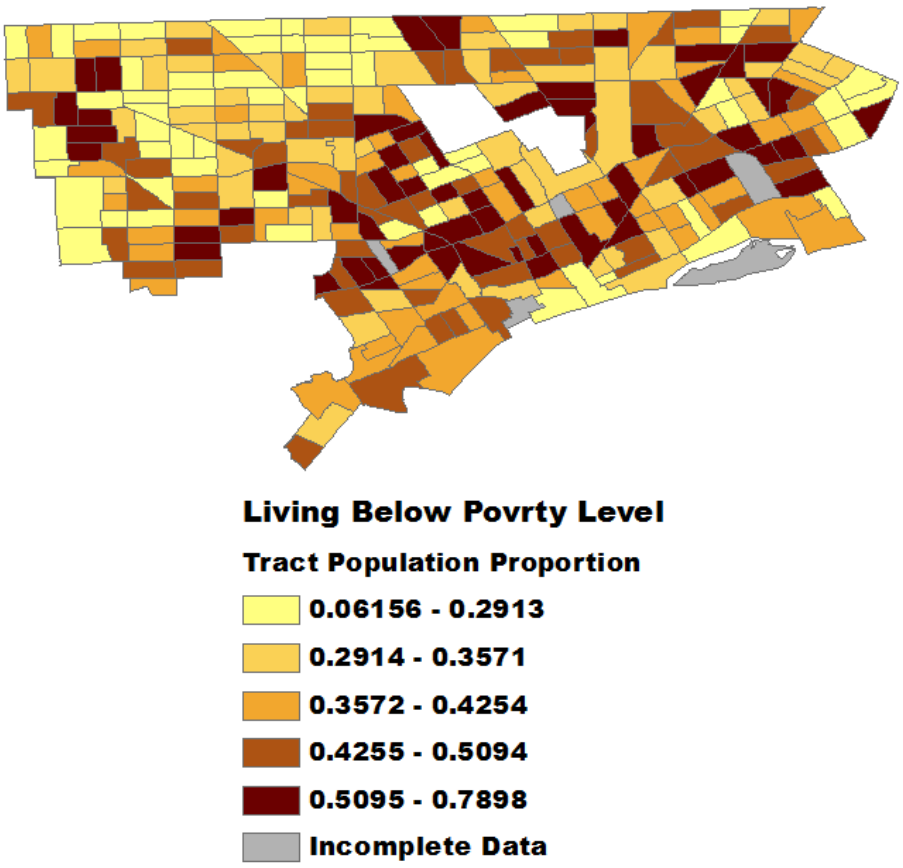
Living Below Povrty Level
Tract Population Proportion
0.06156 - 0.2913
0.2914 - 0.3571
0.3572 - 0.4254
0.4255 - 0.5094
0.5095 - 0.7898
Incomplete Data

A.3 Phoenix

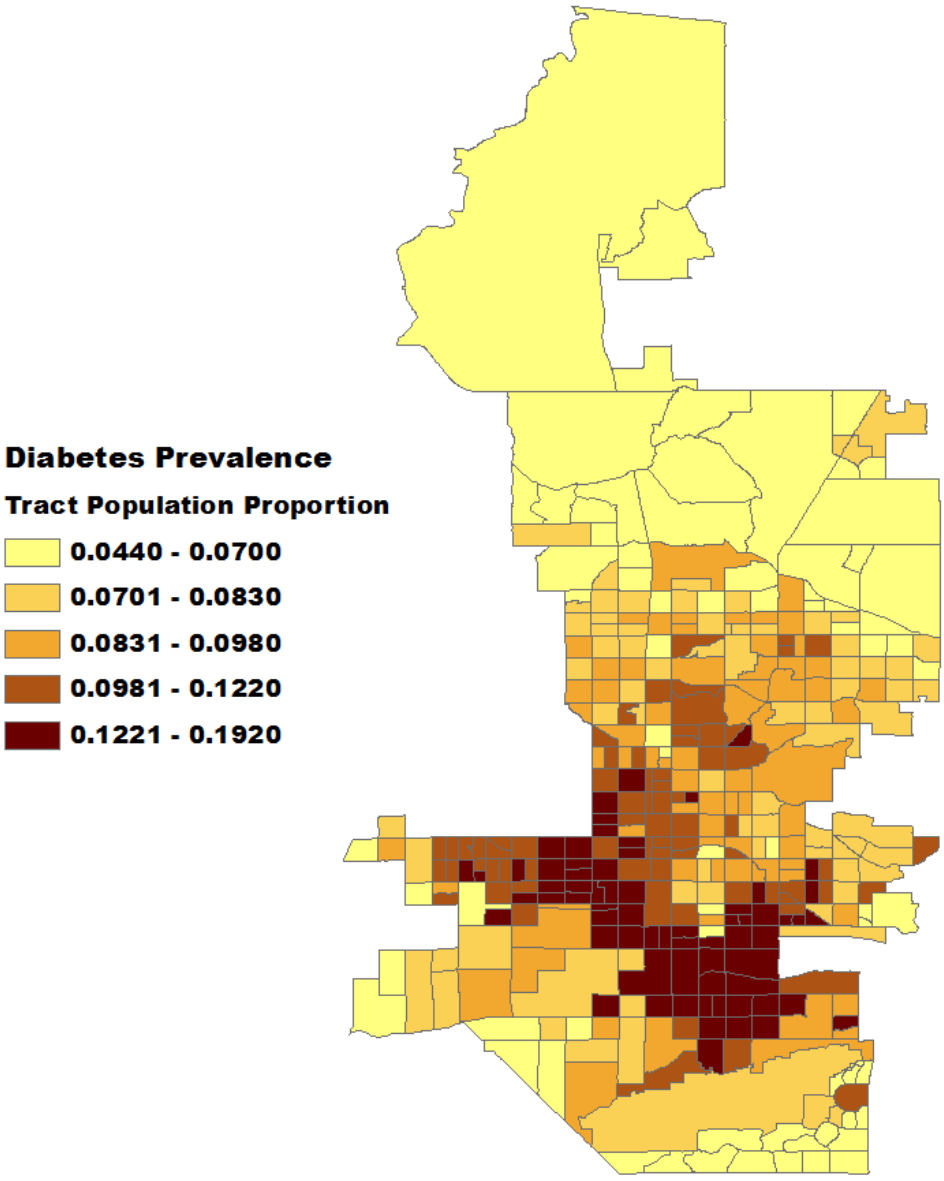
Diabetes Prevalence
Tract Population Proportion
0.0440 - 0.0700
0.0701 - 0.0830
0.0831 - 0.0980
0.0981 - 0.1220
0.1221 - 0.1920

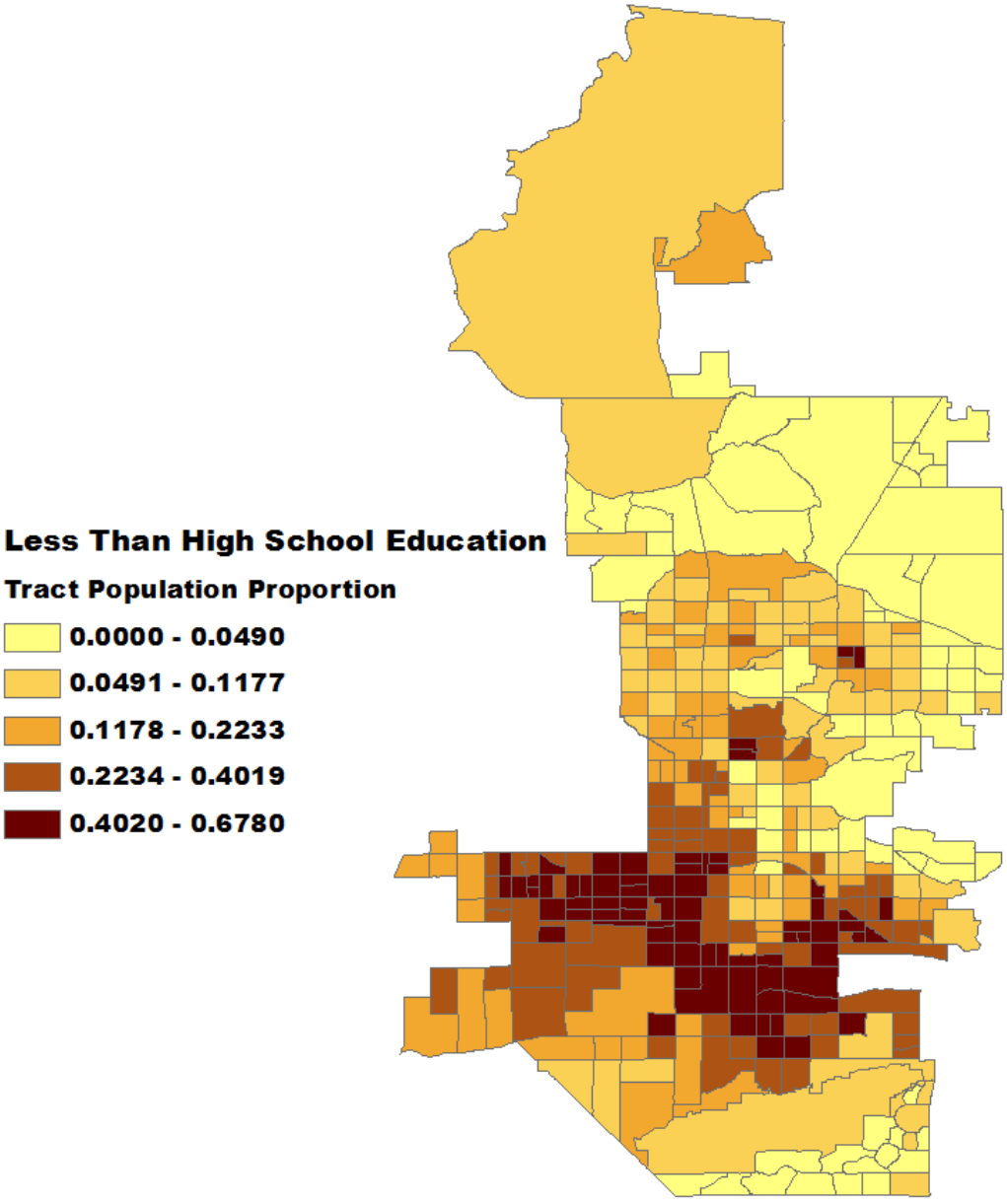
Less Than High School Education
Tract Population Proportion
0.0000 - 0.0490
0.0491 - 0.1177
0.1178 - 0.2233
0.2234 - 0.4019
0.4020 - 0.6780

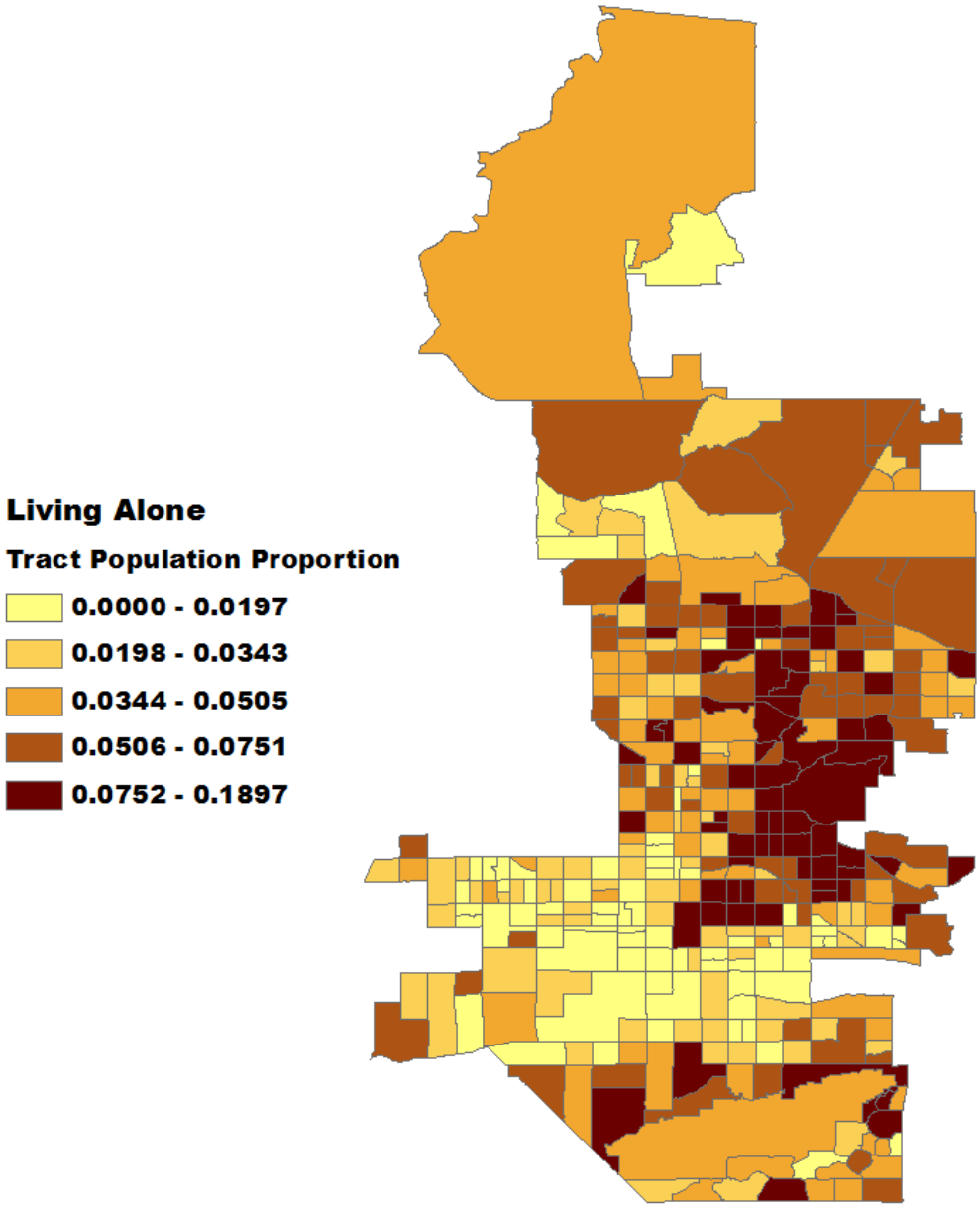
Living Alone
Tract Population Proportion
0.0000 - 0.0197
0.0198 - 0.0343
0.0344 - 0.0505
0.0506 - 0.0751
0.0752 - 0.1897

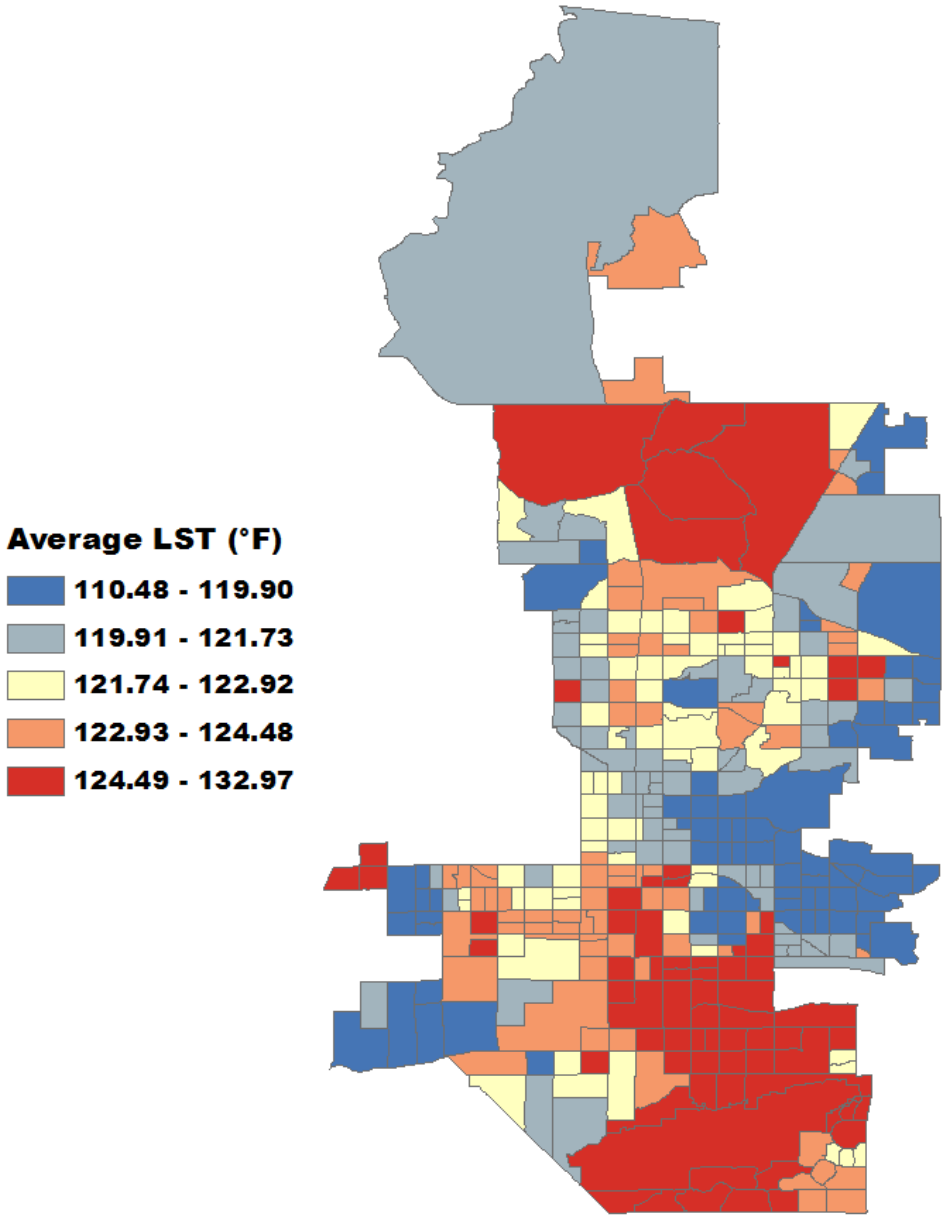
Average LST (°F)
110.48 - 119.90
119.91 - 121.73
121.74 - 122.92
122.93 - 124.48
124.49 - 132.97

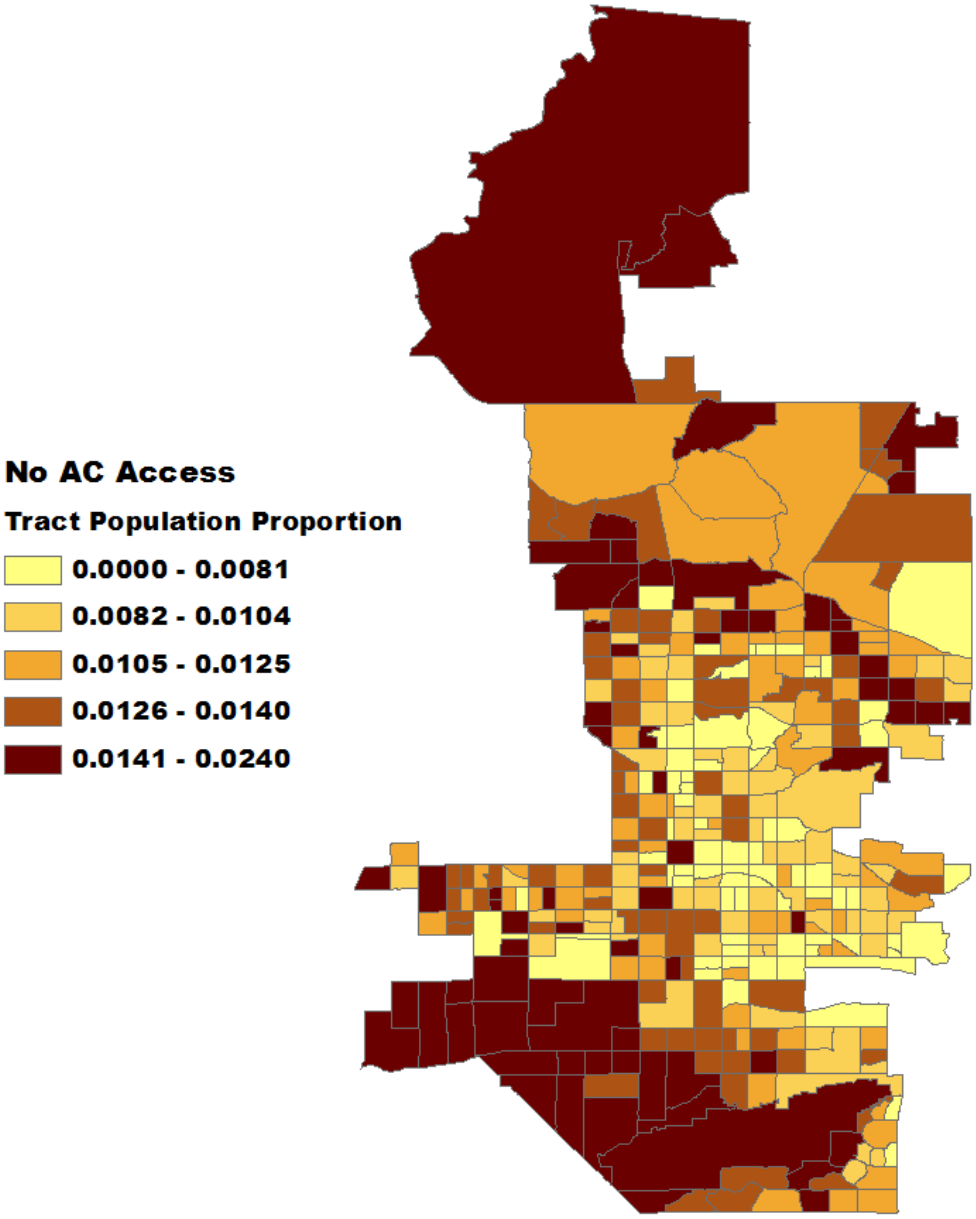
No AC Access
Tract Population Proportion
0.0000 - 0.0081
0.0082 - 0.0104
0.0105 - 0.0125
0.0126 - 0.0140
0.0141 - 0.0240

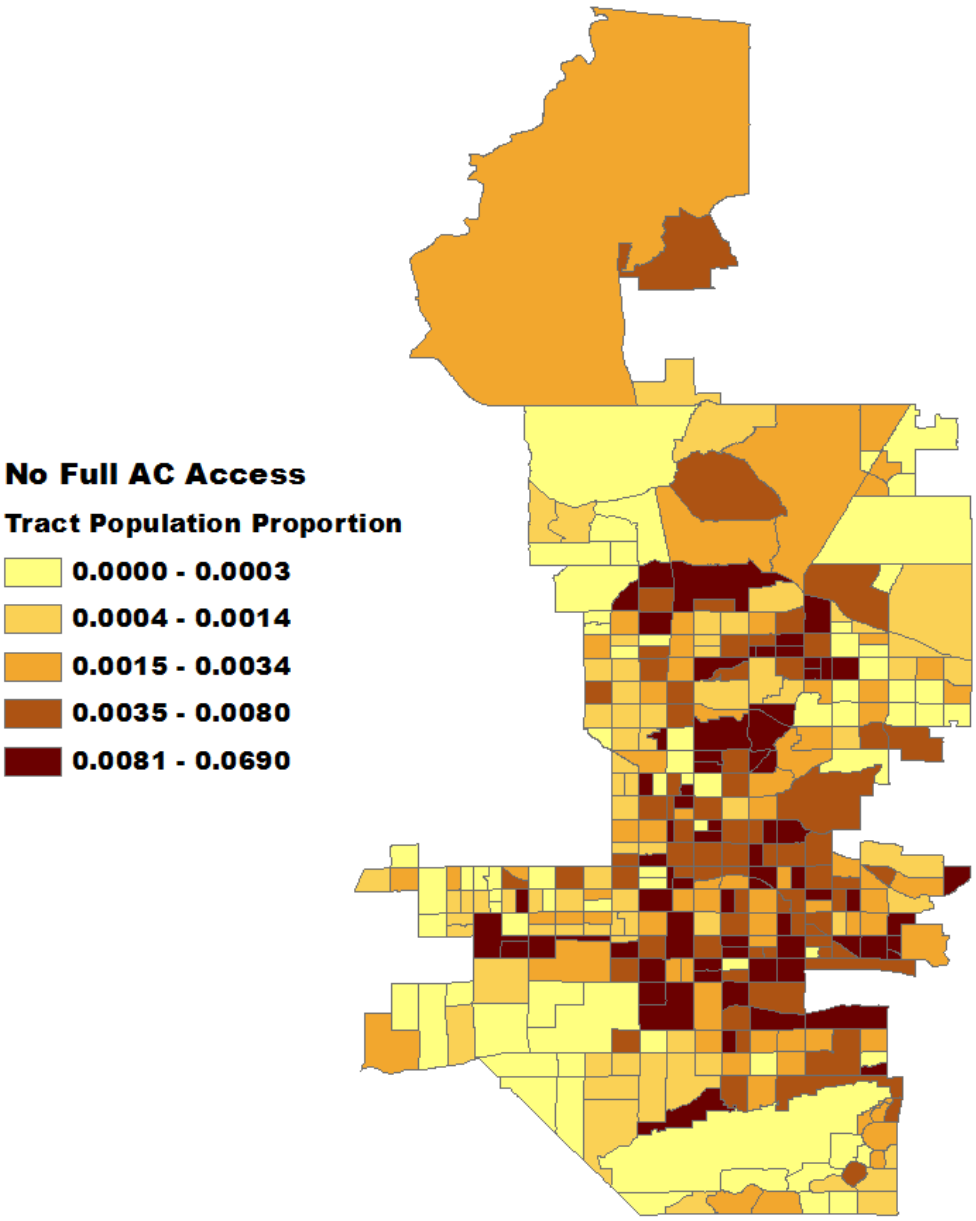
No Full AC Access
Tract Population Proportion
0.0000 - 0.0003
0.0004 - 0.0014
0.0015 - 0.0034
0.0035 - 0.0080
0.0081 - 0.0690

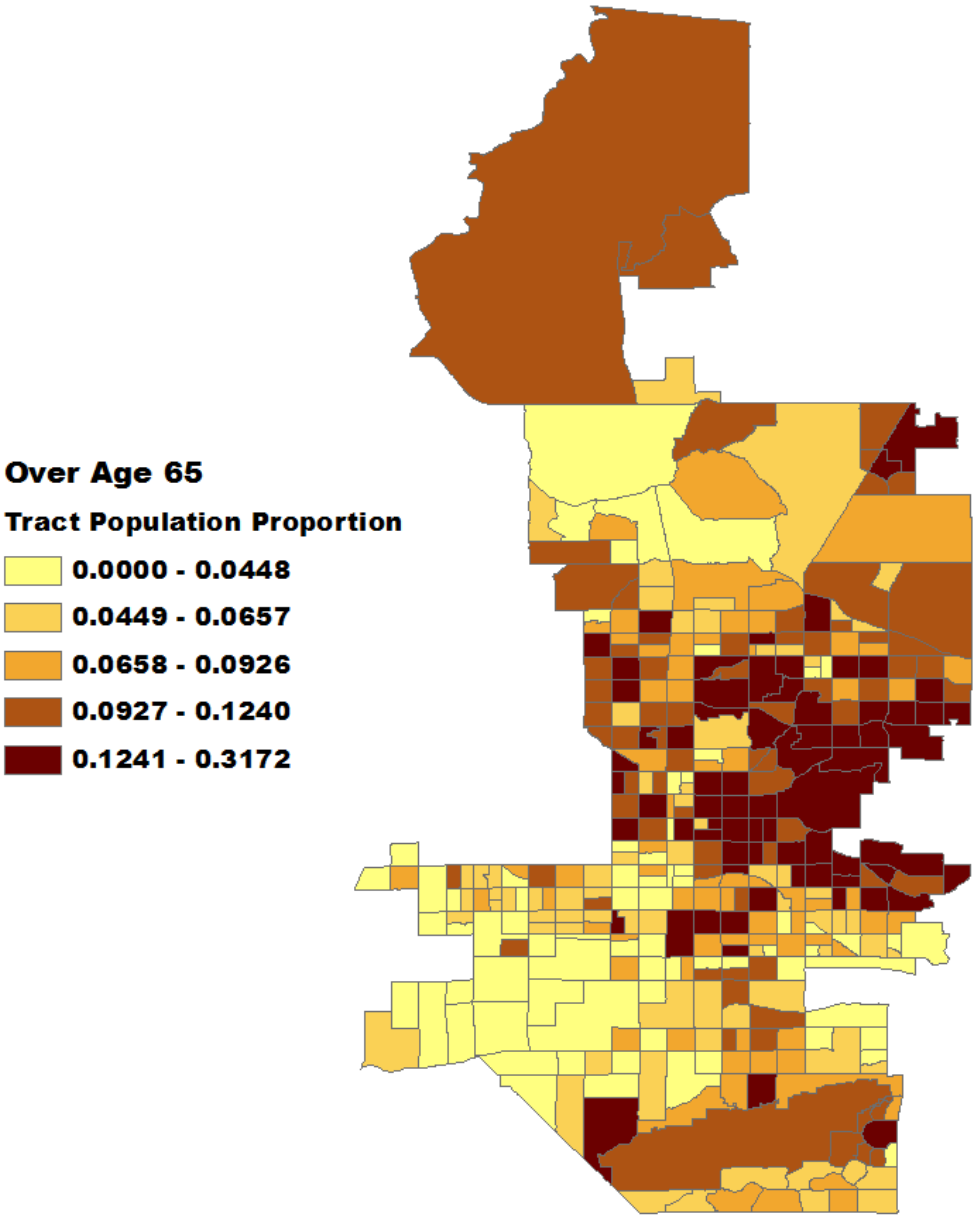
Over Age 65
Tract Population Proportion
0.0000 - 0.0448
0.0449 - 0.0657
0.0658 - 0.0926
0.0927 - 0.1240
0.1241 - 0.3172

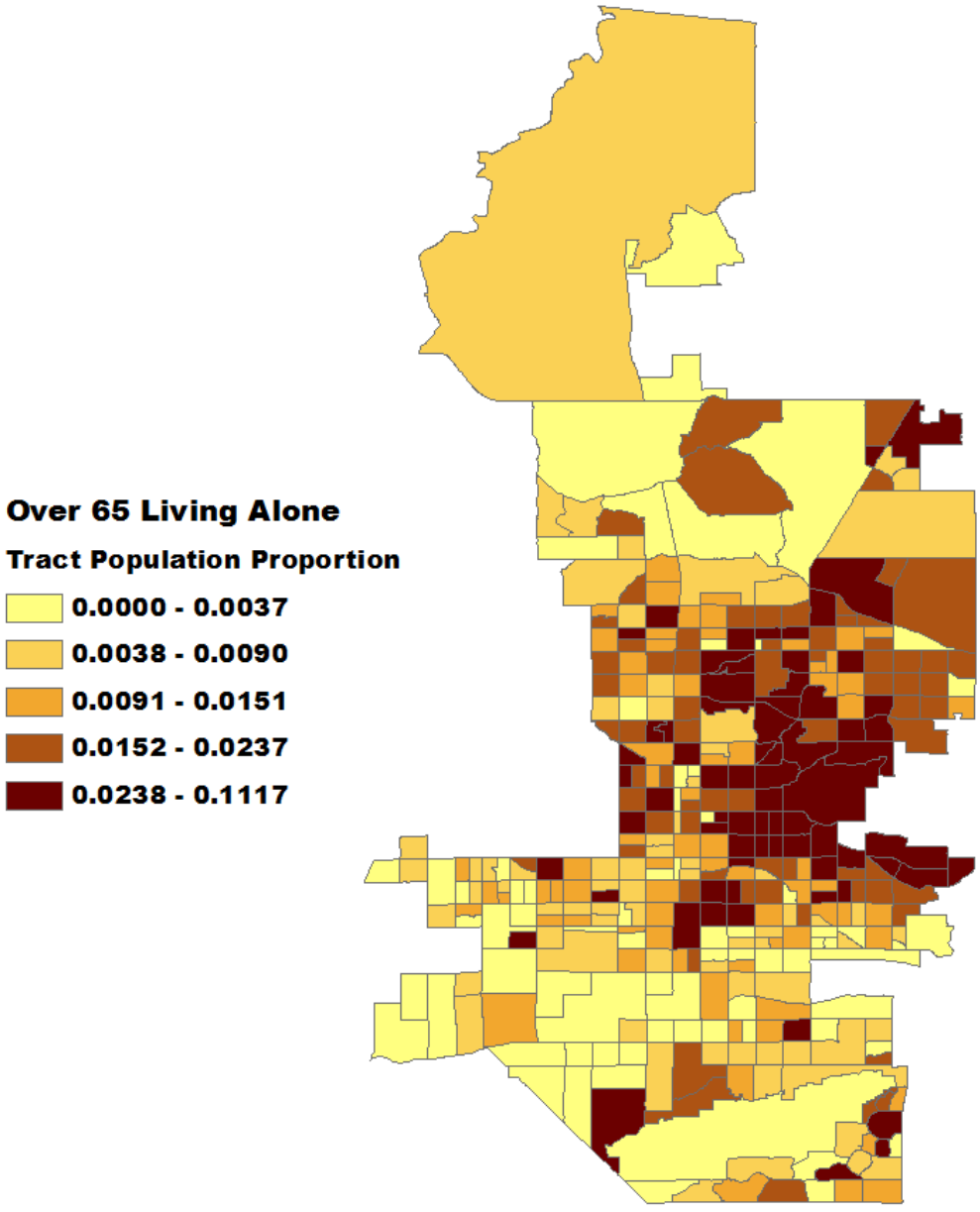
Over 65 Living Alone
Tract Population Proportion
0.0000 - 0.0037
0.0038 - 0.0090
0.0091 - 0.0151
0.0152 - 0.0237
0.0238 - 0.1117

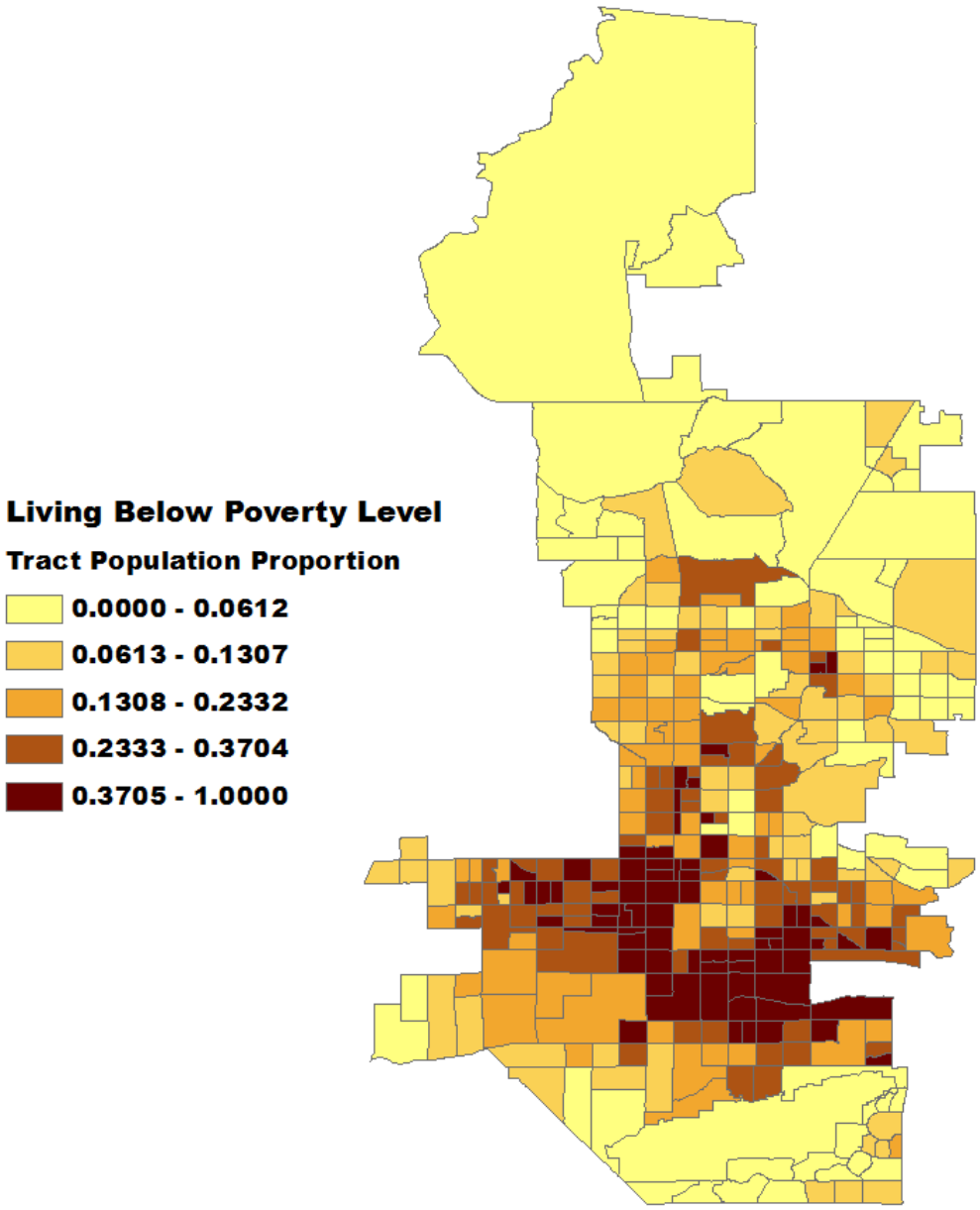
Living Below Poverty Level
Tract Population Proportion
0.0000 - 0.0612
0.0613 - 0.1307
0.1308 - 0.2332
0.2333 - 0.3704
0.3705 - 1.0000

APPENDIX B. HVI INDICATOR DESCRIPTIVE STATISTICS

	Atlanta (N = 127)		Detroit (N = 292)		Phoenix (N = 356)	
	Mean	**Std. Dev.**	**Mean**	**Std. Dev.**	**Mean**	**Std. Dev.**
Diabetes	0.1259	0.0659	0.1817	0.0337	0.0954	0.0285
No AC Access	0.0066	0.0013	0.1021	0.0030	0.0111	0.0031
No Full AC Access	0.0151	0.0159	0.0607	0.0607	0.0051	0.0075
Over Age 65	0.0980	0.0622	0.1192	0.0540	0.0874	0.0512
Nonwhite	0.6320	0.3399	0.8885	0.1634	0.2101	0.1155
Less than High School Education	0.1440	0.1078	0.2367	0.1162	0.2139	0.1755
Living Below Poverty Line	0.2656	0.1691	0.3940	0.1326	0.2222	0.1739
Living Alone	0.0744	0.0494	0.0648	0.0337	0.0494	0.0347
Over 65 and Living Alone	0.0180	0.0166	0.0248	0.0197	0.0156	0.0149
Land Surface Temperature (°F)	99.535	2.926	93.880	2.425	122.30	3.426

Note: All values represent Census tract population proportions except for Land Surface Temperature. N refers to the number of tracts for which there is complete data.

REFERENCES

Abhijith, K. V., & Gokhale, S. (2015). Passive control potentials of trees and on-street parked cars in reduction of air pollution exposure in urban street canyons. Environmental Pollution, 204, 99–108. https://doi.org/10.1016/j.envpol.2015.04.013

American Planning Association. (2011). Policy Guide on Climate Change.

Ahn, B.S.; Choi, S.H. (2012). Aggregation of ordinal data using ordered weighted averaging operator weights. Ann. Oper. Res., 201, 1–16.

Akbari, H. (2002). Shade trees reduce building energy use and CO2 emissions from power plants. Environmental Pollution (Barking, Essex: 1987), 116 Suppl, S119–26. http://doi.org/10.1016/S0269-7491(01)00264-0

Anderson, G., Bell, M. (2011). Heat waves in the United States: Mortality risk during heat waves and effect modification by heat wave characteristics in 43 U.S. communities. Environmental Health Perspectives, 119, 210-218. http://dx.doi.org/10.1289/ehp.1002313

Arnfield, A.J. (2003). Two decades of urban climate research: A review of turbulence, exchanges of energy and water, and the urban heat island. Int. J. Climatol., 23, 1–26.

ASLA. (2011). ASLA green roof demonstration project fact sheet. American Society of Landscape Architects. Retrieved from http://www.asla.org/uploadedFiles/CMS/Green_Roof/Green%20roof%20Fact%20sheet%201-pager%20101111%20final_doc.doc

Aubrecht, C.; Ozceylan, D. (2013). Identification of heat risk patterns in the U.S. National Capital Region by integrating heat stress and related vulnerability. Environ. Int. 56, 65–77.

Baker, I., Peterson, A., Brown, G., & McAlpine, C. (2012). Local government response to the impacts of climate change: An evaluation of local climate adaptation plans.

Landscape and Urban Planning, 107(2), 127–136. http://doi.org/10.1016/j.landurbplan.2012.05.009

Bao, J., Li, X., Yu, C. (2015). The Construction and Validation of the Heat Vulnerability Index, a Review, 7220–7234. http://doi.org/10.3390/ijerph120707220

Basu R., Feng, W, Ostro, B. (2008). Characterizing temperature and mortality in nine California counties. Epidemiology. 19:138–145. doi: 10.1097/EDE.0b013e31815c1da7.

Berardi, U., GhaffarianHoseini, A., GhaffarianHoseini, A. (2014). State-of-the-art analysis of the environmental benefits of green roofs. Applied Energy, 115, 411–428. https://doi.org/10.1016/j.apenergy.2013.10.047

Berko, J., Ingram, D., Saha, S., Parker, J. (2014). Deaths Attributed to Heat, Cold, and Other Weather Events in the United States, 2006–2010. National Health Statistics Reports No. 76. National Center for Health Statistics, Hyattsville, MD. http://www.cdc.gov/ nchs/data/nhsr/nhsr076.pdf

Biesbroek, G. R., Swart, R. J., & van der Knaap, W. G. M. (2009). The mitigation-adaptation dichotomy and the role of spatial planning. Habitat International, 33(3), 230–237. http://doi.org/10.1016/j.habitatint.2008.10.001

Bobb, J., Peng, R., Bell, M., Dominici, F. (2014). Heat-related mortality and adaptation to heat in the United States. Environmental Health Perspectives, 122, 811-816. http://dx.doi.org/10.1289/ehp.1307392

Boeckmann, M., Rohn, I. (2014). Is planned adaptation to heat reducing heat-related mortality and illness? A systematic review. BMC Public Health, 13(1112), 1–13.

Bouchama, A., Knochel, J. (2002). HEAT STROKE. The New England Journal of Medicine, 346(25), 1978–1988

Boumans, R., Phillips, D., Victery, W., Fontaine, T. (2014). Developing a model for effects of climate change on human health and health–environment interactions: heat stress in Austin, Texas. Urban Climate, 8, 78-99.

Braga A., Zanobetti A., Schwartz J. (2002). The effect of weather on respiratory and cardiovascular deaths in 12 U.S. cities. Environ. Health Perspect. 110:859–863. doi: 10.1289/ehp.02110859

Breitner S., Wolf K., Devlin R., Diaz-Sanchez D., Peters A., Schneider A. (2014). Short-term effects of air temperature on mortality and effect modification by air pollution in three cities of Bavaria, Germany: A time-series analysis. Sci. Total Environ. 6:49–61. doi: 10.1016/j.scitotenv.2014.03.048.

Broadbent, A. M., Coutts, A. M., Nice, K. A., Demuzere, M., & Krayenhoff, E. S. (2019). The Air-temperature Response to Green / blue-infrastructure Evaluation Tool (TARGET v1. 0): an efficient and user-friendly model of city cooling. *Geoscientific Model Development*, *12*, 785–803.

Brooks, N.; Adger, W.N.; Kelly, P.M. (2005). The determinants of vulnerability and adaptive capacity at the national level and the implications for adaptation. Glob. Environ. Chang., 15, 151–163.

Bunker, A., Wildenhain, J., Vandenbergh, A., Henschke, N., Rocklöv, J., Hajat, S., & Sauerborn, R. (2016). Effects of Air Temperature on Climate-Sensitive Mortality and Morbidity Outcomes in the Elderly; a Systematic Review and Meta-analysis of Epidemiological Evidence. EBioMedicine, 6, 258–268. http://doi.org/10.1016/j.ebiom.2016.02.034

Bunyavanich, S.; Landrigan, C.P.; McMichael, A.J.; Epstein, P.R. (2003). The impact of climate change on child health. Ambul. Pediatr., 3, 44–52.

Burden, D. (2006). 22 benefits of urban street trees. Retrieved from www.michigan.gov/documents/dnr/22_benefits_208084_7.pdf

Buscail, C., Upegui, E., Viel, J. F. (2012). Mapping heatwave health risk at the community level for public health action. Int J Health Geogr, 11, 38. http://doi.org/10.1186/1476-072X-11-38

Bustinza, R., Lebel, G., Gosselin, P., Bélanger, D., Chebana, F. (2013). Health impacts of the July 2010 heat wave in Quebec, Canada. BMC Public Health, 13, 56. http://dx.doi. org/10.1186/1471-2458-13-56

Centers for Disease Control and Prevention, National Center for Health Statistics. Underlying Cause of Death 1999-2017 on CDC WONDER Online Database, released December 2018. Data are from the Multiple Cause of Death Files, 1999-2017, as compiled from data provided by the 57 vital statistics jurisdictions through the Vital Statistics Cooperative Program. Accessed at http://wonder.cdc.gov/ucd-icd10.html on Jul 12, 2019 10:16:25 PM

Chen, D., Wang, X., Thatcher, M., Barnett, G., Kachenko, A., Prince, R. (2014). Urban Vegetation for Reducing Heat Related Mortality. Environmental Pollution, 192, 275-284.

Curriero, F. C., Heiner, K. S., Samet, J. M., Zeger, S. L., Strug, L., & Patz, J. A. (2002). Temperature and Mortality in 11 Cities of the Eastern United States. American Journal of Epidemiology, 155(1), 80–87.

Cutter, S. L., Barnes, L., Berry, M., Burton, C., Evans, E., Tate, E., & Webb, J. (2008). A place-based model for understanding community resilience to natural disasters. Global Environmental Change, 18(4), 598–606. http://doi.org/10.1016/j.gloenvcha.2008.07.013

Dannenberg, A., Frumkin, H., Jackson, R. (eds). 2011. Making Healthy Places: Designing and building for health, well-being, and sustainability. Island Press. Washington, D.C.

Davis, R., Knappenberger, P., Michaels, P., Novicoff, W. (2003). Changing Heat-Related Mortality in the United States. Environmental Health Perspectives, 111(14), 1712–1718. http://doi.org/10.1289/ehp.6336

Dear, K., & Wang, Z. (2015). Climate and health: mortality attributable to heat and cold. The Lancet, 386, 150–156. http://doi.org/10.1016/S0140-6736(15)60897-2

Diffenbaugh, N. S., & Scherer, M. (2011). Observational and model evidence of global emergence of permanent, unprecedented heat in the 20th and 21st centuries. Climatic Change, 107(3), 615–624. https://doi.org/10.1007/s10584-011-0112-y

Dolney, T.J.; Sheridan, S.C. (2006). The relationship between extreme heat and ambulance response calls for the city of Toronto, Ontario, Canada. Environ. Res., 101, 94–103.

Dousset, B., Gourmelon, F., Laaidi, K., Zeghnoun, A., Giraudet, E., Bretin, P., Mauri, E., Vandentorren, S. (2010). Satellite monitoring of summer heat waves in the Paris metropolitan area. International Journal of Climatology, 31(2), 313–323. http://doi.org/10.1002/joc.2222

Ebi, K.L.; Teisberg, T.J.; Kalkstein, L.S.; Robinson, L.; Weiher, R.F. (2004). Heat watch/warning systems save lives: Estimated costs and benefits for Philadelphia 1995–1998. Bull. Am. Meteorol. Soc. 85, 1067–1073.

Eliasson, I. (2000). The use of climate knowledge in urban planning. Landscape & Urban Planning, 48, 31–44.

Fischer, E. M., Oleson, K. W., & Lawrence, D. M. (2012). Contrasting urban and rural heat stress responses to climate change. Geophysical Research Letters, 39(3), 1–8. https://doi.org/10.1029/2011GL050576

Foster, J., Lowe, A., & Winkelman, S. (2011). The Value of Green Infrastructure for Urban Climate Adaptation. Center for Clean Air Policy.

Fowler, D., Mitchell, C., Brown, A., Pollock, T., Bratka, L., Paulson, J., Noller, A., Mauskapf, R., Oscanyan, K., Radcliffe, R., Vaidyanathan, A., Wolkin, A., Taylor, E. (2013) Heat-related deaths after an extreme heat event — four states, 2012 and United States, 1999–2009. Morbidity and Mortality Weekly Report. 62 (22). 433–436.

Gamble, J., Schmeltz, M., Hurley, B., Hseih, J., Jette, G., & Wagner, H. (2018). Mapping the Vulnerability of Human Health to Extreme Heat in the US.

Gasparrini, A., Guo, Y., Hashizume, M., Lavigne, E., Zanobetti, A., Schwartz, J., Armstrong, B. (2015). Mortality risk attributable to high and low ambient temperature: A multicountry observational study. The Lancet, 386(9991), 369–375. http://doi.org/10.1016/S0140-6736(14)62114-

Gasparrini, A., Guo, Y., Sera, F., Vicedo-Cabrera, A. M., Huber, V., Tong, S., … Armstrong, B. (2017). Projections of temperature-related excess mortality under climate change scenarios. The Lancet Planetary Health, 1(9), e360–e367. http://doi.org/10.1016/S2542-5196(17)30156-0

Habeeb, D., Vargo, J., Stone, B. (2015). Rising heat wave trends in large US cities. Natural Hazards, 76(3), 1651–1665. http://doi.org/10.1007/s11069-014-1563-z

Harlan, S. L., Brazel, A. J., Prashad, L., Stefanov, W. L., Larsen, L. (2006). Neighborhood microclimates and vulnerability to heat stress. Social Science & Medicine, 63, 2847–2863. http://doi.org/10.1016/j.socscimed.2006.07.030

Harlan, S. L., & Ruddell, D. M. (2011). Climate change and health in cities: Impacts of heat and air pollution and potential co-benefits from mitigation and adaptation. Current Opinion in Environmental Sustainability, 3(3), 126–134. https://doi.org/10.1016/j.cosust.2011.01.001

Harlan, Sharon L.; Declet-Barreto, Juan H.; Stefanov, William L., Sarah Santana; Petitti, D. (2013). Neighborhood Effects on Heat Deaths: Social and Environmental Determinants of Vulnerable Places. Environmental Health Perspectives, 121(2), 197–204. http://doi.org/10.1289/ehp.1104625

Hawkins, M. D., Brown, V., Ferrell, J., Hawkins, M. D., Brown, V., & Ferrell, J. (2016). Assessment of NOAA National Weather Service Methods to Warn for Extreme Heat Events. Weather, Climate, and Society, WCAS-D-15-0037.1. https://doi.org/10.1175/WCAS-D-15-0037.1

Hess, J. J., McDowell, J. Z., & Luber, G. (2012). Integrating climate change adaptation into public health practice: Using adaptive management to increase adaptive capacity and build resilience. Environmental Health Perspectives, 120(2), 171–179. http://doi.org/10.1289/ehp.1103515

Ho, H., Knudby, A., Xu, Y., Hodul, M., Aminipouri, M. (2016). A comparison of urban heat islands mapped using skin temperature, air temperature, and apparent temperature (Humidex), for the greater Vancouver area. Science of the Total Environment, 544, 929-938. doi:http://dx.doi.org/10.1016/j.scitotenv.2015.12.021

Hondula, D., Vanos, J., Gosling, S. (2014). The SSC: a decade of climate–health research and future directions. International Journal of Biometeorology, 58, 109–120. http://doi.org/10.1007/s00484-012-0619-6

Hosmer D.W., Lemeshow S. (1980) “A goodness-of-fit test for the multiple logistic regression model.” *Communications in Statistics* A10:1043-1069.

Huang, G., Zhou, W., Cadenasso, M. (2011). Is everyone hot in the city? Spatial pattern of land surface temperatures, land cover and neighborhood socioeconomic characteristics in Baltimore, MD. Journal of Environmental Management, 92 (7). 1753-1759

Jenerette, G. D., Harlan, S. L., Brazel, A., Jones, N., Larsen, L., Stefanov, W. L. (2007). Regional relationships between surface temperature, vegetation, and human settlement in a rapidly urbanizing ecosystem. Landscape Ecology, 22(3), 353–365. http://doi.org/10.1007/s10980-006-9032-z

Johnson, D.P.; Stanforth, A.; Lulla, V.; Luber, G. (2012). Developing an applied extreme heat vulnerability index utilizing socioeconomic and environmental data. Appl. Geogr., 35, 23–31.

Johnson, D.P.; Wilson, J.S.; Luber, G.C. (2009). Socioeconomic indicators of heat-related health risk supplemented with remotely sensed data. Int. J. Health Geogr., 8, doi:10.1186/1476-072X-8-57.

Jones, R. N., Preston, B. L. (2011). Adaptation and risk management. Wiley Interdisciplinary Reviews: Climate Change, 2(2), 296–308. http://doi.org/10.1002/wcc.97

Kalkstein, L., Davis, R. (1989). Weather and Human Mortality: An Evaluation of Demographic and Interregional Responses in the United States. Annals of the Association of American Geographers, 71(1), 44–64.

Kalkstein, L., Greene, S., Mills, D., Samenow, J. (2011) An evaluation of the progress in reducing heat-related human mortality in major US cities. Natural Hazards, 56, 113-129. http://dx.doi.org/10.1007/s11069-010-9552-3

Karl, T., Koss, J. (1984). Regional and National Monthly, Seasonal, and Annual Temperature Weighted by Area, 1895-1983. Historical Climatology Series 4-3, National Climatic Data Center, Asheville, NC

KC, B., Shepherd, J. M., & Johnson, C. (2015). Climate change vulnerability assessment in Georgia. Applied Geography, 62, 62–74. http://doi.org/10.1016/j.apgeog.2015.04.007

Kennedy, D., Stocker, L., & Burke, G. (2010). Australian local government action on climate change adaptation: some critical reflections to assist decision-making. Local Environment, 15(9–10), 805–816. https://doi.org/10.1080/13549839.2010.514602

Kenward, A., Yawitz, D., Sanford, T., & Wang, R. (2014). Summer in the City: Hot and Getting Hotter. Climate Central.

Kloog, I., Chudnovsky, A., Koutrakis, P., Schwartz, J. (2012). Temporal and Spatial Assessments of Minimum Air Temperature Using Satellite Surface Temperature Measurements in Massachusetts, USA. Science of the Total Environment, 432, 85-92. doi:10.1016/j.scitotenv.2012.05.095

Klosterman, R. E. (1983). Fact and value in planning. Journal of the American Planning Association, 49(2), 216–225. http://doi.org/10.1080/01944368308977066

Klosterman, R. E. (2013). Lessons learned about planning. Journal of the American Planning Association, 79(2), 161–169. http://doi.org/10.1080/01944363.2013.882647

Knowlton, K., Lynn, B., Goldberg, R., Rosenzweig, C., Hogrefe, C., Rosenthal, J., Kinney, P. (2007). Projecting heat-related mortality impacts under a changing climate in the New York City region. American Journal of Public Health, 97(11), 2028–2034. http://doi.org/10.2105/AJPH.2006.102947

Knowlton, K., Rotkin-Ellman, M., King, G., Margolis, H., Smith, D., Solomon, G., Trent, R., English, P. (2009). The 2006 California heat wave: Impacts on hospitalizations and emergency department visits. Environmental Health Perspectives, 117, 61-67. http://dx.doi.org/10.1289/ehp.11594

Koppe, C., Kovats, S., Jendritzky, G., & Menne, B. (2004). Heat-waves: risks and responses. Health and Global Environmental Health Series, No.2(2), 124 pp. https://doi.org/10.1007/s00484-009-0283-7

Kovats, R., Hajat, S. (2008). Heat stress and public health: a critical review. Annual Review of Public Health, 29, 41–55. http://doi.org/10.1146/annurev.publhealth.29.020907.090843

Kuras, E. R., Hondula, D. M., & Brown-Saracino, J. (2015). Heterogeneity in individually experienced temperatures (IETs) within an urban neighborhood : insights from a new approach to measuring heat exposure. International Journal of Biometeorology, 59, 1363–1372. http://doi.org/10.1007/s00484-014-0946-x

Kuras, E.R., Hondula, D.M., Brown-Saracino, J. (2016). Heterogeneity in individually experienced temperatures (IETs) within an urban neighborhood: Insights from a new approach to measuring heat exposure. International Journal of Biometeorology, 59, 1363-1372

Lindley, S. J., Handley, J. F., McEvoy, D., Peet, E., Theuray, N. (2007). The Role of Spatial Risk Assessment Adaptation in UK Urban Areas. Built Environment, 33(1), 46–69.

Liu, L., Zhang, Y. (2011). Urban Heat Island Analysis Using the Landsat TM Data and ASTER Data: A Case Study in Hong Kong. Remote Sensing, 3(7), 1535-1552.

Loughnan, M.; Nicholls, N.; Tapper, N.J. (2012). Mapping heat health risks in urban areas. Int. J. Popul. Res., doi:10.1155/2012/518687.

Luber, G., McGeehin, M. (2008). Climate Change and Extreme Heat Events. American Journal of Preventive Medicine, 35(5), 429–435. http://doi.org/10.1016/j.amepre.2008.08.021

Maier, G., Grundstein, A., Jang, W., Li, C., Naeher, L., & Shepherd, M. (2014). Assessing the Performance of a Vulnerability Index during Oppressive Heat across Georgia, United States. American Meteorological Society, 6, 253–264. https://doi.org/10.1175/WCAS-D-13-00037.1

Mallick, J., Rahman, A. (2012). Impact of Population Density on the Surface Temperature and Micro-Climate of Delhi. Current Science, 102, 2847-2863

Manangan, A., Uejio, C., Saha, S., Schramm, P., Marinucci, G., Hess, J. (2014). Assessing health vulnerability to climate change: A guide for health departments. (Climate and Health Technical Report Series). CS249409-A.Centers for Disease Control and Prevention.

Marinucci D., Luber, G., Uejio, C., Saha, S., Hess, J. (2014). Building resilience against climate effects—a novel framework to facilitate climate readiness in public health agencies. International Journal of Environmental Research and Public Health 11.

McPherson, E. G., & Simpson, J. R. (2001). Effects of California's Urban Forests on Energy Use and Potential Savings From Large-Scale Tree Planting. Center for Urban Forest Research, USDA Forest Service.

Measham, T. G., Preston, B. L., Smith, T. F., Brooke, C., Gorddard, R., Withycombe, G., & Morrison, C. (2011). Adapting to climate change through local municipal planning: Barriers and challenges. Mitigation and Adaptation Strategies for Global Change, 16(8), 889–909. http://doi.org/10.1007/s11027-011-9301-2

Mills, D., Schwartz, J., Lee, M., Sarofim, M., Jones, R., Lawson, M., Duckworth, M., Deck, L. (2015) Climate change impacts on extreme temperature mortality in select metropolitan areas in the United States. Climatic Change, 131, 83-95. http://dx.doi.org/10.1007/s10584-014-1154-8

Minnesota Climate and Health Program. (2012). Minnesota extreme heat toolkit. St. Paul, MN.

Mohsin, T., Gough, W. (2012). Characterization and estimation of urban heat island at Toronto: Impact of the choice of rural sites. Theoretical Applications of Climatology, 108, 105-117

Morabito, M., Crisci, A., Gioli, B., Gualtieri, G., Toscano, P., Di Stefano, V., Gensini, G. F. (2015). Urban-hazard risk analysis: Mapping of heat-related risks in the elderly in major Italian cities. PLoS ONE, 10(5), 1–18. http://doi.org/10.1371/journal.pone.0127277

Moser, S. C. (2014). Communicating adaptation to climate change: the art and science of public engagement when climate change comes home. Wiley Interdisciplinary Reviews: Climate Change, 5(3), 337–358. http://doi.org/10.1002/wcc.276

Mullaney, J., Lucke, T., Trueman, S. J. (2015). A review of benefits and challenges in growing street trees in paved urban environments. Landscape and Urban Planning, 134, 157–166. https://doi.org/10.1016/j.landurbplan.2014.10.013

Naughton, M.P.; Henderson, A.; Mirabelli, M.C.; Kaiser, R.; Wilhelm, J.L.; Kieszak, S.M.; Rubin, C.H.; McGeehin, M.A. (2002). Heat-related mortality during a 1999 heat wave in Chicago. Amer. J. Prev. Med., 22, 221–227.

Nayak, S., Shrestha, S., Kinney, P., Ross, Z., Sheridan, S., Pantea, C., (2017). Development of a heat vulnerability index for new york state. Public Health.

Nitschke, M.; Hansen, A.; Bi, P.; Pisaniello, D.; Newbury, J.; Kitson, A.; Tucker, G.; Avery, J.; Dal Grande, E. (2013). Risk factors, health effects and behavior in older people during extreme heat: A survey in south Australia. Int. J. Environ. Res. Public Health, 10, 6721–6733.

Nowak, D. Crane, D., Stevens, J. (2006). Air pollution removal by urban trees and shrubs in the United States. Urban Forestry and Urban Greening, 4. 115-123.

Nowak, D. J., Hirabayashi, S., Bodine, A., & Greenfield, E. (2014). Tree and forest effects on air quality and human health in the United States. Environmental Pollution, 193, 119–129. http://doi.org/10.1016/j.envpol.2014.05.028

O'Neill, M.S.; Zanobetti, A.; Schwartz, J. (2003). Modifiers of the temperature and mortality association in seven US cities. Amer. J. Epidemiol., 157, 1074–1082.

Oke, T. (1987). Boundary Layer Climates (2nd ed.). Routledge. http://doi.org/10.1017/CBO9781107415324.004

Oke, T.R. (1982). The Energetic Basis of the Urban Heat Island. Quarterly Journal of the Royal Meteorological Society, 108, 1–24

Ozceylan, D.; Coskun, E. (2012). The Relationship between Turkey's Provinces' Development Levels and Social and Economic Vulnerability to Disasters. J. Homel. Secur. Emerg., 9, doi:10.1515/1547-7355.1981.

Pandit, R., & Laband, D. N. (2010). Energy savings from tree shade. Ecological Economics, 69(6), 1324–1329. https://doi.org/10.1016/j.ecolecon.2010.01.009

Patz J., Engelberg D., Last J. (2010). The effects of changing weather on public health. Annu. Rev. Public Health. 21:271–307. doi: 10.1146/annurev.publhealth.21.1.271.

Peper, P., McPherson, E., Simpson, J., Gardner, S., Vargas, K., Xiao, Q. (2007). New York City, New York Municipal Forest Resource Analysis, Center for Urban Forest Research. Accessed March 4, 2016 http://www.milliontreesnyc.org/downloads/pdf/nyc_mfra.pdf

Phung, D., Thai, P. K., Guo, Y., Morawska, L., Rutherford, S., & Chu, C. (2016). Ambient temperature and risk of cardiovascular hospitalization: An updated systematic review and meta-analysis. Science of the Total Environment, 550, 1084–1102. http://doi.org/10.1016/j.scitotenv.2016.01.154

Preston, B. L., Yuen, E. J., & Westaway, R. M. (2011). Putting vulnerability to climate change on the map: A review of approaches, benefits, and risks. Sustainability Science, 6(2), 177–202. https://doi.org/10.1007/s11625-011-0129-1

Qin, J., Zhou, X., Sun, C., Leng, H., & Lian, Z. (2013). Influence of green spaces on environmental satisfaction and physiological status of urban residents. Urban Forestry & Urban Greening, 12(4), 490–497. http://doi.org/10.1016/j.ufug.2013.05.005

Quay, R. (2010). Anticipatory Governance. Journal of the American Planning Association, 76(4), 496–511. http://doi.org/10.1080/01944363.2010.508428

Reid, C., O'Neill, M., Gronlund, C., Brines, S., Brown, D., Diez-Roux, A., Schwartz, J. (2009). Mapping community determinants of heat vulnerability. Environmental Health Perspectives, 117(11), 1730–1736. http://doi.org/10.1289/ehp.0900683

Rinner, C.; Patychuk, D.; Bassil, K.; Nasr, S.; Gower, S.; Campbell, M. (2010). The role of maps in neighborhood-level heat vulnerability assessment for the city of Toronto. Cartogr. Geogr. Inf. Sci., 37, 31–44.

Robinson, P. (2001). On the Definition of a Heat Wave. Journal of Applied Meteorology, 40, 762–775.

Rocklov, J.; Forsberg, B.; Ebi, K.; Bellander, T. (2014). Susceptibility to mortality related to temperature and heat and cold wave duration in the population of Stockholm County, Sweden. Glob. Health Action, doi:10.3402/gha.v7.22737.

San Francisco Department of Public Health. (2014). Community Resiliency Indicator Maps, San Francisco Climate & Health Program. https://sfclimatehealth.org/maps/

Sander, H., Polasky, S., Haight, R. (2010). The value of urban tree cover: A hedonic property price model in Ramsey and Dakota Counties, Minnesota, USA. Ecological Economics, 69. 1646-1656.

Schwartz, J. (2005). Who is sensitive to extremes of temperature? A case-only analysis. Epidemiology, 16, 67–72.

Scott, K., McPherson, E., Simpson, J. (1998). Air pollution uptake by Sacremento's urban forest. Journal of Arboriculture, 24. 223-234.

Semenza, J.C.; McCullough, J.E.; Flanders, W.D.; McGeehin, M.A.; Lumpkin, J.R. (1999). Excess hospital admissions during the July 1995 heat wave in Chicago. Am. J. Prev. Med., 16, 269–277.

Seroka C, Kaiser P, Heany J. (2011). Mapping heat vulnerability in Michigan. (MPHI Annual Report).

Shashua-Bar, L., Pearlmutter, D., & Erell, E. (2009). The cooling efficiency of urban landscape strategies in a hot dry climate. Landscape and Urban Planning, 92(3–4), 179–186. https://doi.org/10.1016/j.landurbplan.2009.04.005

Sherbakov, T., Malig, B., Guirguis, K., Gershunov, A., & Basu, R. (2018). Ambient temperature and added heat wave effects on hospitalizations in California from 1999 to 2009. Environmental Research, 160(May 2017), 83–90. http://doi.org/10.1016/j.envres.2017.08.052

Sheridan, S. C. (2007). A survey of public perception and response to heat warnings across four North American cities: an evaluation of municipal effectiveness. International Journal of Biometeorology, 52, 3–15. http://doi.org/10.1007/s00484-006-0052-9

Smoyer, K. E. (1998). Putting risk in its place: Methodological considerations for investigating extreme event health risk. Social Science and Medicine, 47(11), 1809–1824. http://doi.org/10.1016/S0277-9536(98)00237-8

Stocker, L., Burke, G., Kennedy, D., & Wood, D. (2012). Sustainability and climate adaptation: Using Google Earth to engage stakeholders. Ecological Economics, 80, 15–24. https://doi.org/10.1016/j.ecolecon.2012.04.024

Stone, B. J. (2007). Urban and Rural Temperature Trends in Proximity to Large US Cities: 1951-2000. International Journal of Climatology, 27, 1801–1807. http://doi.org/10.1002/joc

Stone, B., Vargo, J., Liu, P., Habeeb, D., DeLucia, A., Trail, M., Hu, Y. Russell, A. (2014). Avoided heat-related mortality through climate adaptation strategies in three US cities. PLoS ONE, 9(6). http://doi.org/10.1371/journal.pone.0100852

Stone, B.; Hess, J.J.; Frumkin, H. (2010). Urban form and extreme heat events: Are sprawling cities more vulnerable to climate change than compact cities? Environ. Health Perspect., 118, 1425–1428.

Stone, Brian. (2012). The city and the coming climate: climate change in the places we live. Cambridge ; New York: Cambridge University Press.

Sugawara, H., Shimizu, S., Takahashi, H., Hagiwara, S., Narita, K., Mikami, T., & Hirano, T. (2015). Thermal Influence of a Large Green Space on a Hot Urban Environment. Journal of Environment Quality, 0(0), 0. https://doi.org/10.2134/jeq2015.01.0049

Sun, X.; Sun, Q.; Zhou, X.; Li, X.; Yang, M.; Yu, A.; Geng, F. (2014). Heat wave impact on mortality in Pudong New Area, China in 2013. Sci. Total Environ., 493, 789–794.

Tallis, M., Taylor, G., Sinnett, D., Freer-Smith, P. (2011). Estimating the removal of atmospheric particulate pollution by the urban tree canopy of London, under current and future environments. Landscape and Urban Planning, 103. 129-138.

Tapsell, S.M.; Penning-Rowsell, E.C.; Tunstall, S.M.; Wilson, T.L. (2002). Vulnerability to flooding: Health and social dimensions. Philos. Trans. R. Soc. A, 360, 1511–1525.

Tate, E. (2012). Social vulnerability indices: A comparative assessment using uncertainty and sensitivity analysis. Nat. Hazards. 63, 325–347.

Tate, E. (2013). Uncertainty Analysis for a Social Vulnerability Index. Annals of the Association of American Geographers, 103(3), 526–543. http://doi.org/10.1080/00045608.2012.700616

Thornton, P.E., M.M. Thornton, B.W. Mayer, Y. Wei, R. Devarakonda, R.S. Vose, and R.B. Cook. 2016. Daymet: Daily Surface Weather Data on a 1-km Grid for North America, Version 3. ORNL DAAC, Oak Ridge, Tennessee, USA. https://doi.org/10.3334/ORNLDAAC/1328

Tjur, T. (2009) "Coefficients of determination in logistic regression models—A new proposal: The coefficient of discrimination." *The American Statistician* 63: 366-372.

Toloo, G. S., Fitzgerald, G., Aitken, P., Verrall, K., & Tong, S. (2013). Are heat warning systems effective ? Environmental Health, 12(27). http://doi.org/10.1186/1476-069X-12-27

Tomlinson, C.J.; Chapman, L.; Thornes, J.E.; Baker, C.J. (2011). Including the urban heat island in spatial heat health risk assessment strategies: A case study for Birmingham, UK. Int. J. Health Geogr., 10, 42, doi:10.1186/1476-072X-10-42.

Turner, D.P., W.D. Ritts, and M. Gregory. 2006. BigFoot NPP Surfaces for North and South American Sites, 2002-2004. ORNL DAAC, Oak Ridge, Tennessee, USA. https://doi.org/10.3334/ORNLDAAC/1270

Turvey, R. (2007). Vulnerability assessment of developing countries: The case of small-island developing states. Dev. Policy Rev., 25, 243–264.

US Global Change Research Program. (2016). The Impacts of Climate Change on Human Health in the United States: A Scientific Assessment. Washington DC.

Vargo, J., Xiao, Q., & Liu, Y. (2015). The Performance of the National Weather Service Heat Warning System against Ground Observations and Satellite Imagery. Advances in Meteorology, 2015, 1–15. https://doi.org/10.1155/2015/649614

Velarde, M. D., Fry, G., & Tveit, M. (2007). Health effects of viewing landscapes – Landscape types in environmental psychology. Urban Forestry & Urban Greening, 6(4), 199–212. https://doi.org/10.1016/j.ufug.2007.07.001

Vescovi, L.; Rebetez, M.; Rong, F. (2005). Assessing public health risk due to extremely high temperature events: Climate and social parameters. Clim. Res., 30, 71–78.

Voorhees, A., Fann, N., Fulcher, C., Dolwick, P., Hubbell, B., Bierwagen, B., Morefield, P. (2011). Climate Change-Related Temperature Impacts on Warm Season Heat Mortality: A Proof-of-Concept Methodology Using BenMAP. Environmental Science & Technology, 45, 1450-1457. doi:dx.doi.org/10.1021/es102820y

Wang, Y., Nordio, F., Nairn, J., Zanobetti, A., & Schwartz, J. D. (2018). Accounting for adaptation and intensity in projecting heat wave-related mortality. Environmental Research, 161(July 2017), 464–471. http://doi.org/10.1016/j.envres.2017.11.049

Weng, Q., Rajasekar, U., Hu, X. (2011). Modeling Urban Heat Islands and Their Relationship with Impervious Surface and Vegetation Abundance by Using ASTER Images. IEEE Transactions on Geoscience and Remote Sensing, 49(10), 4080–4089.

Wilhelmi, O., Hayden, M. (2010). Connecting people and place:Anew framework for reducing urban vulnerability to extreme heat. Environ. Res. Lett., 5, 014021, doi:10.1088/ 1748-9326/5/1/014021.

Wilson, B., Chakroborty, A. (2017). Chicago Heat Vulnerability. Online Resource. Retreived from http://chicagoheatvulnerability.org/

Winkler, J.A., G.S. Guentchev, M. Liszewska, Perdinan, and P.-N. Tan. (2011): Climate scenario development and applications for local/regional climate change impact assessments: An overview for the non-climate scientist. Part II: Considerations when using climate change scenarios. Geography Compass, 5/6, 301– 328. DOI 10.1111/j.1749-8198.2011.00426.x.

Wolf, J.; Adger, W.N.; Lorenzoni, I.; Abrahamson, V.; Raine, R. (2010). Social capital, individual responses to heat waves and climate change adaptation: An empirical study of two UK cities. Glob. Environ. Chang., 20, 44–52.

Wolf, T.; McGregor, G. (2013). The development of a heat wave vulnerability index for London, United Kingdom. Weather Clim. Extremes, 1, 59–68.

Wolf, T.; McGregor, G.; Analitis, A. (2014). Performance assessment of a heat wave vulnerability index for greater London, United Kingdom. Weather Clim. Soc., 6, 32–46.

Wolf, T., Chuang, W., Mcgregor, G. (2015). On the Science-Policy Bridge : Do Spatial Heat Vulnerability Assessment Studies Influence Policy? International Journal of Environmental Research and Public Health, 12, 13321–13349. http://doi.org/10.3390/ijerph121013321

World Health Organization. (2004). International Statistical Classification of Dis- eases and Related Health Problems, 10th Revision (ICD–10), 2nd ed. World Health Organization, Geneva, Switzerland. http://www.who.int/classifications/icd/ICD-10_2nd_ed_ volume2.pdf

Xu, Z.; Sheffield, P.E.; Su, H.; Wang, X.; Bi, Y.; Tong, S. (2014). The impact of heat waves on children's health: A systematic review. Int. J. Biometeorol., 58, 239–247.

Ye, X., Wolff, R., Yu, W., Vaneckova, P., Pan, X., Tong, S. (2012). Ambient temperature and morbidity: A review of epidemiological evidence. Environmental Health Perspectives, 120, 19-28. http://dx.doi.org/10.1289/ehp.1003198

Yuan, F., Bauer, M. E. (2007). Comparison of impervious surface area and normalized difference vegetation index as indicators of surface urban heat island effects in Landsat imagery. Remote Sensing of Environment, 106(3), 375-386. doi:10.1016/j.rse.2006.09.003

Zeng, Q., Li, G., Cui, Y., Jiang, G., & Pan, X. (2016). Estimating Temperature-Mortality Exposure-Response Relationships and Optimum Ambient Temperature at the Multi-City Level of China. International Journal of Environmental Research and Public Health, 13(3), 279. http://doi.org/10.3390/ijerph13030279

Zhou, Y., Shepherd, J. (2010). Atlanta’s urban heat island under extreme heat conditions and potential mitigation strategies. Natural Hazards, 52(3), 639–668. http://doi.org/10.1007/s11069-009-9406-z

Zhu, Q.; Liu, T.; Lin, H.L.; Xiao, J.P.; Luo, Y.; Zeng, W.L.; Zeng, S.Q.; Wei, Y.; Chu, C.; Baum, S.; et al. (2014). The spatial distribution of health vulnerability to heat waves in Guangdong Province, China. Glob. Health Action, 7, doi:10.3402/gha.v7.25051.